

Design Methodology and Numerical Optimization of Ultrasonic Transducers for Spinal Surgery

THÈSE N° 4328 (2009)

PRÉSENTÉE LE 6 MARS 2009

À LA FACULTÉ SCIENCES ET TECHNIQUES DE L'INGÉNIEUR

LABORATOIRE D'ACTIONNEURS INTÉGRÉS

PROGRAMME DOCTORAL EN SYSTÈMES DE PRODUCTION ET ROBOTIQUE

ÉCOLE POLYTECHNIQUE FÉDÉRALE DE LAUSANNE

POUR L'OBTENTION DU GRADE DE DOCTEUR ÈS SCIENCES

PAR

Daniel PORTO

acceptée sur proposition du jury:

Prof. M.-O. Hongler, président du jury

Prof. Y. Perriard, directeur de thèse

Dr J.-M. Breguet, rapporteur

Dr D. Damjanovic, rapporteur

Dr J. Murphy, rapporteur



ÉCOLE POLYTECHNIQUE
FÉDÉRALE DE LAUSANNE

Suisse
2009

Abstract

Nowadays, the general trend towards to minimally invasive interventions is present in all the medical domains. For the surgical intervertebral spinal disc cutting or removal domain, it is particularly a necessity because the manual methods currently employed are tedious, time consuming and taxing on the hands of the practitioner. In that context, new devices that are small enough to pass through a small opening in the skin or through a small portal are required. A detailed analysis of current cutting methods that are or could be used for disc and disc nucleus removal provided that *ultrasonics* technology should be investigated as a possible solution.

The study of ultrasonics technology to fulfil the overall cutting function needed for spinal annulus and nucleus disc material removal is based on a design methodology that breaks down the overall cutting function in many partial functions. The applied design methodology consists in drawing a complete catalogue of solutions for each partial function. Based on a predetermined choice of criteria for each partial function, the evaluation and the classification of each solution allows determination of the best solutions for each partial function. A new ultrasonic transducer designed device composed of a piezoelectric stack for the source of energy and movement, a transmission partial function with rods or discs, an amplification partial function with exponential horns and the cutting partial function solutions is detailed.

Existing analytical methods for the design of ultrasonic transducers are mostly based on quarter wavelength segments used to build the transducer. The modeling of that transducers with a finite element method (FEM) avoids building the prototypes and constitutes progress. Analytical models different from the quarter wavelength approach have already been developed and are very useful when used in an optimization process. Furthermore, when the geometry of the analyzed model is not straightforward, a FEM optimization approach to solve that kind of problems can be a valid solution too.

Some existing optimization algorithms and other already developed pseudo-gradient methods applied to optimize the analytical models of the ultrasonic transducers are not valid for numerical optimizations where the computing time is a key factor. This leads to the development a new genetic algorithm (GA) optimization methods. One advantage being that the number of parameters to be optimized does not change the complexity of the algorithm unlike other algorithms. Three GAs with improvements done on different parts are discussed, implemented and tested. One GA is chosen to optimize the transducer model with numerical methods. As the main drawback with

FE optimizations is the amount of computation time spent for each simulation, this creates a need to develop numerical 2D models that can be quickly simulated but with accurate results. Ultrasonic transducer prototypes are also built and measured. As the prototype has to be used for the cutting or the removal of spinal disc material, the cutting effect of the prototypes has been tested and evaluated.

Keywords: Design methodology, numerical optimization, ultrasonic transducer, spinal surgery, spinal disc, FEM, FEA, genetic algorithm, optimization, finite element, piezoelectric transducer, medical transducer

Résumé

De nos jours, une tendance générale pour des interventions moins invasives se fait ressentir dans tous les domaines médicaux. Dans le domaine de la chirurgie des disques intervertébraux et en ce qui concerne la découpe ou l'enlèvement des disques intervertébraux, c'est particulièrement devenu une obligation car les méthodes manuelles actuelles sont fastidieuses, prennent beaucoup de temps et sont ardues pour les mains des chirurgiens. Dans ce contexte, de nouveaux appareils qui sont assez petits pour passer à travers une petite incision dans la peau ou à travers une petite ouverture sont fortement demandés. Une analyse détaillée des méthodes de découpe actuelles qui sont ou qui pourraient être utilisées pour l'enlèvement des disques (annulus) et des noyaux mous à l'intérieur (nucleus) a conclu que la *technologie ultrasonique* devrait être analysée comme possible solution.

L'étude de la technologie ultrasonique pour remplir la fonction générale de découpe dont on a besoin pour l'enlèvement du tissu de l'annulus et du nucleus de la colonne vertébrale est basée sur une méthodologie de conception qui sépare la dite fonction générale de découpe en plusieurs fonctions partielles. La méthodologie de conception appliquée consiste à dresser un catalogue complet de solutions pour chaque fonction partielle. En se basant sur des critères préalablement choisis pour chaque fonction partielle, l'évaluation et la classification de chacune des solutions permet de déterminer les meilleures solutions pour chaque fonction partielle. Lors de la conception d'un nouveau dispositif, le transducteur ultrasonique sera composé d'une pile piézoélectrique comme source d'énergie et de mouvement, une fonction partielle de transmission avec des tiges ou des disques, une fonction partielle d'amplification avec des cornets exponentiels et des solutions détaillées pour la fonction partielle de découpe.

Les méthodes analytiques existantes pour la conception des transducteurs ultrasoniques sont basées principalement sur la méthode typique des segments quart-d'onde qui sont utilisés pour construire un transducteur. La modélisation de ces transducteurs avec une méthode par éléments finis (FEM) évite de fabriquer les prototypes et constitue donc un progrès. Des modèles analytiques différents de l'approche par segments quart-d'onde ont déjà été développés et sont très utiles lorsqu'ils sont utilisés dans un processus d'optimisation. De plus, lorsque la géométrie du modèle analysé n'est pas évidente, une optimisation par une approche éléments finis permettrait de résoudre ce genre de problèmes et pourrait être une solution valable également.

Certains algorithmes d'optimisation existants et d'autres algorithmes développés basés sur une méthode de pseudo-gradient, et qui ont déjà été appliqués

pour l'optimisation des modèles analytiques de transducteurs ultrasoniques, ne sont pas valables pour les optimisations numériques où le temps de calcul est un facteur clé. Ceci nous a conduit à développer une nouvelle méthode d'optimisation basée sur les algorithmes génétiques. Un avantage de cette méthode étant que le nombre de paramètres à optimiser ne change pas la complexité de l'algorithme, à la différence des autres algorithmes. Trois algorithmes génétiques avec des améliorations apportées sur des parties différentes de l'algorithme sont discutés, implémentés et testés. Un algorithme génétique est choisi pour l'optimisation du modèle du transducteur par des méthodes numériques. Etant donné que le plus grand désavantage des optimisations par éléments finis est la quantité de temps de calcul nécessaire pour chaque simulation, ceci a créé le besoin de développer des modèles numériques 2D qui peuvent être simulés rapidement mais avec des résultats précis. Les transducteurs ultrasoniques ont également été fabriqués et mesurés. Puisque le prototype doit être utilisé pour la découpe ou l'enlèvement du tissu des disques de la colonne vertébrale, le pouvoir de découpe des prototypes a été testé et évalué.

Mots-clés: Méthodologie de conception, optimisation numérique, transducteur ultrasonique, chirurgie de la colonne vertébrale, disque intervertébral, algorithmes génétiques, optimisations, éléments finis, transducteur piézoélectrique, transducteur médical

Acknowledgements

I would like to express my gratitude to all the people who have contributed to this work with their help, their advice, support, encouragement and inspiration.

I would especially like to thank Prof. Y. Perriard who gave me the opportunity to do my thesis at LAI as well as for his advice and support and encouragements during these years have permitted the achievement of this thesis work.

Prof. M.-O. Hongler for presiding the thesis jury and Dr. J.-M. Breguet, Prof. D. Damjanovic and Dr J. Murphy for having accepted to be part of the jury and the time they spent in reading and criticizing this work.

Thanks to all the members, friends and colleagues of the LAI laboratory. Special thanks to my different officemates: J. Persson, J. Murphy and O. Scaglione. Thank you J. Maridor for having read and corrected this manuscript.

Particular thanks to J.Murphy, who first was a colleague, then an officemate and finally a friend. Thank you for all your support and the hours spent in discussions about the project, for your friendship and for all the reasons that have made this work possible.

Thank you Vero, for these four years supporting me and with the affection and love she gives to me.

A meus pais, Josefa e Secundino, con todo o meu cariño, gracias pola vosa axuda e apoio ó longo destes tantos anos. Este traballo vai adicado a vós. Gracias por todo.

Table of Contents

1	Introduction	1
1.1	Introduction	1
1.2	Background	2
1.3	State of the Art	3
1.3.1	Criteria for Power Source Selection	3
1.3.2	Selection Matrix and Results	3
1.3.3	Numerical Methods	5
1.4	Reading Instruction	6
2	Design Methodology	9
2.1	Introduction	9
2.2	Transmission Partial Function	11
2.2.1	Selection Criteria	11
2.2.2	Proposed Solutions	11
2.2.2.1	Bendable Tube with Internal Sliding Wire	11
2.2.2.2	Linked Tube with Internal Sliding Wire	14
2.2.2.3	Resonant Beam	14
2.2.2.4	Resonant Horn	15
2.2.2.5	Resonant Beam Inside Tube with Rotating Head	15
2.2.2.6	Rubber Inside Flexible Tube	16
2.2.2.7	Resonant Beam with Small Flexible Tube Filled with Rubber	16
2.2.2.8	Resonant Horn with Small Flexible Tube Filled with Rubber	16
2.2.2.9	Bellows Coupling	17

	2.2.2.10	Bendable Tube with Internal Sliding Wire on Guides	17
	2.2.2.11	Flexible Tube with Electrical Wires	18
	2.2.2.12	Flexible Tube with Incompressible Liquid	18
	2.2.2.13	Combination Resonant Beam and Flexible Tube with Incompressible Liquid	19
	2.2.3	Conclusions	19
2.3		Amplification Partial Function	22
	2.3.1	Selection Criteria	22
	2.3.1.1	Pass-Fail Criteria	22
	2.3.1.2	Merit Criteria	22
	2.3.2	Proposed Solutions	24
	2.3.2.1	Resonant Horn	24
	2.3.2.2	Expanding Ball	25
	2.3.2.3	Impact Printer Concept	25
	2.3.2.4	Scissored Beams	26
	2.3.2.5	Pinching Fingers	26
	2.3.2.6	Cantilevered Foot	27
	2.3.2.7	Rotational Lever	27
	2.3.2.8	Bow Strain	28
	2.3.2.9	4 Bar Linkage	28
	2.3.2.10	Molecular Scale Mechanical Amplifier	29
	2.3.2.11	Bimorph Trimorph	30
	2.3.2.12	Dual Fixed End Bimorph	30
	2.3.2.13	Hydraulic	31
	2.3.2.14	Integrated Lever	31
	2.3.3	Solution Augmentations	32
	2.3.3.1	Multiple Element Resonator	32
	2.3.3.2	Free Mass	33
	2.3.3.3	Constrained Mass	33
	2.3.4	Conclusions	34
2.4		Cutting Partial Function	36
	2.4.1	Selection Criteria	36
	2.4.1.1	General Selection Criteria	36
	2.4.1.2	Function Specific Criteria	37
	2.4.2	Proposed Solutions	37
	2.4.2.1	Blade Tip	37
	2.4.2.2	Blade with Fixed Base	38

2.4.2.3	Blade Needle	38
2.4.2.4	Scissors Ball	39
2.4.2.5	Scissors Piezo	39
2.4.2.6	Cavitation Jet	40
2.4.2.7	Multiple Pyramidal Cutter	41
2.4.2.8	Curved Shank Cutter	41
2.4.2.9	Rasp	41
2.4.2.10	Apposing Cutters	42
2.4.2.11	Apposing Cutters II	42
2.4.2.12	Resonant Tube	43
2.4.2.13	Resonant Tube with Sharpened Screen	43
2.4.2.14	Large Area Tip	44
2.4.3	Solution Ratings	44
2.4.4	Conclusions	46
2.4.4.1	Cutting Solutions	46
2.4.4.2	Material Removal Solutions	46
2.4.4.3	Material Shaping Solutions	46
2.4.4.4	Coagulation Solutions	47
2.4.4.5	Overall	47
2.5	Overall Conclusion	47

3 Piezoelectrics and Waves 49

3.1	Elastic Material Properties	49
3.1.1	Elasticity Modulus E_Y	50
3.1.2	Poisson coefficient ν	50
3.2	Piezoelectricity Equations	51
3.3	Velocity and Wavelength	53
3.3.1	Wavelength	54
3.4	Numerical or Finite Element Equations	55
3.4.1	Elements	57
3.4.2	Analysis Types	58
3.5	Impedance and Admittance	59
3.6	Equivalent Circuit	59

4 Optimization Methods 61

4.1	Complete Output Mapping	62
4.2	Response Surface Methods	62
4.3	Gradient Methods	63
4.3.1	Pseudo-Gradient Method	64

4.3.2	Other Search Techniques	64
4.4	Genetic Algorithms	64
4.4.1	Main Concepts	65
4.4.1.1	Individual Representation	66
4.4.1.2	Initial Population	66
4.4.1.3	Fitness Function vs Objective Function	66
4.4.1.4	Parents Selection Rules	67
4.4.1.5	Parents Reproduction Rules	67
4.4.1.6	Replacement Strategy	69
4.4.1.7	Stop Criterion	69
4.4.2	Constraints and Convergence Problems	69
4.4.2.1	Optimization with Constraints	69
4.4.2.2	Premature Convergence and Population Diversity	70
4.5	Basic and New Genetic Algorithms	70
4.5.1	Preliminary Considerations	70
4.5.2	Basic Algorithm	71
4.5.3	Conditional Genetic Operators	72
4.5.4	Crossover Rules and Integrated Local Search	73
4.5.4.1	Local Search	75
4.5.5	Combination of Both Improvements	75
4.6	Test Functions	77
4.6.1	Algorithms Comparison	78
4.6.2	Algorithms Testing	79
4.6.3	Population and Children Size	81
4.7	MATLAB and ANSYS Implementation	82
4.8	Conclusion	83

5 Numerical Simulations and Optimizations 85

5.1	Introduction	86
5.2	Ultrasonic Transducer Parts	86
5.2.1	Piezoelectric Stack	86
5.2.2	Transmission Discs	87
5.2.3	Amplification Horns	87
5.2.4	Full Transducer Model	88
5.3	First Prototype	88
5.3.1	Displacement Amplitude	89
5.3.2	Impedance	90
5.3.3	Displacement and Impedance Comparisons	91

5.3.4	Mesh Size Effect	91
5.3.5	Optimization Objective Function	92
5.4	Second Prototype	93
5.4.1	Displacement Amplitude	93
5.4.2	Impedance	94
5.4.3	Amplitude and Impedance	94
5.4.4	Cannulation Size Effect	95
5.5	GAO Prototype	98
5.5.1	Transducer Model	98
5.5.2	Optimization Parameters	98
5.5.3	Results and Discussion	98
5.5.4	Conclusion	100
6	Measurements and Testings	103
6.1	Electronics	104
6.2	First Prototype Measurements	105
6.3	Second Prototype Measurements	106
6.3.1	Cracked Parts and Cannulation	106
6.3.2	Piezoelectric Stack Mounting	108
6.3.3	Displacement and Impedance Measurements	109
6.4	Cutting Testings	112
6.4.1	Test Setup	112
6.4.2	Test Results	113
6.5	Conclusions	114
7	Conclusions	117
7.1	Overview	117
7.2	Originality	118
7.3	Outlook	119
	Appendices	129
A	Technology Narrowing	131
B	Material Properties	133
B.1	Aluminium Alloy EN-AW-7075	133
B.2	Titanium Alloy T-6Al-4V-STA	133
B.3	Piezoelectric PZ-28	133
B.4	Piezoelectric PZ-54	134

C Mechanical Drawings	135
C.1 First Prototype	135
C.2 Second Prototype	142
C.3 test Bench	157
D Test Functions	161
D.1 Ackley Function	161
D.2 Rastrigin Function	161
D.3 Zakharov Function	161
Curriculum Vitae	162

Chap 1

Introduction

Summary

1.1	Introduction	1
1.2	Background	2
1.3	State of the Art	3
1.3.1	Criteria for Power Source Selection	3
1.3.2	Selection Matrix and Results	3
1.3.3	Numerical Methods	5
1.4	Reading Instruction	6

1.1 Introduction

Nowadays, everyone suffers or knows someone who suffers from back pain. This is not surprising because back pain is one of the most frequent complaints in the world. In some cases, surgical intervention has to be done and different manual methods are already used to cut the human tissue or to remove the spinal disc. Nevertheless, surgeons are not always fully satisfied due to the tedious, time consuming and the taxing nature of the existing devices.

Another important trend in the medical domain is all that concerns the minimally invasive surgery. These kind of procedures are less invasive to the patient, so they recover faster, result in shorter hospital stays, allows outpatient treatment, and reduces health care costs.

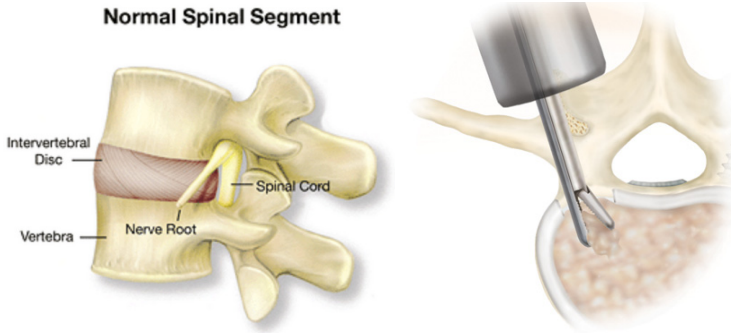


Figure 1.1: Normal Spinal Disc Segment and Manual Disc Removal Technique

The purpose of this project is to develop a set of surgical hand-pieces for use in the minimally invasive cutting, coagulating and removal of soft tissue, cartilage and bone.

1.2 Background

This thesis has been elaborated at the LAI (Laboratoire d'Actionneurs Intégrés) during the period 2004-2008.

A strong collaboration with a full-time engineer (John Murphy) at LAI from the Medtronic Inc. and the support of the Swiss Government through the CTI program has allowed the realization of this project.

The project itself was born somewhere in Texas. At that time, John Murphy, with the support of the executive team, had the idea to study a new technology to cut or remove the spinal discs with minimal invasive methods. This project was large enough to require two persons during four years and the subject treated in two thesis works.

The first thesis work has been undertaken and already successfully finished by Murphy [12]. So, this thesis is seen as a complementary part of the overall subject of *Ultrasonic Transducers for Spinal Surgery*. As this thesis treats themes that have not been discussed in details in [12], the two thesis complement each other and many cross-references are done.

1.3 State of the Art

The technological state of the art is undertaken as a first pass in narrowing a technology that will be suitable for disc and disc nucleus removal and has two major purposes. The first is to decide whether there is a good opportunity to realize a design with one of the technologies that have been considered and the second is to eliminate any technologies that are not viable. This reduces the amount of time that one must spend in finding a solution as the project becomes more focused.

1.3.1 Criteria for Power Source Selection

A list of criteria that are considered to allow for the different technologies considered to be down selected is presented in Table 1.1. The criteria are based on initial feedback from sessions with other company groups.

Table 1.1: Power Source Selection Criteria

Criterion	Value	Description
C1	Boolean	Power provided by the surgical device
C2	1-10	Measures the ability of the technology to target different tissue types
C3	1-10	Measures the degree of possible steering and maneuvering in limited access portal
C4	1-10	Ablative capabilities
C5	1-10	Ability to provide a cautery effect

1.3.2 Selection Matrix and Results

A matrix with specific values assigned to the criteria found in Table 1.1 is filled out. For each assignment there is a justification that was used to assign the value corresponding to how well the criterion in question was met. This matrix serves to down select to some technologies or a technology that is promising for the research to be performed. For clarity reasons, only four cutting methods are exposed in Appendix A, Table A.1.

The preliminary results are taken as an average of the different parameters on a 10 point scale and are presented in Table 1.2.

Table 1.2: Power Source Results

#	Cutting Method	Value
1	Scalpel	1
2	Ultrasonic	8.75
3	Electromechanical Shaver	2.5
4	Rongeur	1.25
5	Power Rongeur	1.5
6	Drill	1.5
7	Power Saw	1.5
8	Water Jet	3
9	Electro Surgical Generator (ESG)	7.5
10	Plasma Cutter	6.5
11	Laser	7.75
12	Milling	1.75
13	Grinding	1.5
14	Turning	1.5
15	Charged Particle Beam (CPB)	6.25
16	Electro Discharge Machining (EDM)	6
17	Flame	5.25

Data in Table 1.2 show clearly that *ultrasonics* should be the technology to investigate as a solution for the rapid removal of spinal nucleus and annulus disc material.

While the results of the *Laser* came in a close second in overall score, there is one area that should be considered more strongly than others when deciding which technology to choose. That area is the ability of the technology to target different materials for removal. If one considers that a different frequency *Laser* must be used to target different materials it makes more sense to pursue a technology that can have a wide range of outputs frequencies and possible material selectivity just by varying the input frequency of the drive signal. In order to select different materials with a laser, the material to be cut must be opaque and the material to be spared must be translucent. When one considers the two materials in question one sees that the nucleus is relatively clear in comparison with the annulus material. This does not lend itself well to the removal of just the nucleus and not the annulus because any frequency that will see the nucleus as opaque will also see the annulus as opaque. If the reverse were true and the annulus were clear in comparison to the nucleus, a laser might be better suited, because one desires to remove just the nucleus or both the nucleus and annulus. In this case though, one must also consider how difficult it is to generate just the correct frequency that will

ablate the nucleus and leave the annulus intact. These frequencies might not be available for most types of high-powered lasers.

Some other technologies such as *Plasma*, *Electro Surgery*, and *Electro Discharge Machining* (EDM) show some promise, but rely on the electrical properties of the subject as a return path for the energy introduced to the surgical site. This has been considered and found to be less desirable than a technology that relies only on the tissue to be cut and the energy source being applied to that tissue. EDM is particularly nice in regards to its ability to steer the electrode as it can be quite small and flexible. The problem that is encountered is the fluid in the wound site that is conductive and tends not to allow the EDM process to occur. For other methods, the wound site in question with its high water content might tend to present a challenging environment where the shortest path to the tissue to be removed might not be the actual path of the applied energy due to variations in the electrical properties of the wound.

Charged Particle Beams (CPB) have been considered and ruled out due to the difficult nature in steering the particle beam after having been accelerated. Considering the high voltages that are necessary to accelerate the particles, the beam would have to be accelerated before it left the power console. This would require steering the beam down some type of a guide. This seems far too complicated when one considers that *ultrasonics* receive a higher score in all categories as well.

Other methods that do not provide power to the surgical site from a power console are not considered as one of the primary concerns is to ameliorate the amount of work required by the surgeon as well as reduce the time it takes to do a disc removal by purely mechanical means.

The overall conclusion is that *ultrasonics* is the technology that should be pursued. In particular, studies should be done to determine how plausible it is to steer a resonant horn and still provide sufficient power and frequency selectivity to the target tissue. Or whether it is required to generate the ultrasonics by another way that has not been used in surgery up to date, but could revolutionize ultrasonic surgical handpieces and extend their use in all types of minimally invasive procedures.

1.3.3 Numerical Methods

When designing a new transducer, there is the typical method said of quarter wavelength elements. This method consists in building a new transducer with

different parts of length $\lambda/4$ and putting them together. The advantage is that the analytical equations are well-known; nevertheless, there is always some time spent to adapt the realized, measured and evaluated prototypes to guarantee their correct behavior.

Another method that has shown excellent results is the complete analytical modeling of the elements constituting the transducer. Any new transducer responding to any desired characteristic can easily be optimized and conceived from that model [12].

The last method of interest is the finite element method (FEM). When considering full 3D models, this method does not help too much in finding new transducer designs due to the amount of time spent in only one simulation. 3D models are rather used to verify the characteristics of a transducer with determined parameters.

Nevertheless, simplified numerical models can be found and 2D models can be used to design, simulate, measure and validate the transducers. This simplification reduces tremendously the calculation time for one simulation from 5 min to 5 s; and allows envisioning some kind of optimization process with FEM only.

1.4 Reading Instruction

The thesis is presented in the following manner:

Chapter 2 introduces a design methodology that is applied to develop a device for the removal of spinal disc material. The transducer is decomposed into three partial functions: transmission, amplification and cutting. For each partial function, a list of criteria is chosen and the proposed solutions are evaluated among each criterion.

In Chapter 3, the theory governing the waves and the piezoelectricity domain are discussed. Finite element theory is also introduced and the adaptations are discussed.

Chapter 4 deals with some optimization methods. Some pseudo-gradient methods have already been employed to optimize an ultrasonic transducer. The main concepts of a new optimization method based on genetic algorithms are introduced. A basic algorithm is implemented and three improvements are done. The first of concern is the conditional genetic operators, the second concerns the crossover rules and the last algorithm takes the two improvements into account. The developed algorithms are tested with some well-known functions and a set of parameters results for future optimizations.

Chapter 5 concerns the finite element (FE) simulations and optimizations. The first prototype is simulated for some important parameters and allows a validation of the FE models. The second prototype addresses the cannulation effect. Finally, a prototype is optimized using exclusively FE simulations.

In Chapter 6 the measurements and built prototypes are discussed to understand the encountered problems.

Chapter 7 ends with an overview of the thesis contents and the main results obtained. Some perspectives and the originality of this work are also mentioned.

Chap 2

Design Methodology

Summary

2.1	Introduction	9
2.2	Transmission Partial Function	11
2.2.1	Selection Criteria	11
2.2.2	Proposed Solutions	11
2.2.3	Conclusions	19
2.3	Amplification Partial Function	22
2.3.1	Selection Criteria	22
2.3.2	Proposed Solutions	24
2.3.3	Solution Augmentations	32
2.3.4	Conclusions	34
2.4	Cutting Partial Function	36
2.4.1	Selection Criteria	36
2.4.2	Proposed Solutions	37
2.4.3	Solution Ratings	44
2.4.4	Conclusions	46
2.5	Overall Conclusion	47

2.1 Introduction

A design methodology strongly based on [4] is applied and adapted to the current project.

The proposed basic method can be summarized in the four following phases in the development of a project:

1. the project

- choose an objective: market analysis, trend study, questions to customers, patent,...
- set or decide the development objectives (development proposition)

2. the design

- work out the requirements or specifications
- decide
- set up the overall function and decompose it in partial functions
- set up catalogues of solutions and objects for a given function
- find the solutions to the partial functions in the development context
- combine the functions to fulfil the overall function
- study the different concept alternatives
- technical and economical estimation of the different alternatives of the concept
- decide

3. the construction

- set up a scale outline of each alternative of the concept
- technical estimation and economical of the outlines (estimate the worst solutions)
- set up a re-examined and corrected construction
- optimize the configuration zones
- determine the optimized construction
- decide

4. the elaboration

- develop and optimize the components
- elaborate the documentation (drawings, list parts, instructions)
- build and test a prototype
- control the costs
- decide
- manufacture

The objective is to develop a new disruptive minimally invasive technology for the cutting, coagulation and removal of cartilage, and bone, and for the cutting and coagulating of soft tissue. The technical objective is to design

and develop a series of surgical hand-pieces that can be driven from a common source of energy housed in a portable control console or the hand-piece itself.

First of all, it has been necessary to choose (from a list of chosen criteria) a technology of construction in order to reduce the number of possible solutions, which is the *ultrasonics* technology. Then, it is possible to decompose the overall function of cutting spinal disc material in partial functions of *transmission*, *amplification* and *cutting*. For each partial function, a catalogue of solutions is determined following some selection criteria and evaluated as precisely as possible.

2.2 Transmission Partial Function

The scope of this section is to discuss the results of a preliminary study of methods to transmit ultrasonics from an actuator/amplifier to a cutter in an ultrasonic surgical handpiece.

2.2.1 Selection Criteria

Different methods of transmitting the power from the actuator and amplification section of the handpiece have been proposed and a set of criteria are chosen to evaluate the efficacy. These methods are compared using different criteria as a means to assess their viability. The criteria are described in Table 2.1.

2.2.2 Proposed Solutions

The proposed solutions to solve the problem of transmitting the ultrasonic energy from the actuator/amplification section to the cutting section of the handpiece are described.

2.2.2.1 Bendable Tube with Internal Sliding Wire

Description This solution consists of a wire that is encased in a flexible housing. The wire is excited mechanically by ultrasonics from one end in an *axial* or *rotational* direction. The ultrasonics propagate along the wire and are transferred to the cutting section.

Table 2.1: Transmission Selection Criteria

	Criterion	Description
P	Price	expected cost of a given solution. This is just an educated guess and is meant only to identify solution that might be too cost prohibitive at this early state of the project.
m	Mass/Weight	a comparative number between the different methods proposed for a solution.
S	Volume/Size	a comparative number between the different methods proposed for a solution.
AT	Ability to Transmit and Amplify	this number is a yes/no, four/one respectively.
F	Flexibility	this is a value based on how well the device can be flexed and is a measure of the possibility for guiding or steering the transmission section of the handpiece.
D	Disposability	This is a measure of how easily a solution could be used as a disposable. At first thought, one might think that anything can be thrown away but certain items, for example batteries or devices with heavy metals, might have special considerations when they are disposed of.
E	Efficiency	this is a measure of how well the power can be transmitted from the transducer-amplifier section to the cutting location. Poor efficiency means loss of power and effectiveness as well as heat generation that could be uncomfortable or unsafe for the user or patient.
EF	Efficiency when Flexing	this measure the ability to change the direction of cutting using the same transmission section.
CA	Ability to Cut and Transmit	this is a yes/no evaluation and is a measure of whether or not the transmission section could be adapted to perform the cutting as well.
M	Manufacturability	a quick stab at how easy it would be to realize a given solution. This was mainly base on the next item Complexity.
C	Complexity	a measure of how complicated the transmission section is in relation to parts count and tolerances.
R	Reliability	a measure of how long a device could be expected to work. This item also ties in with the complexity and manufacturability.
f	Ability to Transmit High Frequencies	Since the frequencies in question are quite elevated for mechanical devices it is necessary that a particular solution allows for their transmission. This value is a measure of the proposed solution to perform this function.
PS	User and Patient Safety	this value highlights any perceived issues that might need to be considered that concern patient or user safety.
PT	Power Transmission Capability	this is a measure of how much power the solution can transmit before there is a danger of it failing.

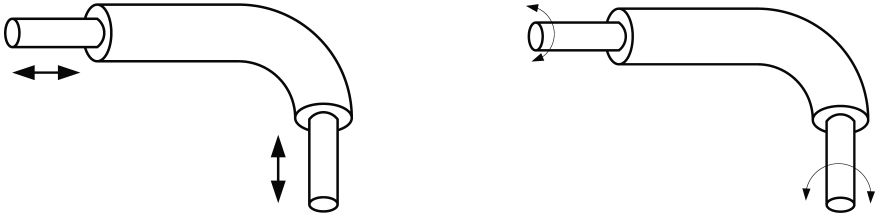


Figure 2.1: Sliding Wire Axial and Rotational

Remarks This solution should be relatively cheap to produce, as there are items on the market that are very similar if not the same. The volume and material selections should not make weight a problem. Cables currently available with a single strand can be made much smaller than is required for this application.

These solutions should be more flexible than most but the ability to transmit high frequencies decreases as the flexibility of the wire increases, because the stiffness depends on the cross sectional area of the wire. The natural frequency does increase with a shorter wire so this solution might be good for a short distance in combination with another more efficient solution to get the length needed. The natural frequency in rotation should be a little higher than the one allowing for transmission of higher frequencies because the stiffness of the wire in rotation is higher than it is in flexure.

This solution could be lossy if the wire needs to be under tension to pre-load a spring mass at the cutting end. The frictional losses could increase rapidly if the normal force between the cable and the housing increases. When compared with other solutions that only have structural losses, the sliding action of the wire on the housing make this solution less attractive. The use of low coefficient of friction materials could help. Another aid might be that the frequencies in question are high and this tends to decrease the friction. Bending the cable could further increase the normal force between the cable and housing and considerably increase the frictional losses.

The wire is very simple and involves only a case of some sort, possibly a liner, and a wire, but is still more complex than a beam or like solution. Although simple, it might drive a more complex solution for either the amplifier or the cutter, because a reliable mechanism to clamp and tension the wire might be necessary.

2.2.2.2 Linked Tube with Internal Sliding Wire

Description This solution consists of a wire that is encased in a flexible housing. The wire is exited mechanically by ultrasonics from one end in an *axial* or *rotational* direction. The housing consists of linked sections that interlock and can provide more axial stiffness along the length of the housing than the cable described in Section 2.2.2.1.

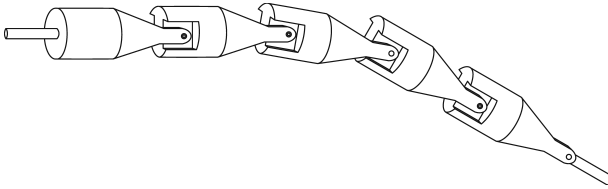


Figure 2.2: Linked Tube with Internal Sliding Wire

Remarks This is the same solution as Bendable Tube with Internal Sliding Wire - Axial and will have similar loss characteristics, frequency transmission ability etc. The difference lies in the housing in that it could provide better coupling with the stationary portion of the actuator and allow for the structure to handle more load in tension. The downside is that it would be less flexible and be harder to make.

2.2.2.3 Resonant Beam

Description This solution consists of a beam that extends from the amplification section of the handpiece to the cutting section. The beam could be solid or a hollow tube and have many different shapes. Ideally the beam would be driven at its resonant frequency. The beam could also have *axial*, *flexural* or *rotational* possibilities.

Remarks The resonant beam is an attractive solution in that it has very low losses, but it limits the ability to steer the device. It was ranked very low for efficiency while bending as it is a rigid beam but under small bending it should still transmit rather well.



Figure 2.3: Resonant Beam

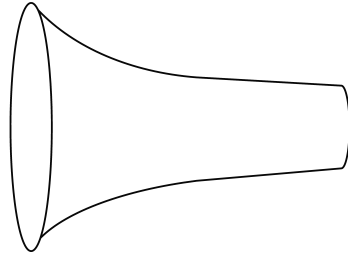


Figure 2.4: Resonant Horn

2.2.2.4 Resonant Horn

Description This solution consists of a resonant horn that is driven by a piezoelectric actuator. Horns can be of various shapes depending on the desired resonance and motion.

Remarks The resonant horns have high efficiency and have the added benefit that they can amplify the signal as well as transmit the power. This solution lacks in flexibility, as the structure is rigid, but could be coupled to another method of transmission to get some flexibility back into the transmission section.

2.2.2.5 Resonant Beam Inside Tube with Rotating Head

Description This solution consists of a transmitting beam that moves, without contact, inside a rigid tube that is mounted to the stationary portion of the actuator. Affixed to the other end of the tube is a rotating head that is driven from the back by the transmitting beam. The interface between the beam and the rotating head can be matched such that considerable motion can be coupled to the head over a range of angles.

Remarks The solution provides some flexibility at the tip but the complexity and part tolerances could make the part hard to manufacture and drive up the cost. While the head can rotate the access to the site might still be limited if the head were too short or too long. Finding the perfect length could be a real problem, as different lengths might be needed. This solution could also be very lossy if tolerances are not kept very tight.

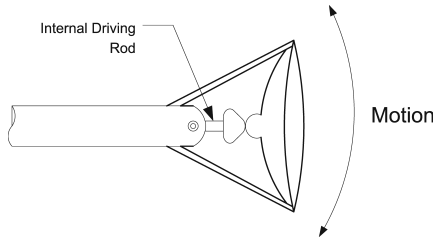


Figure 2.5: Floating Head

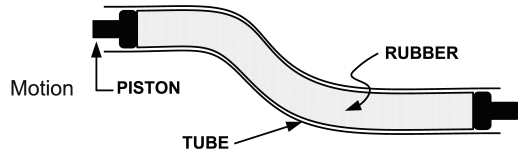


Figure 2.6: Rubber Inside Flexible Tube

2.2.2.6 Rubber Inside Flexible Tube

Description This solution consists of a rubber material encased in a flexible tube that provides radial stiffness. The rubber is excited and the tube is fixed to the stationary portion of the actuator. The tube may or may not be necessary.

Remarks Currently there is not a good feel for the losses in this system. Literature shows that the stiffness of rubber materials increases and the loss angle decreases as the material deformation decreases, but no similar uses were noted, as the literature usually refers to the damping of sound and not its transmission. Some stiffer, denser rubbers have been known to transmit frequencies up to a few Megahertz. It might be possible that a short section of rubber could be used to transmit the energy if the impedances are well matched.

2.2.2.7 Resonant Beam with Small Flexible Tube Filled with Rubber

Description This solution is a combination of the *Rubber Inside Flexible Tube* (Sec. 2.2.2.6) and the *Resonant Beam - Axial, Flexural, or Rotational* (Sec. 2.2.2.3).

Remarks This solution has the added benefits of flexibility where needed but improved transmission over a purely rubber solution.

2.2.2.8 Resonant Horn with Small Flexible Tube Filled with Rubber

Description This solution is a combination of the *Rubber Inside Flexible Tube* (Sec. 2.2.2.6) and the *Resonant Horn* (Sec. 2.2.2.4).

Remarks This solution has the added benefits over the Resonant Beam with Small Flexible Tube Filled with Rubber in that it will also amplify the motion from the actuator.

2.2.2.9 Bellows Coupling

Description This solution consists of a bellows type coupler connected between two transmission sections. The bellows coupling allows the cutting tip to be steered. *Axial* or *rotational* directions possible.



Figure 2.7: Bellows Coupling

Remarks The bellows coupling in the axial direction suffers from an inability to transmit high frequencies. Production of the device could be problematic, but there are commercially available bellows couplings that could be employed. Bellows couplings are usually expensive, so the price of the device might be prohibitive if it needs to be disposable. The bellows coupling used with rotational transmission has a higher capability to transmit high frequencies than the axial bellows coupling.

2.2.2.10 Bendable Tube with Internal Sliding Wire on Guides

Description This solution consists of a wire that is encased in a flexible housing. The wire is exited mechanically by ultrasonics from one end in an *axial* or *rotational* direction. The ultrasonics propagate along the wire and are transferred to the cutting section. Contact with the wire occurs only where the guides are located in the cable.

Remarks This solution is very similar to Bendable Tube with Internal Sliding Wire - Axial. This solution should have about the same losses but could suffer from problems if the wire were to bunch up or bind at the guide and the losses could be much larger. Also the manufacture of the cable could be more difficult which could drive up the cost.

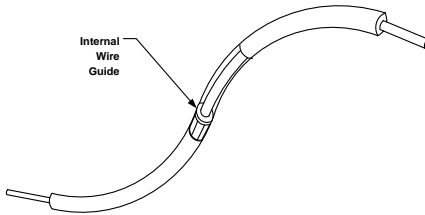


Figure 2.8: Bendable Tube with Internal Sliding Wire on Guides

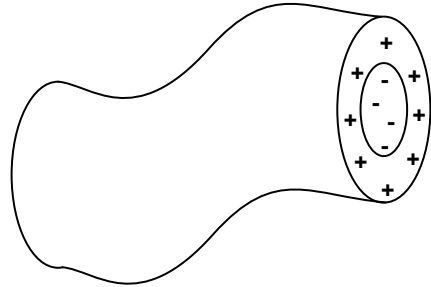


Figure 2.9: Flexible Electrical Cable

2.2.2.11 Flexible Tube with Electrical Wires

Description This solution consists of conductive wires encased in a housing that are used to transfer power to the actuator.

Remarks Although this solution is the best as far as the transmission sections are considered, it requires that the actuator, amplifier, and cutting section to be in vivo. Due to the limited size of the access and the spinal disc, this might not be possible. There are also some safety issues that need to be overcome because the voltage required to drive the actuator is on the order of 100 V and upwards.

2.2.2.12 Flexible Tube with Incompressible Liquid

Description This method of power transmission utilizes an incompressible liquid in a piece of tubing. The liquid is driven at one end by a piston connected to an actuator or amplifier. The liquid at the other end of the transmission section drives another piston that is connected to the cutting section of the handpiece.

Remarks This solution provides for a very flexible transmission section but suffers from an inability to transmit high frequencies. At pressures of about one atmosphere the liquid will begin to cavitate and most of the power to be transmitted will be lost in the interaction of the cavitating liquid with the transmission tube. At pressures of about one atmosphere the liquid will begin to cavitate unless the frequency is very high and most of the power to be

transmitted will be lost in the interaction of the cavitating liquid within the transmission tube.

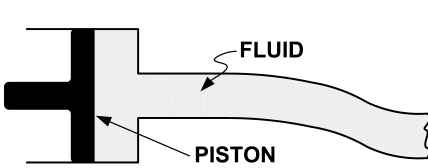


Figure 2.10: Flexible Tube with Incompressible Liquid

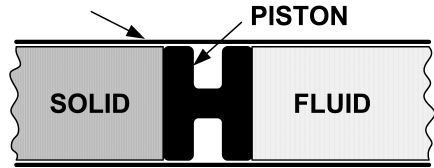


Figure 2.11: Combination Resonant Beam and Flexible Tube with Incompressible Liquid

2.2.2.13 Combination Resonant Beam and Flexible Tube with Incompressible Liquid

Description This method of power transmission utilizes the incompressible liquid in a piece of tubing coupled with a resonant beam. The liquid is driven at one end by a piston connected to the resonant beam. The liquid at the other end of the transmission section drives a piston that is connected to the cutting section of the handpiece.

Remarks This solution provides for a very flexible transmission section and gains from the low loss of the resonant beam, but still suffers from an inability to transmit high frequencies. At pressures of about one atmosphere the liquid will begin to cavitate unless the frequency is very high and most of the power to be transmitted will be lost in the interaction of the cavitating liquid within the transmission tube.

2.2.3 Conclusions

Rigid structures certainly provide for the lowest losses in the transmission section, but do not allow for the cutting section of the handpiece to be guided. It might be possible to use a more lossy solution for a small section of the transmission section to allow for the possibility of better access to the surgical site. This could be employed in a separate disposable that could be used to clean up the site while the bulk of the work can be done with the main rigid attachment. Based on this information, the transmission section should

consist of a resonant horn coupled with a beam for transmission of the power to the cutting section or to an auxiliary flexible transmission section.

The flexible tube with rubber, or just a plain rubber section for transmission of energy at some bend radius is also a solution that shows some promise but will require investigation. Available literature focuses on rubber's ability to absorb high frequencies and not its ability to transmit it. After producing an amplifier and transmission section, some testing should be performed to see if there is any merit in pursuing this type of solution. A stiff, dense rubber should be chosen and some testing performed.

Perhaps the best solution as far as the transmission section is concerned is to use a flexible tube with wires that can drive an actuator that is located in the surgical site. This solution is the most flexible and will have very low losses, but puts some tough restraints on the actuator section. The actuator must have a high power output and provide for amplification of the ultrasonic signal and be in a very small package. This in itself might be enough to exclude it from the possibilities. A further problem, if the actuator is a piezoelectric solution, is that piezoelectric actuators require voltages that can be rather large. This would require that the actuator be shielded to a great extent and could have some safety concerns.

The evaluations of each of the proposed solutions are shown in Table 2.2.

Table 2.2: Transmission Merit Comparisons

Solution	P	m	S	A	T	F	D	E	E	F	C	A	M	C	R	f	PS	PT	Score	
Bendable Tube w/internal sliding wire Axial	4	4	4	1	4	4	2	1	1	4	3	2	4	2	4	2	4	2	2.8	
Bendable Tube w/internal sliding wire Rot	4	4	4	1	4	4	2	1	1	3	2	2	4	2	4	2	4	2	2.67	
Linked Tube w/internal sliding wire Axial	4	3	4	1	3	4	2	1	1	2	1	2	4	2	4	2	4	2	2.4	
Linked Tube w/internal sliding wire Rot	2	2	4	1	3	4	2	1	1	2	1	2	4	2	4	2	4	2	2.2	
Resonant Beam Axial	4	3	4	2	1	4	4	1	4	4	4	4	4	4	4	4	4	4	3.4	
Resonant Beam Rot	4	3	4	2	1	4	4	1	4	4	4	4	4	4	4	4	4	4	3.4	
Resonant Horn	2	3	3	4	1	2	4	1	4	3	3	4	4	4	4	4	4	4	3.07	
Resonant Beam Inside tube w/rotating Head	1	2	2	3	2	2	3	2	4	1	1	1	3	4	4	4	4	4	2.33	
Rubber inside flexible tube	4	3	4	1	4	4	4	U	U	1	3	3	3	3	3	3	4	4	2.83	
Resonant Beam w/small flexible tube filled with rubber	3	3	4	1	3	4	U	U	U	1	3	3	3	3	3	3	4	4	2.83	
Resonant Horn w/small flexible tube filled with rubber	2	3	3	4	3	4	U	U	U	1	3	3	3	3	3	3	4	4	2.83	
Bellows Coupling Axial	2	3	3	2	3	3	4	3	1	2	2	3	1	4	1	4	1	4	2.47	
Bellows Coupling Rot	2	3	3	2	3	3	3	3	3	1	2	2	3	3	3	3	4	3	2.67	
Beam with rotational tip	2	3	4	1	2	4	4	2	4	3	2	4	2	4	2	4	4	4	3	
Rotating shaft	4	3	4	1	3	4	4	2	1	4	4	4	2	1	4	4	2	4	3.07	
Bendable Tube w/internal sliding wire on guides Axial	3	3	4	1	4	4	2	2	1	2	3	2	3	4	2	3	4	2	2.67	
Bendable Tube w/internal sliding wire on guides Rot	3	3	4	1	4	4	2	2	1	2	3	2	2	4	2	4	2	4	2.6	
Flexible Tube with electrical wires	4	4	4	1	4	4	4	4	1	4	4	4	1	4	4	4	2	4	3.47	
Flexible Tube with incompressible liquid	2	3	4	4	4	4	3	3	1	2	3	2	1	3	2	1	3	3	2.8	
Resonant Beam w/small flexible tube filled with incompressible liquid	2	3	4	4	4	3	4	3	3	1	2	3	2	1	3	2	1	3	4	2.8

2.3 Amplification Partial Function

2.3.1 Selection Criteria

The selection criteria were divided into two categories. The first set was used as a pass-fail evaluation. If the solution could not adequately meet the selection criteria, then it was eliminated from consideration. The second set of criteria included the first set as well as additional criteria, and was used to evaluate solutions on a merit basis. Values of 1-4 were assigned for each criteria and an average value calculated for each remaining solution. A subset of these same criteria was also used to evaluate solution augmentations (see Section 2.3.3).

2.3.1.1 Pass-Fail Criteria

This set of criteria is used to eliminate solutions from consideration if they could not sufficiently meet any one of the following:

Table 2.3: Definition of Pass-Fail Criteria

Criterion	Description
Gain Rating	the ability of the solution to gain up the output from the transducer.
Price	expected cost of a given solution. This is just an educated guess and is meant only to identify solution that might be too cost prohibitive at this early state of the project.
Volume/Size	a comparative number between the different methods proposed for a solution.
Ability to Amplify High Frequencies	since the frequencies in question are quite elevated for mechanical devices it is necessary that a particular solution allows for their amplification. This value is a measure of the proposed solution to perform this function.
Power Transmission Capability	this is a measure of how much power the solution can transmit before there is a danger of it failing.

2.3.1.2 Merit Criteria

Different methods of transmitting the power from the actuator and amplification section of the handpiece have been proposed and a set of criteria is chosen to evaluate the solutions. The criteria are in Table 2.4.

Table 2.4: Amplification Selection Criteria

	Criterion	Description
G	Gain Rating	the ability of the solution to gain up the output from the transducer
RR	Requires Resonance for amplification	a yes/no answer
P	Price	Expected cost of a given solution. This is just an educated guess and is meant only to identify solution that might be too cost prohibitive at this early state of the project.
m	Mass/Weight	a comparative number between the different methods proposed for a solution.
S	Volume/Size	a comparative number between the different methods proposed for a solution
AT	Ability to Amplify and Transmit	this number is a yes/no, four/one respectively.
D	Disposability	This is a measure of how easily a solution could be used as a disposable. At first thought, one might think that anything can be thrown away but certain items, for example batteries or devices with heavy metals, might have special considerations when they are disposed of.
E	Efficiency	this is a measure of how many losses are associated with the solution. Poor efficiency means loss of power and effectiveness as well as heat generation that could be uncomfortable or unsafe for the user or patient.
CA	Ability to Cut and Amplify	this is an evaluation whether or not the amplification section could be adapted to perform the cutting as well. This could be done by integrating a cutter onto the end of the amplification section.
M	Manufacturability	a quick stab at how easy it would be to realize a given solution. This was mainly base on the next item Complexity.
C	Complexity	a measure of how complicated the transmission section is in relation to parts count and tolerances.
R	Reliability	a measure of how long a device could be expected to work. This item also ties in with the complexity and manufacturability.
f	Ability to Amplify High Frequencies	Since the frequencies in question are quite elevated for mechanical devices it is necessary that a particular solution allows for their amplification. This value is a measure of the proposed solution to perform this function.
PS	User and Patient Safety	this value highlights any perceived issues that might need to be considered that concern patient or user safety.
PT	Power Transmission Capability	this is a measure of how much power the solution can transmit before there is a danger of it failing.

2.3.2 Proposed Solutions

Solutions proposed to solve the problem of transmitting the ultrasonic energy from the actuator/amplification section to the cutting section of the handpiece.

2.3.2.1 Resonant Horn

Description So named for a shape that resembles a horn, the resonant horn can be tapered or stepped. Gain is developed along the horn as a larger mass moves the smaller mass farther out along the horn. A gain of around 1 is realized up to the resonance of the horn where it can be 10 or larger. Figure 2.12 depicts a typical tapered horn. The taper can be exponential, conic, or stepped.

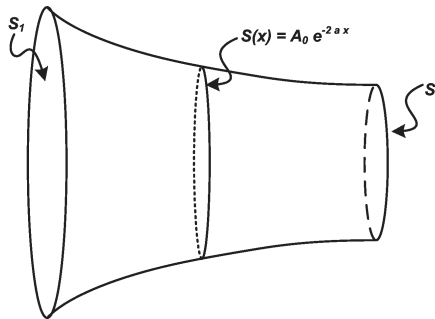


Figure 2.12: Resonant Horn

Remarks There is a reason that the resonant horn is used in many ultrasonic applications; it has low losses, high gain, is relatively easy to produce, has good frequency response, and has good power transmission capabilities. The cost is a little higher than some other solutions, but it would not be necessary to dispose of this portion of the handpiece if this solution is selected. Care must be taken to ensure that internal stresses in the horn design do not cause premature failure of the device. As horns can change frequencies as they age, it would be beneficial to have an adaptive drive algorithm that determines the required resonant drive frequency.

2.3.2.2 Expanding Ball

Description This solution consists of a ball that is driven from the backside by a driving rod. Attached to the surface are rods that transmit the ultrasonic energy to the cutting site. The solution requires that the drive mechanism pass through a stationary tube that is connected to the outside portion of the ball.

Remarks This solution is plagued with problems. Low gain, difficulty of production, reliability issues to name a few. It really has nothing to offer when compared to the other proposed solutions.

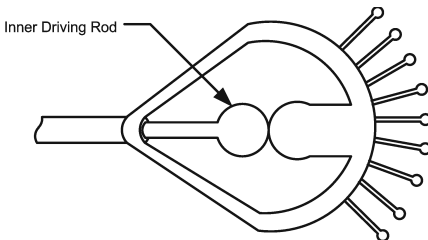


Figure 2.13: Expanding Ball

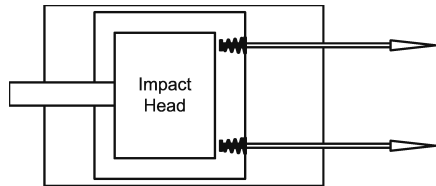


Figure 2.14: Impact Printer Concept

2.3.2.3 Impact Printer Concept

Description This solution consists of a mass that is driven into multiple impacts with a smaller cutting mass much the way that a dot matrix printer functions. Gain is provided by the impact of a large mass with the small mass of the cutter.

Remarks The impact can provide a large gain, but will most likely suffer from the inability to ensure that the cutter is always impacting the driving mass. This is especially true when the cutter is loaded. This solution also is not as attractive as some others because it would be harder to manufacture due to its increased complexity and the tolerances required ensuring that the transmission mass always impacts the cutting mass.

2.3.2.4 Scissored Beams

Description This solution consists of two beams fixed at a fulcrum. The beams are driven by a piezoelectric stack sandwiched between one end of the two beams. Gain is provided by the length of the beams and the location of the fulcrum. Beams would need to be bent back toward each other for better cutting.

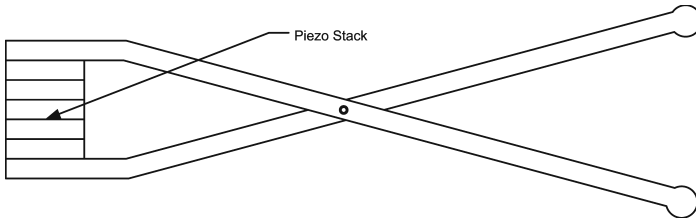


Figure 2.15: Scissored Beams

Remarks Volume and size as well as a limited ability to transmit high frequencies exclude this solution from consideration. Since the gain is determined by the length of the beams, they would have to be quite long. This lowers the natural frequency and reduces that ability to transmit high frequencies. This is not a good solution to the problem.

2.3.2.5 Pinching Fingers

Description Pinching fingers consists of fingers drawn together and driven with a ball from the rear that results in their expansion and contraction. The idea is that the material would enter between the fingers when they are open and be cut or pulled away as they close.

Remarks This is another solution that is plagued with problems. The gain associated with driving the fingers is less than one and a positive gain could only be realized with a resonant solution. This becomes very hard to do if there is contact with the other fingers. Also, manufacturing the fingers and ensuring that spacing is correct for pinching could be next to impossible. This solution would also suffer from large changes in output based on loading.

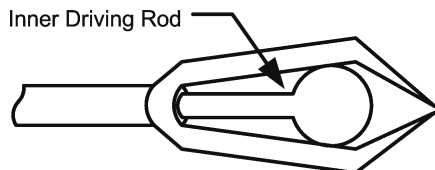


Figure 2.16: Pinching Fingers

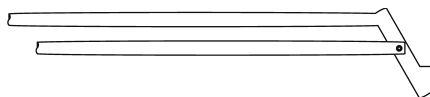


Figure 2.17: Cantilever Foot

2.3.2.6 Cantilevered Foot

Description This solution consists of a foot fixed at a fulcrum on the end of a stiff support. A piezo stack connected by a second stiff support drives one end of the foot. The other end of the foot is used for cutting. The gain is determined by the length of the foot and the position of the fixed stiff support that serves as a fulcrum.

Remarks This solution provides for gain without resonance but requires the foot to be long in order to get a suitable gain. It could also suffer from an inability to transmit high frequencies due to the required length of the foot and the length and cross section of the fulcrum support. Moving the fulcrum to the driving end of the foot could provide for a larger gain, but would require that the system be driven in resonance.

2.3.2.7 Rotational Lever

Description The rotational lever consists of a rotational actuator and a lever attached to the actuator. As the actuator turns, the lever moves roughly axially as the angle of movement is very small.

Remarks This solution has two shortcomings that should exclude it from the possibilities. The biggest problem is that it has to be long in order to get any gain. The actuator must already be fairly large to get a good amount of power and attaching a lever to an actuator that is already fairly large in diameter would make the handpiece too large. The solution also suffers from a low gain factor and with a longer lever the natural frequency will suffer. This will reduce the capacity to transmit high frequencies.

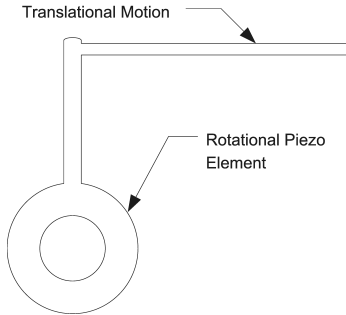


Figure 2.18: Rotational Lever

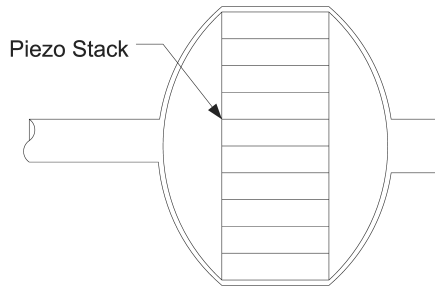


Figure 2.19: Bow Strain

2.3.2.8 Bow Strain

Description The Bow Strain is made up of a double bow inside which there is a sandwiched piezo stack, the bow strain amplifier provides for very large gains. The bow and piezo stack are located transverse to the motion of the driven transmission section.

Remarks It has been used quite successfully in many applications that require high gain in a relatively short distance. Several bows can be placed in series to increase the gain at the added cost of another piezo stack for each bow. One thing that might be problematic could be the manufacturing. It could be difficult to manufacture the bow and the piezo stack to match well, so that a good preload is ensured. This could result in a large variability between handpieces and the possibility that some would work and others would not. If the bow strain is chosen as the solution, these points should be addressed with a known solution in hand before continuing. One possibility would be to provide for a mechanism for manually setting the preload of the actuator, but this comes at the added cost of adjusting each one. It will be necessary to do this for all the piezo stacks used, so it might not be that big of a problem.

2.3.2.9 4 Bar Linkage

Description This solution consists of four bars fixed in such a manner that they flex in much the same way as the bow strain amplifier. The stack and the amplifier are also located transverse to the motion of the driven transmission section.

Remarks This solution provides for an overall good gain and good transmission characteristics. It suffers somewhat in manufacturability from a complexity and part tolerance standpoint. Any misalignment of the beams will cause degradation of the amplifiers performance.

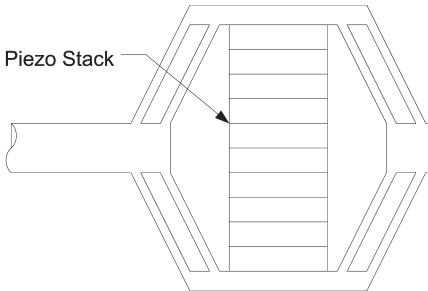


Figure 2.20: 4 Bar Linkage

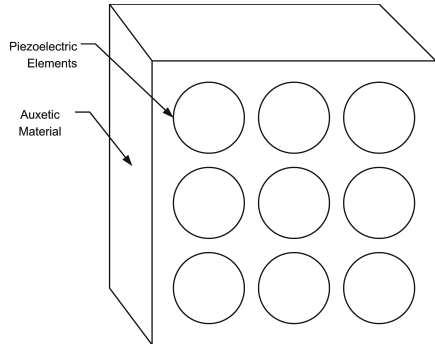


Figure 2.21: Molecular Scale Mechanical Amplifier

2.3.2.10 Molecular Scale Mechanical Amplifier

Description The Molecular Scale Mechanical Amplifier is a relatively new concept and relies on the strange properties of Auxetic materials. These are materials that expand instead of contract radially when subjected to axial tension. This solution would consist of a matrix of active piezo elements and Auxetic materials.

Remarks This solution has some very promising and exciting prospects. Materials have been found that are very rigid and have negative Poisson's ratios of -11 . This means that a gain of 11 could be obtained with a material that is even stiffer than the piezo element and very high frequencies could be achieved. The drawback is that the materials, nanotubes, are currently very hard to produce and cost in the neighborhood of \$30 per gram for the worst performing of the materials. As the materials are produced in bulk the price should come down and this might be a solution in the future. One thing of note is that by using electrodes made of Auxetic metals, of which there are many, a gain of two could be realized over a similar piezo stack with normal metal electrodes.

2.3.2.11 Bimorph Trimorph

Description The bimorph has been used extensively as an actuator. They consist of, as far as piezo actuators are concerned, of two thin piezo elements pressed together with an electrode in the middle. When the elements are supplied with power of opposite polarity, one shortens and the other lengthens so that a bending motion is produced.

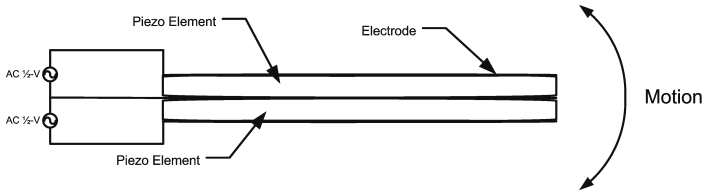


Figure 2.22: Bimorph Trimorph

Remarks Bimorphs provide high gain but at the expense of stiffness and natural frequency. This means that they are not a viable solution for this project.

2.3.2.12 Dual Fixed End Bimorph

Description This method uses two bimorphs with ends fixed to provide for axial actuation. Each bimorph is allowed to bend in opposite directions and, since their ends are attached, the bending provides for an axial movement.

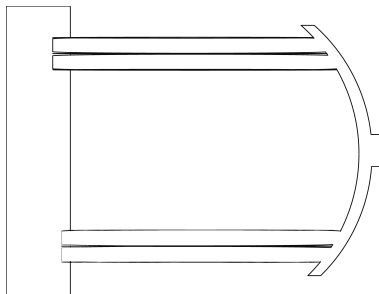


Figure 2.23: Dual Fixed End Bimorph

Remarks This solution suffers from the same problems that a single bimorph suffers: low stiffness and low natural frequency. This does not allow it to transmit high frequencies.

2.3.2.13 Hydraulic

Description A piezo stack drives a piston that forces liquid along a tapered or stepped channel. At the other end of the channel there is another piston that is driven by the liquid. The transmission section is connected to the second piston.

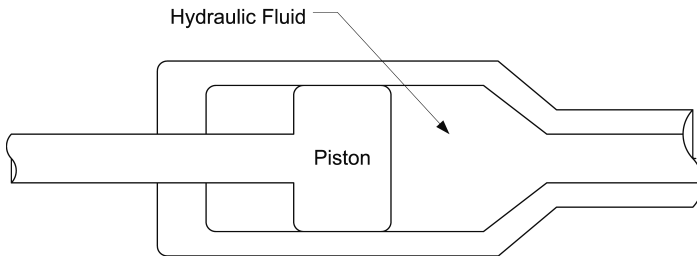


Figure 2.24: Hydraulic Amplifier

Remarks A hydraulic actuator is nice in that it can provide a high gain across a large frequency band. It does not suffer from the resonant frequency requirement of many mechanical actuators. Where it does have a problem is power transmission capabilities at smaller diameters. When the diameter is small a very high frequency, in the neighborhood of 500 kHz, is required to ensure that the liquid does not cavitate if any amount of power is to be transmitted. This frequency is well above what one could reasonably expect a handpiece to operate.

2.3.2.14 Integrated Lever

Description A L-shaped lever fixed at the short end of the L. A piezo stack pushes against the short length of the L causing the lever to rotate about the fixed point. Axial motion is provided at the end of the long section of the L, as the angle traversed is very small.

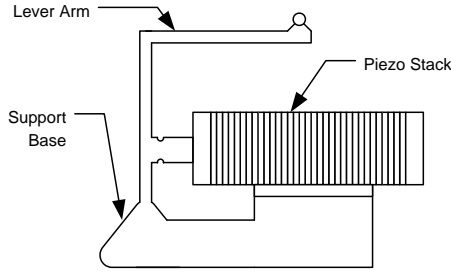


Figure 2.25: Integrated Lever

Remarks This solution has been used to great success in piezo actuator design and actuators of this type are readily available in a multitude of sizes and natural frequencies. A problem that results from the lever is a reduction in the natural frequency.

2.3.3 Solution Augmentations

2.3.3.1 Multiple Element Resonator

Description The Multiple Element Resonator consists of multiple piezo elements in series driven by the same power source.

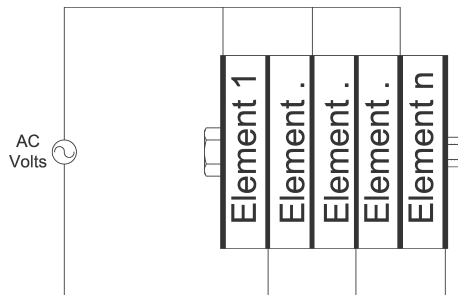


Figure 2.26: Multiple Element Piezoelectric Stack

Remarks This solution is a must for reducing the required voltage of the handpiece. Normally a deflection of a few microns, one must subject a piezo crystal to around 1000 V. With a multiple element stack the voltage can be reduced to 100 V or less because the electric field in each thinner element

nears the value a larger element would see with 1000 V. While the cost for the piezo stack makes disposability unattractive this portion of the handpiece can be kept, and the overall cost is not that high. This should be the basis upon which the rest of the handpiece is built.

2.3.3.2 Free Mass

Description This solution consists of a beam that extends from the amplification section of the handpiece to the cutting section. The beam could be solid or a hollow tube and have many different shapes. Ideally the beam would be driven at its resonant frequency. Inside or by some means a free mass constrained in the transmission section. This free mass is allowed to strike the transmission section in such a way that the normal ultrasonic cutting action is augmented by the impulse generated by the free mass impact.

Remarks This is a worthwhile pursuit for augmentation of the cutting action, but is not an overall solution for the amplification section. It is still required to agitate the free mass by some other means, which requires applying the ultrasonics and amplifying them. This solution could be lossy and could be done better by attaching the free mass with a spring or otherwise constraining the mass. For this see the next section 4.3 Constrained Mass.

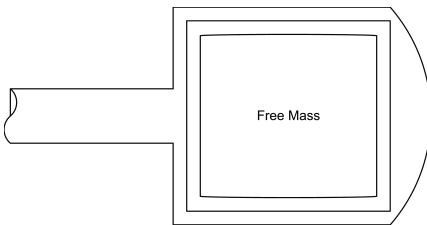


Figure 2.27: Free Mass

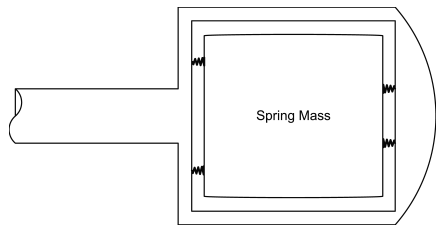


Figure 2.28: Constrained Mass

2.3.3.3 Constrained Mass

Description This augmentation solution is almost exactly the same as the previous, but differs in that the mass is suspended from the transmission section by a spring or other constraining mechanism. This allows the mass to move only in the direction of desired motion.

Remarks This has the added benefit over the free mass of lower losses and more predictable behavior.

2.3.4 Conclusions

An initial elimination of solutions was done using the following requirements: the necessity to transmit high frequencies, the gain, the volume and size, the cost, and the power transmission capability. Table 2.5 shows the results of this analysis.

Table 2.5: Pass Fail Solution Analysis

Solution	G	P	S	fp	PT	Score
Resonant Horn Exponential	1	1	1	1	1	1
Expanding Ball	1	1	1	1	1	1
Impact Printer Head	1	1	1	1	1	1
Scissored Beam	1	1	0	0	1	0
Pinching Fingers	0	1	1	1	1	0
Cantilevered Foot	1	1	0	1	1	0
Cam	1	1	0	1	1	0
Bow Strain	1	1	1	1	1	1
4 Bar Linkage	1	1	1	1	1	1
Molecular Scale Mechanical Amplifier	1	0	1	1	1	0
Bimorph Trimorph	1	1	1	0	1	0
Hydraulic	1	1	1	1	0	0
Dual Fixed End Bimorphs	1	1	1	0	1	0
Integrated Lever	1	1	1	1	1	1

Attractive prospects were the resonant horn, the multiple element tuned resonator, the bow strain amplifier, the 4 bar linkage, and the integrated lever actuator. The resonant horn had by far the best rating, but the bow strain, integrated lever, and 4 bar linkages show considerable promise and could prove interesting because they can provide for amplification without resonance. That means that over a broad range of frequencies they can produce a gained output. This could be particularly beneficial in selecting different tissues with the cutter. The drawback is that these amplifier sections are transverse to the direction of amplification and might require the handpiece to be wider than a longitudinal section.

Another interesting finding was the prospect of auxetic materials (Molecular Scale Mechanical Amplifier). Currently, there are no real solutions for the amplifier using these materials. They are far too expensive, but the use of

Auxetic metals as electrodes in the actuator could provide an additional gain of two for the piezo-stack.

These results suggest that the primary focus for the amplification section should be a resonant horn but that the bow strain, integrated lever, and 4 bar linkage designs should be investigated for amplifier design to see if they can match the performance of the resonant horn. If so, one of them could provide a better overall design.

Following the initial pass-fail elimination of solutions, the solutions were then graded using the merit criteria. A number from 1-4 was used to evaluate the solution against each criterion. Overall poor performance of the solution, measured by a score under 2.7 was used to exclude: the expanding ball, and the impact printer concept. Table 2.6 shows the results.

Table 2.6: Merit Comparisons of Narrowed Solutions

Solution	G	RR	P	m	S	AT	D	E	CA	M	C	R	fp	PS	PT	Score
Resonant Horn Exponential	4	Y	2	4	4	4	3	4	4	3	4	4	4	4	4	3.69
Expanding Ball	1	Y	2	3	3	1	3	3	1	2	2	2	3	4	4	2.54
Impact Printer Head	2	N	2	4	3	1	3	4	1	2	2	3	3	4	3	2.69
Bow Strain	4	N	3	4	4	1	1	3	1	2	3	4	4	4	4	2.92
4 Bar Linkage	4	N	3	4	4	1	1	3	1	2	2	3	4	4	4	2.77
Integrated Lever	4	N	3	4	4	1	1	4	1	3	3	4	2	4	4	2.92

One further item to consider is that cutting augmentation that can be provided by a free mass or a constrained mass, and by using multiple piezoelectric elements in the actuator (see Section 2.3.3).

By using a mass that is accelerated and allowed to strike the cutter or transmission section in the axial plane the cutting can be sped up especially through hard materials. The multiple-element tuned resonator is a must as it has the capacity to considerably lower the required handpiece voltage from thousands of volts to one hundred volts or less. Ratings for the augmentation solutions are in Table 2.7.

Table 2.7: Augmentation Solution Merit Analysis

Solution	G	P	m	S	D	E	M	C	R	fp	PS	PT	Score
Free Mass	2	4	4	3	4	1	3	3	4	4	4	2	3.17
Constrained Mass	2	3	3	3	4	3	3	3	4	4	4	3	3.25
Multiple Element Stack	3	2	4	4	1	2	3	3	4	4	3	4	3.08

2.4 Cutting Partial Function

The scope of this section is to discuss the results of a preliminary study of methods to cut with an ultrasonic surgical handpiece.

2.4.1 Selection Criteria

For the cutter function of the handpiece, it is necessary to separate the solutions into the following different functions: material removal, material shaping, and cutting.

- Material Removal - the primary function is to remove material as quickly as possible. This function would include any solution that will break large amounts of tissue up into small enough pieces to be removed quickly by suction or other means.
- Material Shaping - the function is to shape material. This includes roughing endplates or the removal of small amounts of material in a controlled manner, as to shape the endplate or spinal materials in preparation for an implant or other need.
- Cutting - the function is to cut material. This could be used to access the site of the operation, to clean up after other removal procedures etc.
- Cautery - this function is to cauterize material. This function can be used to control bleeding or seal vessels or other structures. It might be possible to close a disc after placement of nucleus replacement.

2.4.1.1 General Selection Criteria

Table 2.8 contains the criteria and definitions of all the cutting partial functions.

Table 2.8: Cutting General Selection Criteria

Criterion	Description
S	Size
f	Natural Frequency
D	Disposability
M	Manufacturability
PT	Power Transmission Ability

2.4.1.2 Function Specific Criteria

The following criteria in Table 2.9 are necessary to rate the different functions of the cutter. All solutions will be graded using the following as a means to identify solutions that might possibly used to perform more than one function.

Table 2.9: Cutting Function Specific Criteria

Criterion	Description
MR	Material Removal - the ability of the solution to breakup or vaporize material so that it may be removed quickly from the surgical site. This criterion is specific to the material removal solutions.
SE	Shaping effectiveness - the ability of the solution to shape spinal tissue and bone. This criterion is specific to the material shaping function.
CES	Cutting Effectiveness On Soft Tissue - the ability of the solution to cut through soft tissue quickly and effectively. The criterion is specific to the cutter cutting function.
CEC	Cutting Effectiveness On Coarse Materials - the ability of the solution to cut through coarse material quickly and effectively. While some solutions might do well with for soft tissue, they might have little or no effect on the disk annulus or bone. The criterion is specific to the cutter cutting function.
CA	Cautery - the ability of the solution to provide a cautery effect.

2.4.2 Proposed Solutions

Solutions proposed to solve the problem of cutting with the ultrasonic energy from the actuator/amplification and transmission section are presented.

2.4.2.1 Blade Tip

Description There is a simple blade with a tip which allows cutting. The blade can have different shapes, depending on the cutting manner. A blade with a tip is shown in Figure 2.29. The cutting is done only along an axis with an ultrasonic movement.

Another possible shape for the blade is like a knife as shown in Figure 2.29. The movement of cutting is also done in a single axis. It could also be possible to cut in other directions: horizontally, vertically and the combination of the two directions that is an elliptical movement.

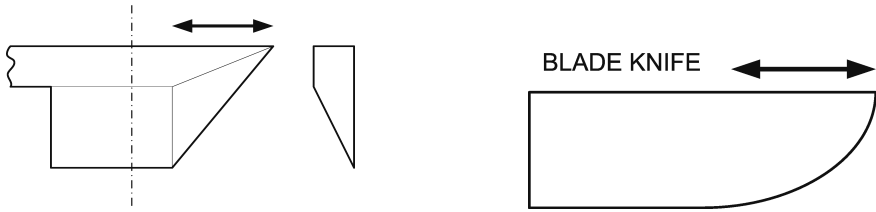


Figure 2.29: Simple Blade with a Tip and Knife Blade

Remarks These kinds of blades are useful to cut soft tissue but require some pressure on soft tissue to permit cutting. To cut harder tissue or bones, a rough or seriated blade would certainly be better. Wider blades can be used to provide some cauterizing effect while cutting so two functions can be realized at the same time.

2.4.2.2 Blade with Fixed Base

Description This solution is already in use in the market for cutting soft tissue. It consists of a blade that moves in contact with a fixed support. The fixed support allows local pressure to be applied to the tissue to cut, and provides protection for tissues that are below the base.

Remarks This solution has been used with great success for cutting and coagulating soft tissue. Usefulness will most likely be limited for cutting tougher tissues. The solution suffers from losses in movement that are dependent on the angle of the base, as the movement is transformed into two axes at the base. A variant could allow the base to move in one direction and the blade in the other thereby increasing the relative motion. Blade angle and shape variations allow for cutting and coagulating at the same time.

2.4.2.3 Blade Needle

Description A needle, as shown in Figure 2.31, can do a very accurate cutting with an ultrasonic movement. Transmission of the movement is done in a single direction that is the direction of the tip.

Remarks This can be a good solution for accurate cutting. The contact surface is not very big, so coagulation in soft tissue could be a problem. A hollow tip could be used for harvesting of hard materials for testing etc.

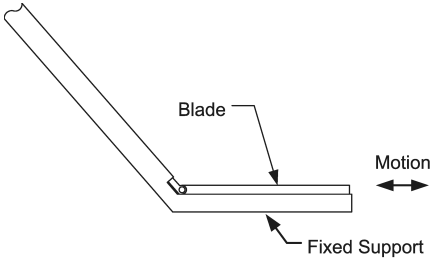


Figure 2.30: Blade with a Fixed Base

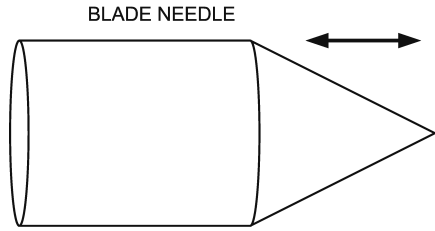


Figure 2.31: Needle Blade

2.4.2.4 Scissors Ball

Description The working principle is based on a pair of scissors as shown in Figure 2.32. A ball or similar structure could move horizontally, providing a vertical movement to the scissors. The vertical movement transmits to the cutting ends through a fixed point. This solution would provide a large amount of energy to a very small area and might facilitate the cutting of tougher materials. A problem would be getting the material into the shears to the cutting area.

Remarks The size of the cutter and drive mechanism could make a solution based on this problematic. This solution could provide some cautery effect depending on the shape of the blade.

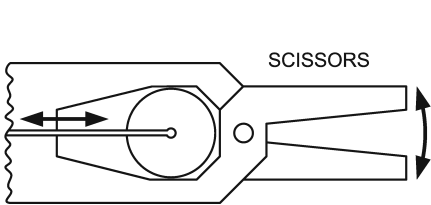


Figure 2.32: Scissors Ball

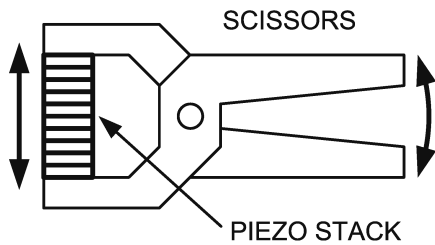


Figure 2.33: Scissors Piezo

2.4.2.5 Scissors Piezo

Description The working principle is always the pair of scissors. The difference with the preceding system is that the vertical movement is directly done

with a piezoelectric element.

Remarks The piezoelectric stack could preclude use in some cutting zones. This solution could provide some cautery effect depending on the shape of the blade.

2.4.2.6 Cavitation Jet

Description The cavitation jet generates a jet of cavitating water or liquid by means of ultrasonics that is directed out of the matching horn toward the tissue to be removed. The cavitation liquid enters the apparatus through the irrigation inlets, which can be pointed toward the cavitation generator and can be continuously supplied or pulsed.

Remarks The generator surface could be shaped to maximize the cavitation effect and provide a focal point for the cavitation beam. First harmonics could be used to generate the beam with second harmonics injected at intervals to cause a timed, simultaneous collapse of the cavitation bubbles. This could be done in a manner that would allow the bubble stream to reach the tissue before collapsing thereby exacting the largest effect on the target tissue. It might be necessary to have a short horn to get the material close to the generator. This solution could require a large amount of liquid in order to keep the generator supplied and functioning continuously and could be attractive for use in arthroscopy as large amounts of irrigation are typically supplied to the site anyway.

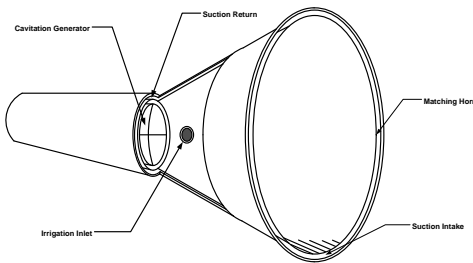


Figure 2.34: Cavitation Jet

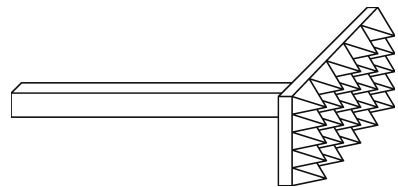


Figure 2.35: Multiple Pyramidal Cutter

2.4.2.7 Multiple Pyramidal Cutter

Description This solution consists of a flat head shaped with multiple pyramidal cutting extensions. The head would be driven longitudinally and could also benefit from rotational motion.

Remarks The raised tips might localize cutting energies and allow for easier material penetration. Holes could be made through the head at the intersections of the bases of the pyramids to allow material to pass through passively or by active suction. Irrigation could be supplied around the outside through a separate conduit.

2.4.2.8 Curved Shank Cutter

Description Consist of a cutter on a bent shaft. If driven at resonance the shaft will amplify the motion. The input shaft motion is longitudinal while the cutter motion will be elliptical.

Remarks The elliptical motion of the blade would tend to dig into the target material, which could assist in the cutting process. This solution has been employed by another manufacturer to cut bone in dental applications. The shape of the cutter can be varied to provide cutting and coagulation.

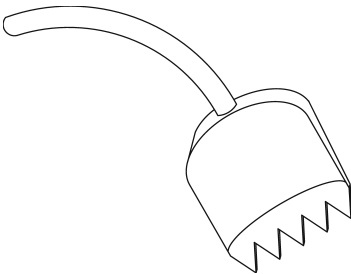


Figure 2.36: Curved Shank Cutter

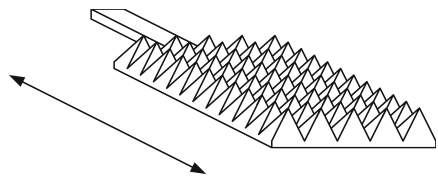


Figure 2.37: Rasp

2.4.2.9 Rasp

Description This cutter/shaper is very similar to the Multiple Pyramidal Cutter. The only real difference is the direction of motion.

Remarks This solution could be very interesting for shaping material and could take on many different shapes from that of a file to a very coarse rasp. This solution could be particularly interesting for shaping of the endplates after removal of the spinal disc.

2.4.2.10 Apposing Cutters

Description Consists of two apposing cutters driven at resonance by a longitudinal drive that is translated to a vertical/elliptical cut by the shape of the connecting rods and the blades.

Remarks This could provide the same kind of cut as the Curved Shank Cutter but allow a cut to be made straight into a hole with many different shapes that would depend only on the shape of the cutters and the motion. This would allow, for instance, the drilling of a square hole. The blades can be shaped in a manner that would cause them to have an elliptical motion, which would assist in boring operations.

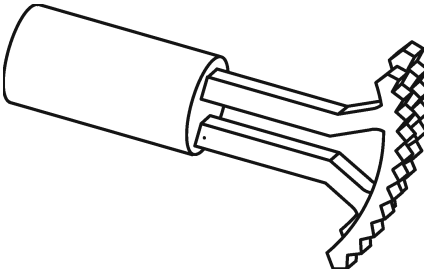


Figure 2.38: Apposing Cutters

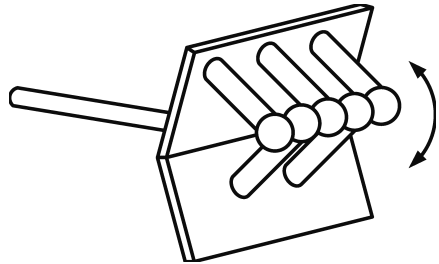


Figure 2.39: Apposing Cutters II

2.4.2.11 Apposing Cutters II

Description Apposing plates connected in a vee and driven in resonance by a connecting rod. The rods on the face of the vee move in opposite directions.

Remarks The cutter would cause local cavitation that might be augmented by the compression of the material caused by the rods moving in opposite directions. Some amplification will result from the rods being located out along the plates. The device shown in Figure 2.39 would probably not work that

well, as the two sides of the cutter would have different resonant frequencies. To have a better solution the two sides of the cutter should be matched in the number and size of the elements.

2.4.2.12 Resonant Tube

Description Consists of a tube driven horizontally and/or rotationally at resonance. The tube end could be sharpened or have teeth that would facilitate cutting.

Remarks One problem that this solution could have is that a tube of material could be cut and could still be connected to the surrounding tissue at the end and it might be necessary to pierce the material through both sides before it could be removed with suction or manually.

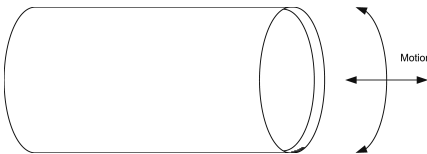


Figure 2.40: Resonant Tube

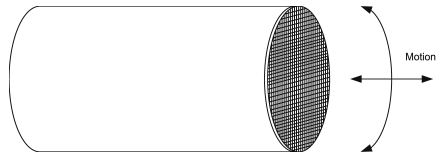


Figure 2.41: Resonant Tube with Sharpened Screen

2.4.2.13 Resonant Tube with Sharpened Screen

Description This is a version of the Resonant Tube that contains a screen in the end. The screen could be used to cut the material into smaller pieces while the rotational movement might cut the pieces off. The fragments could then be easily evacuated through the tube via suction. The size of the screen could be changed to keep the resonant frequency high or select different fragment sizes.

Remarks While this solution might solve the problems noted in the Resonant Tube it could be difficult to drive the entire screen at resonance as the length of the wires in the screen vary. A possible solution to this might be to use a square tube and make the members that make up the screen thicker.

2.4.2.14 Large Area Tip

Description The large area tip is a resonant tip that has a large contact area with the tissue.

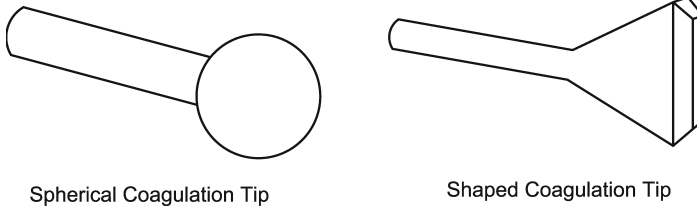


Figure 2.42: Large Area Tips

Remarks The goal is to cause localized coagulation. The tip could have many different shapes and sizes.

2.4.3 Solution Ratings

The cutting section of the handpieces must provide several functions and therefore the solution comparison tables were broken down by these functions. This allows for easy assessment of best of fit for a given function. The different functions considered are:

- Cutting - Soft Material
- Cutting - Coarse Material
- Material Removal
- Material Shaping
- Coagulation

Tables 2.10-2.14 show the comparisons of the different solutions based on the already defined criteria of Tables 2.8 & 2.9.

Each solution was assigned a weight from 1 to 4 for secondary criterion and a weight from 1 to 10 for a primary criterion.

Table 2.10: Cutting Solution Comparisons - Soft Material

Solution	S	f	D	M	MR	SE	CES	CEC	CA	PT	Mean
Blade Tip	4	4	4	4	2	1	6	2	3	2	3.2
Blade Needle	4	4	4	4	1	2	7	2	1	2	3.1
Blade with Fixed Base	3	3	3	3	1	2	8	1	3	2	2.9
Scissors Ball	2	2	2	2	1	1	8	1	3	2	2.4
Scissors Piezo	1	2	1	2	1	1	8	1	3	2	2.2
Curved Shank Cutter	4	3	4	4	3	3	5	3	3	3	3.5

Table 2.11: Cutting Solution Comparisons - Coarse Material

Solution	S	f	D	M	MR	SE	CES	CEC	CA	PT	Mean
Blade Tip	4	4	4	4	2	1	3	6	3	2	3.3
Blade Needle	4	4	4	4	1	2	2	2	1	2	2.6
Blade with Fixed Base	3	3	3	3	1	2	4	3	3	2	2.7
Scissors Ball	2	2	2	2	1	1	3	3	3	2	2.1
Scissors Piezo	1	2	1	2	1	1	3	3	3	2	1.9
Curved Shank Cutter	4	3	4	4	3	3	2	8	3	3	3.7

Table 2.12: Material Removal Solutions

Solution	S	f	D	M	MR	SE	CES	CEC	CA	PT	Mean
Cavitation Jet	3	4	3	2	9	1	3	3	1	4	3.3
Multiple Pyramidal Cutter	4	4	4	3	7	2	1	1	2	4	3.2
Apposing Cutters	4	4	4	3	4	2	1	1	1	3	2.7
Apposing Cutters II	2	3	4	2	4	2	1	2	2	3	2.5
Resonant Tube	4	4	4	4	5	1	2	2	1	4	3.1
Resonant Tube with Sharp-ened Screen	4	3	4	3	7	1	2	2	1	4	3.1

Table 2.13: Material Shaping Solutions

Solution	S	f	D	M	MR	SE	CES	CEC	CA	PT	Mean
Rasp	4	4	4	3	2	9	1	1	2	4	3.4

Table 2.14: Coagulation Solutions

Solution	S	f	D	M	MR	SE	CES	CEC	CA	PT	Mean
Large Area Tip	4	4	4	4	1	1	2	2	9	4	3.5

2.4.4 Conclusions

2.4.4.1 Cutting Solutions

Cutting solutions were broken into two different types: one that would function to cut soft tissue and the other to cut coarse. Soft tissue cutters could be added at a later date to help gain access to the disk area and provide an overall expansion of the product line to include all types of tissues.

For cutting of soft tissue, a simple blade seems to be the overall best solution, but it is not without some issues. In order for it to cut material some pressure must be supplied to the tissue to be cut, and this could result in a loss of control. A solution to this problem would be to use the blade with a fixed support. Some movement and maneuverability is lost but the trade off could be worth it.

For cutting of coarse materials the curved shaft cutter is an attractive solution. This method is already in the market for use in the dental industry and provides for very accurate cutting with minimal lateral tissue damage. Additionally, the cut bone tends to bleed less than if cut by other methods.

A look should also be taken at the ultrasonic needle. This could be an effective method for harvesting bone material for testing or if the needle is large enough, used to harvest bone for an implant somewhere else in the body.

2.4.4.2 Material Removal Solutions

Three solutions for material removal appear to be viable and should be given further study. These are the Cavitation Jet, the Multiple Pyramidal Cutter, and the Resonant Tube with Sharpened Screen.

The cavitation jet is a novel concept and will most likely require some prototypes for analysis. Most literature concerning the cutting effect produced by ultrasonics mentions the effect due to cavitation in the material. This method would take full advantage of this effect but introduces it at the surface of the tissue as a means to break it into small pieces. Cavitation is known to destroy steel impellers in pumps as well as destroy other very tough materials; so the application to the removal of biologic materials appears to be a logical step.

2.4.4.3 Material Shaping Solutions

Only one solution was considered for the function: the Rasp. Different shapes, degrees of roughness etc. could be used for different effects. This function

could be very interesting for use when the endplates need to be roughened or shaped after the disc has been removed.

2.4.4.4 Coagulation Solutions

Again only one solution was considered for this solution and that was the Large Area Tip. These tips could be made in different shapes and sizes to allow for different levels of coagulation.

2.4.4.5 Overall

Finally it should be stated that many of the proposed solutions will provide some level of results in secondary functions. This could allow for procedure specific cutters to be made that would allow a complicated series of steps to be done with fewer steps or provide a new procedure to be developed that might not be possible with current solutions.

2.5 Overall Conclusion

As an overall conclusion, the designed ultrasonic transducer used for the cutting of spinal disc material will be composed by a combination of one or several transmission partial function solutions, one or more amplification partial function solutions and different cutting partial function solutions; as is it can be seen in Figure 2.43.

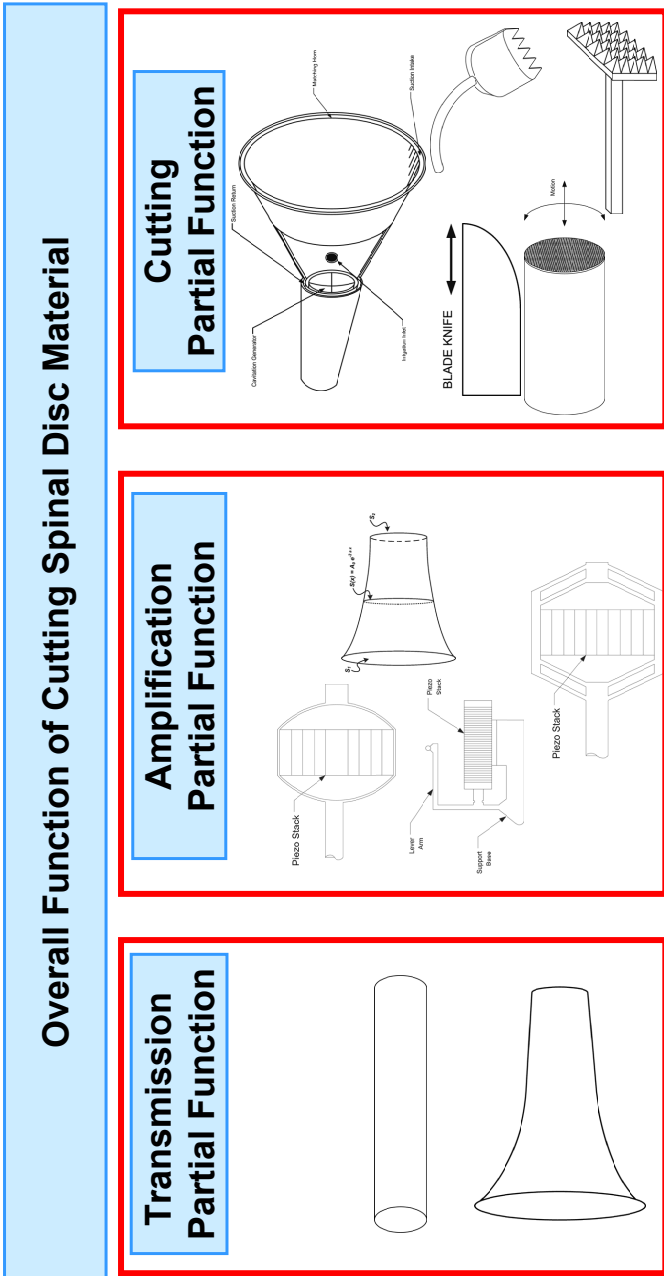


Figure 2.43: Combination of the Different Partial Function Solutions

Chap 3

Piezoelectrics and Waves

Summary

3.1	Elastic Material Properties	49
3.1.1	Elasticity Modulus E_Y	50
3.1.2	Poisson coefficient ν	50
3.2	Piezoelectricity Equations	51
3.3	Velocity and Wavelength	53
3.3.1	Wavelength	54
3.4	Numerical or Finite Element Equations	55
3.4.1	Elements	57
3.4.2	Analysis Types	58
3.5	Impedance and Admittance	59
3.6	Equivalent Circuit	59

3.1 Elastic Material Properties

A material has an *elastic behavior* if it takes back its initial dimensions when the effect of the applied forces stops. The elastic deformation is reversible. In the middle of the 17th century, Hooke stated that a deformation (mechanical strain, ϵ or S_{kl}) in an elastic body was proportional to the applied stress or constraint (σ or T_{ij}). In small deformations, the elastic behavior of most materials is approximately a linear relationship known as Hooke's law:

$$T_{ij} = c_{ijkl} S_{kl} \quad \text{with} \quad i, j, k, l = 1, 2, 3 \quad (3.1)$$

with

$$c_{ijkl} = \frac{\partial T_{ij}}{\partial S_{kl}} \quad (3.2)$$

From Equation 3.1 we obtain the following corresponding relation:

$$S_{ij} = s_{ijkl} T_{kl} \quad \text{with } i, j, k, l = 1, 2, 3 \quad (3.3)$$

The s_{ijkl} terms are called the *elastic compliance* coefficients.

3.1.1 Elasticity Modulus E_Y

The elasticity or Young's modulus E_Y is defined by the Hooke's law linking the axial stress σ to the relative resulting axial strain ϵ (Figure 3.1).

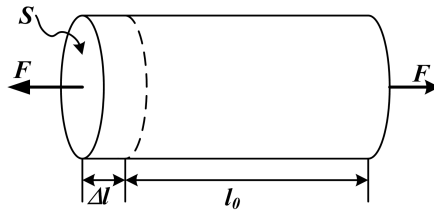


Figure 3.1: Young's Modulus Definition

$$E_Y = \frac{\sigma}{\epsilon} \quad \text{N/m}^2 \quad (3.4)$$

where $\epsilon = \frac{\Delta l}{l_0}$; $\sigma = \frac{F}{S} = E_Y \epsilon$ [N/m²] and $F = \left(\frac{SE_Y}{l_0} \right) \Delta l$ [N]

3.1.2 Poisson coefficient ν

The Poisson's coefficient ν is defined as the ratio lateral deformation to the longitudinal deformation ratio due to a stress applied in the longitudinal direction. In an isotropic body $\epsilon_x = \epsilon_y$. The extension in ϵ is defined positive and the shortening negative.

$$\nu = \frac{-\epsilon_x}{\epsilon_z} \quad (3.5)$$

3.2 Piezoelectricity Equations

Some dielectric materials have the following reciprocal relationships:

- they can be polarized under the action of a mechanical stress;
- in the absence of mechanical constraint, their dimensions are modified when they are polarized by the action of an external electrical field.

These properties constitute the *piezoelectricity* and the materials in which it appears are said to be piezoelectric.

The constitutive relationship of piezoelectric materials for linear behavior are:

$$T = c^E S - e E \quad (3.6)$$

$$D = e S + \epsilon^S E \quad (3.7)$$

or equivalently in a matrix form

$$\begin{bmatrix} T \\ D \end{bmatrix} = \begin{bmatrix} c^E & e \\ e & -\epsilon^S \end{bmatrix} \begin{bmatrix} S \\ -E \end{bmatrix} \quad (3.8)$$

It is also possible to write the piezoelectric equations in the following form:

$$S = s^E T + d^t E \quad (3.9)$$

$$D = d T + \epsilon^T E \quad (3.10)$$

where a description of all matrix variables used is shown in Table 3.1.

The elasticity or stiffness matrix c can be written directly in uninverted form c or in inverted form c^{-1} as a general anisotropic symmetric matrix:

$$c = \begin{bmatrix} c_{11} & c_{12} & c_{13} & c_{14} & c_{15} & c_{16} \\ & c_{22} & c_{23} & c_{24} & c_{25} & c_{26} \\ & & c_{33} & c_{34} & c_{35} & c_{36} \\ & & & \text{Symmetric} & c_{44} & c_{45} & c_{46} \\ & & & & & c_{55} & c_{56} \\ & & & & & & c_{66} \end{bmatrix} \quad (3.11)$$

Table 3.1: Piezoelectric Matrices

Symbol	Vector Size	Units	Definition
T	6 x 1	N/m ²	stress vector (also referred to as σ)
S	6 x 1	-	strain vector (also referred to as ϵ)
D	3 x 1	C/m ²	electric displacement (flux density) vector
E	3 x 1	N/C	electric field vector
s	6 x 6	m ² /N	compliance matrix (s^E evaluated at constant electric field or short-circuit)
c	6 x 6	N/m ²	stiffness matrix (c^E evaluated at constant electric field or short-circuit)
e	3 x 6	C/m ²	piezoelectric matrix relating stress/electric field (e^t transposed)
d	3 x 6	C/N	piezoelectric matrix relating strain/electric field (d^t transposed)
ϵ	3 x 3	F/m	dielectric permittivity matrix (ϵ^S evaluated at constant strain or mechanically clamped, ϵ^T at constant stress or mechanically free)

For the piezoelectric materials, the stiffness c reduces to the simplified matrix

$$c = \begin{bmatrix} c_{11} & c_{12} & c_{13} & & & \\ & c_{11} & c_{13} & & & \\ & & c_{33} & & & \\ \text{Symmetric} & & & c_{44} & & \\ & & & & c_{44} & \\ & & & & & c_{66} \end{bmatrix} \quad (3.12)$$

If the coefficient c_{66} is not available or not given by the manufacturer, it can be determined from the relation $c_{66} = (c_{11} - c_{12})/2$.

As the stiffness matrix is the inverse of the compliance matrix, they are linked by

$$c = s^{-1} \quad \text{then} \quad c \cdot s = s \cdot c = I \quad (3.13)$$

where I is the identity matrix.

The piezoelectric stress matrix \mathbf{e} relates the electric field vector \mathbf{E} to the stress vector \mathbf{T} and reduces to the following form with piezoelectric materials:

$$\mathbf{e} = \begin{bmatrix} e_{11} & e_{12} & e_{13} & e_{14} & e_{15} & e_{16} \\ e_{21} & e_{22} & e_{23} & e_{24} & e_{25} & e_{26} \\ e_{31} & e_{32} & e_{33} & e_{34} & e_{35} & e_{36} \end{bmatrix} = \quad (3.14)$$

$$= \begin{bmatrix} 0 & 0 & 0 & 0 & e_{15} & 0 \\ 0 & 0 & 0 & e_{15} & 0 & 0 \\ e_{31} & e_{31} & e_{33} & 0 & 0 & 0 \end{bmatrix} \quad (3.15)$$

The piezoelectric stress matrix \mathbf{e} can also be input as a piezoelectric strain matrix \mathbf{d} using the elasticity matrix \mathbf{c} :

$$\mathbf{e} = \mathbf{c}^E \cdot \mathbf{d} \quad (3.16)$$

The anisotropic dielectric matrix at constant strain ϵ^S is of the form:

$$\epsilon^S = \begin{bmatrix} \epsilon_{11}^S & \epsilon_{12}^S & \epsilon_{13}^S \\ & \epsilon_{22}^S & \epsilon_{23}^S \\ \text{Symm} & & \epsilon_{33}^S \end{bmatrix} = \epsilon_0 \begin{bmatrix} \kappa_{11}^S & \kappa_{12}^S & \kappa_{13}^S \\ & \kappa_{22}^S & \kappa_{23}^S \\ \text{Symm} & & \kappa_{33}^S \end{bmatrix} = \quad (3.17)$$

$$= \begin{bmatrix} \epsilon_{11}^S & 0 & 0 \\ & \epsilon_{11}^S & 0 \\ \text{Symm} & & \epsilon_{33}^S \end{bmatrix} = \epsilon_0 \begin{bmatrix} \kappa_{11}^S & & \\ & \kappa_{11}^S & \\ \text{Symm} & & \kappa_{33}^S \end{bmatrix} \quad (3.18)$$

where $\kappa^S = \frac{\epsilon^S}{\epsilon_0}$ is the relative permittivity and $\epsilon_0 = 8.854 \cdot 10^{-12}$ [F/m] the vacuum permittivity.

The dielectric matrix can also be input as a dielectric permittivity matrix at constant stress ϵ^T :

$$\epsilon^S = \epsilon^T - \mathbf{e} \cdot \mathbf{d}^t \quad (3.19)$$

3.3 Velocity and Wavelength

The propagation velocity v in a material depends on the Young's Modulus E_Y and density ρ ratio:

$$v = \sqrt{\frac{E_Y}{\rho}} = \sqrt{\frac{c_{11}^E}{\rho}} \quad \text{N/m}^2 \quad (3.20)$$

More generally, acoustic waves have velocity $(c^D/\rho)^{1/2}$ if a piezoelectric field is created parallel to the propagation direction; if not, the velocity is $(c^E/\rho)^{1/2}$.

3.3.1 Wavelength

Another important parameter often used is the wavelength λ where:

$$\lambda = \frac{v}{f} \quad \text{m} \quad (3.21)$$

The quarter wavelength $\lambda/4$ for the typical materials used in the project are shown in Figure 3.2 for metal materials and in Figure 3.3 for piezoelectric materials.

The ultrasonic frequency range used in the simulations goes from 20 kHz to 40 kHz in the left figures and from 20 kHz to 25 kHz in the right ones.

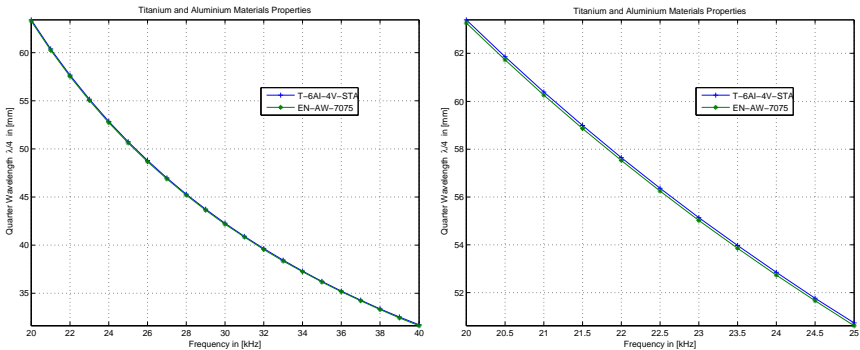


Figure 3.2: Quarter Wavelength $\lambda/4$ for Metal Materials Used

From the curves in Figure 3.2, the aluminium alloy and titanium alloy materials have almost the same wavelengths. At the frequency f of 22.5 kHz, the quarter wavelength $\lambda/4$ for aluminium alloy EN-AW-7075 is equal to 56.24 mm; and for the titanium alloy TI-6Al-4V-STA, $\lambda/4$ is 56.36 mm. A difference of 0.12 mm over the 56.24 mm represents a variation of 0.2%, which is not significant.

From the curves in Figure 3.3, the piezoelectric materials PZ-54 and PZ-28 have a variation of 5% in their wavelengths. At the frequency f of 22.5 kHz, the quarter wavelength $\lambda/4$ for PZ-54 is 33.95 mm; and for the PZ-28, $\lambda/4$ is 35.67 mm.

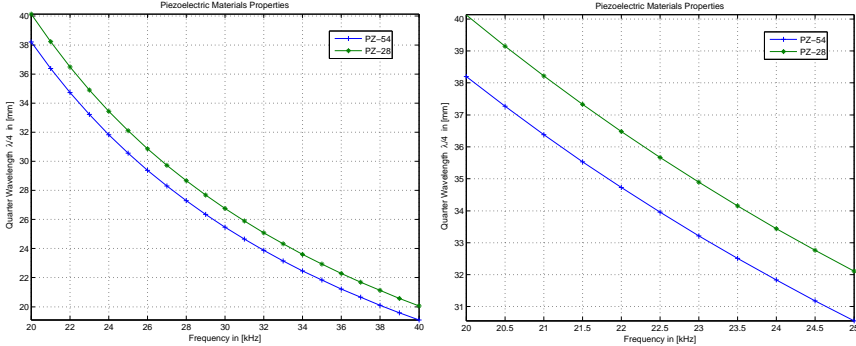


Figure 3.3: Quarter Wavelength $\lambda/4$ for Piezoelectric Materials

Mostly, when designing ultrasonic transducers, the length of the different parts is a half or quarter wavelength.

3.4 Numerical or Finite Element Equations

With FEA softwares, it can be considered that the general form of the relationship [9] between nodal loads, boundary conditions and reaction forces is

$$\{R\} = [K] \{u\} - \{F\} \quad (3.22)$$

with:

- $\{R\}$ reaction matrix
- $[K]$ stiffness matrix
- $\{u\}$ displacement matrix
- $\{F\}$ load matrix

The finite element discretization is performed by establishing nodal solution variables and element shape functions over an element domain which approximate the solution.

$$\{u_c\} = [N^u]^t \{u\} \quad (3.23)$$

$$V_c = \{N^V\}^t \{V\} \quad (3.24)$$

where:

- $\{u_c\}$ = displacements within the element domain in the x, y, z directions
- V_c = electrical potential within element domain
- $[N^u]$ = matrix of displacement shape functions
- $\{N^V\}$ = vector of electrical potential shape function
- $\{u\}$ = vector of nodal displacements
- $\{V\}$ = vector of nodal electrical potential

Expanding these definitions:

$$[N^u]^t = \begin{bmatrix} N_1 & 0 & 0 & \cdots & N_n & 0 & 0 \\ 0 & N_1 & 0 & \cdots & 0 & N_n & 0 \\ 0 & 0 & N_1 & \cdots & 0 & 0 & N_n \end{bmatrix} \quad (3.25)$$

$$\{N^V\}^t = (N_1 \ N_2 \ \cdots \ N_n) \quad (3.26)$$

where N_i is the shape function for node i

$$\{u\} = [UX_1 \ UY_2 \ UZ_3 \ \cdots \ UX_n \ UY_n \ UZ_n]^t \quad (3.27)$$

$$\{V\} = \left\{ \begin{array}{c} V_1 \\ V_2 \\ \cdots \\ V_n \end{array} \right\} \quad (3.28)$$

where n is number of nodes of the element.

Then the strain $\{S\}$ and the electric field $\{E\}$ are related to the displacements and the potentials, respectively, as:

$$\{S\} = [B_u]\{u\} \quad (3.29)$$

$$\{E\} = -[B_V]\{V\} \quad (3.30)$$

$$[B_u] = \begin{bmatrix} \frac{\partial}{\partial x} & 0 & 0 \\ 0 & \frac{\partial}{\partial y} & 0 \\ 0 & 0 & \frac{\partial}{\partial z} \\ \frac{\partial}{\partial y} & \frac{\partial}{\partial x} & 0 \\ 0 & \frac{\partial}{\partial z} & \frac{\partial}{\partial y} \\ \frac{\partial}{\partial z} & 0 & \frac{\partial}{\partial x} \end{bmatrix} \quad (3.31)$$

$$[B_V] = \left\{ \begin{array}{c} \frac{\partial}{\partial x} \\ \frac{\partial}{\partial y} \\ \frac{\partial}{\partial z} \end{array} \right\} \{N^V\}^T \quad (3.32)$$

After the application of the variational principle and finite element discretization [2], the coupled finite element matrix equation derived for a one element model is:

$$\begin{aligned} & \begin{bmatrix} [M] & [0] \\ [0] & [0] \end{bmatrix} \begin{Bmatrix} \{\dot{u}\} \\ \{\ddot{V}\} \end{Bmatrix} + \begin{bmatrix} [C] & [0] \\ [0] & [0] \end{bmatrix} \begin{Bmatrix} \{\dot{u}\} \\ \{\dot{V}\} \end{Bmatrix} + \\ & + \begin{bmatrix} [K] & [K^z] \\ [K^z]^t & [K^d] \end{bmatrix} \begin{Bmatrix} \{u\} \\ \{V\} \end{Bmatrix} = \begin{Bmatrix} \{F\} \\ \{L\} \end{Bmatrix} \end{aligned} \quad (3.33)$$

where a dot above a variable denotes a time derivative. The following equations provide an explanation of the submatrices in Equation 3.33:

3.4.1 Elements

In ANSYS, some elements have the piezoelectric capability. These elements are said *coupled-field* because they intermix the displacements UX, UY, UZ solutions with the electric charge reaction VOLT solution. Table 3.2 summarizes the different available elements for piezoelectric analysis.

Table 3.2: Piezoelectric Capability in ANSYS Elements

Element	2D or 3D	DOFs	Nodes	Shape
PLANE13	2D	UX, UY, VOLT	4	quadrilateral
PLANE223	2D	UX, UY, VOLT	8	quadrilateral
SOLID5	3D	UX, UY, UZ, VOLT	8	brick
SOLID98	3D	UX, UY, UZ, VOLT	10	tetrahedron
SOLID226	3D	UX, UY, UZ, VOLT	20	brick
SOLID227	3D	UX, UY, UZ, VOLT	10	tetrahedron

There are 2D elements or 3D elements where the calculations can be done at different nodes. At each node the UX, UY, UZ and VOLT solutions are calculated. The different shapes for the 2D elements are shown in Figure 3.4 and the shapes available for the 3D elements in Figure 3.5.

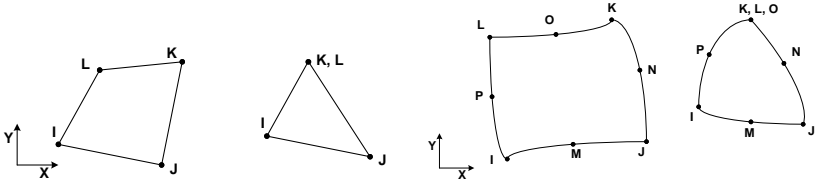


Figure 3.4: Piezoelectric 2D Elements

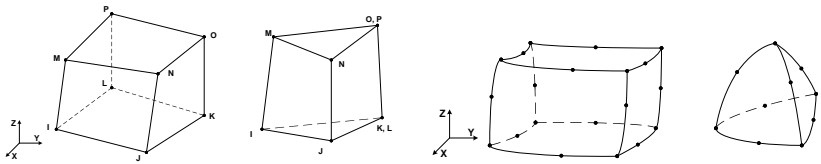


Figure 3.5: Piezoelectric 3D Elements

3.4.2 Analysis Types

Different types of analysis can be done in ANSYS. The main analysis methods used in this project are the *static*, *modal* and *harmonic* analysis.

A static analysis calculates the effects of steady loading conditions on a structure, while ignoring inertia and damping effects, such as those caused by time-varying loads. Static analysis determines the displacements, stresses, strains, and forces in structures or components caused by loads that do not induce significant inertia and damping effects.

Modal analysis is used to determine the natural frequencies and mode shapes of a structure. The natural frequencies and mode shapes are important parameters in the design of a structure for dynamic loading conditions. They are also required if you want to do a spectrum analysis or a mode superposition harmonic or transient analysis.

Any sustained cyclic load that varies sinusoidally (harmonically) with time (as does the piezoelectric stack in this work) will produce a sustained cyclic response (a harmonic response) in a structural system. Harmonic response analysis gives the ability to predict the sustained dynamic behavior of the structures, thus enabling verification of whether or not the designs will successfully overcome resonance, fatigue, and other harmful effects of forced vibrations.

3.5 Impedance and Admittance

The *electric current* I is defined as the flow of accumulated charges Q through a conductor. When considering a harmonic analysis, i.e. the charges vary sinusoidally, the electric current and the accumulated charges are related by

$$I = \frac{dQ}{dt} = j \omega Q = j 2 \pi f Q \quad \text{A} \quad (3.34)$$

where $\omega = 2\pi f$ is the operating frequency.

Admittance Y is calculated as I/V_a where V_a is the applied potential (voltage).

$$Y = \frac{1}{Z} = \frac{I}{V_a} \quad \Omega \quad (3.35)$$

3.6 Equivalent Circuit

A piezoelectric ceramic element exposed to an alternating electric field changes dimensions cyclically, according to the frequency of the field. Every ceramic element has a unique frequency, or resonance frequency f_r , at which it vibrates most readily in response to the electrical input, and most efficiently converts the electrical energy input into mechanical energy. At this resonance frequency f_r , the behavior of the element can be described by the equivalent electrical circuit in Figure 3.6.

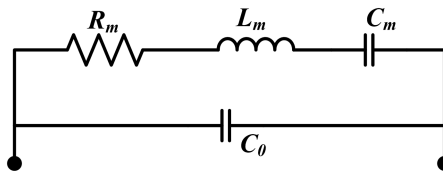


Figure 3.6: Equivalent Circuit

- C_0 = (capacitance of transducer below f_r) - (capacitance C_m)
- C_m = capacitance of mechanical circuit
- L_m = inductance of mechanical circuit
- R_m = resistance caused by mechanical losses

Chap 4

Optimization Methods

Summary

4.1	Complete Output Mapping	62
4.2	Response Surface Methods	62
4.3	Gradient Methods	63
4.3.1	Pseudo-Gradient Method	64
4.3.2	Other Search Techniques	64
4.4	Genetic Algorithms	64
4.4.1	Main Concepts	65
4.4.2	Constraints and Convergence Problems	69
4.5	Basic and New Genetic Algorithms	70
4.5.1	Preliminary Considerations	70
4.5.2	Basic Algorithm	71
4.5.3	Conditional Genetic Operators	72
4.5.4	Crossover Rules and Integrated Local Search	73
4.5.5	Combination of Both Improvements	75
4.6	Test Functions	77
4.6.1	Algorithms Comparison	78
4.6.2	Algorithms Testing	79
4.6.3	Population and Children Size	81
4.7	MATLAB and ANSYS Implementation	82
4.8	Conclusion	83

Different methods have been implemented and tested in order to optimize a given problem when a maximum or a minimum has to be found. Some methods have already been explained and used to optimize the analytical the complete piezoelectric transducer model [12]. The considered methods are mentioned without going into details.

The development of an optimization method requiring less simulations is desired. The main problem with FE simulations is the calculation time of a single new geometry (time is spent in creating the geometry mesh that includes all the nodes; and to calculate the desired solution). A new genetic algorithm is developed based and tested in order to use it in the further step of full FE optimizations.

4.1 Complete Output Mapping

As said in [12], the simplest and most straightforward optimization method is to perform a complete mapping of all possible combinations of input parameters to the system and then choose the combination that comes closest to the desired result. The drawback of this method is the increasing number of tests with the number of parameters.

4.2 Response Surface Methods

Another considered method [5, 12] is the Design of Experiments (DoE) methodology that can be used for a system optimization.

The most common plan of experiments consists in varying one single parameter at time. This simple plan does not take into account the interactions between the parameters. The benefit of the *factorial plans* in comparison to classical plans (one parameter at a time) resides in that all the parameters are simultaneously varied, and in a structured manner.

To explore the experimental space of N parameters (or factors) and two levels, it is necessary to run 2^N experiments (e.g. with $N = 10$ parameters, $2^{10} = 1024$ experiments needed). With factorial plans, it is evident that the trials grow exponentially and that is the reason why these plans become quickly very time consuming and unworkable.

To predict the response of a system in a determined region of an experimental domain, where no experiments have been carried out, it is necessary to do trials distributed over the full domain. For that purpose, an empirical model has to be used that is often called the *response surface*. In an optimization approach of a system, the Doehlert plan is a good candidate that has been satisfactory used and described by Fernandez Lopez [5].

Nevertheless, as already said, the response surface methods are well-suited for problems with few degrees of freedom (DOF), parameters or variables to be optimized.

4.3 Gradient Methods

In the classic theory of maxima and minima, as shown in Figure 4.1 with one parameter, $y = f(x)$ represents the solution of the system to be optimized. The f function describing the behavior of the system can be analytical or not. The solution y can have one or more maxima (respectively minima) corresponding to points where $\partial f / \partial x = 0$ that are called *local maxima* (respectively *local minima*). The biggest local maximum is called the *global maximum* (respectively the *global minimum*).

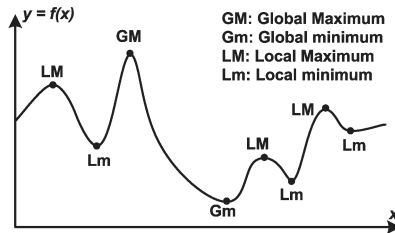


Figure 4.1: Local and Global Maxima or Minima

When considering a set of n parameters and $\{x_1, x_2, \dots, x_n\}$ the values for each parameter, the system is defined by the function $f \equiv f(\mathbf{x}) = f(x_1, x_2, \dots, x_n)$. In the case that $f(\mathbf{x})$ is determined experimentally (or may be the results of FE simulations), a discrete approximation to the gradient ∇f is used.

$$\nabla f(\mathbf{x}) = \frac{\partial f(x_1, x_2, \dots, x_n)}{\partial x_i} \quad \text{for } i = 1, \dots, n \quad (4.1)$$

The search of stationary solutions (local maxima or minima) in a multidimensional space leads to solve the gradient identity $\nabla f(\mathbf{x}) = 0$.

4.3.1 Pseudo-Gradient Method

The *pseudo-gradient* method that has been developed and described by Murphy [12], has also been satisfactory used with the complete analytical model of the studied piezoelectric ultrasonic transducer.

The pseudo-gradient is a trick used to reduce the number of terms involved in the gradient calculation. The procedure uses an initial coordinate in the system parameter space and an experimental plan around the point to calculate the pseudo-gradient. A normalization is done against its largest term and scaled by a factor α . This allows the application of a known step size to the parameter with the greatest effect on the output. The normalized numerical gradient is added to the current coordinate \mathbf{X}_c to find a new coordinate \mathbf{X}_n .

Faster algorithms can be developed by eliminating the cross and squared terms involved in the pseudo-gradient calculation. The accuracy of the gradient is reduced but with a small step size this compromise can work nicely.

4.3.2 Other Search Techniques

Murphy [12] has improved the pseudo-gradient method by randomly choosing a point of departure. Incorrect representation problems of the real surface due to step sizes that are too large have also been overcome.

An unlimited number of search techniques can be developed and imagination is the only limitation to find ingenious features.

4.4 Genetic Algorithms

The *genetic algorithm* (GA) is a search method used to optimize mathematical or engineering quite complicated problems (that can be constrained or not), and often multidimensional [3, 13, 16].

GA repeatedly modify during successive generations a population of different sub-optimal solutions of a given problem. The *selection* process consists in keeping a number of individuals of the current generation, depending on some criteria, and produces children for the next generation. Over successive

generations, the population evolves toward an optimal solution. The *fitness* function evaluates, for a given solution, its degree of optimality; the evaluation of this function is essential to the selection process. The *fitness* must not to be mistaken for the *objective* function.

Interestingly enough that GA can be applied to particular optimization problems, in which some discontinuity or differentiability problems could appear. GA can be applied to problems with many degrees of freedom (DOF), to which DoE methods (Sec. 4.2) do not give satisfactory enough results.

4.4.1 Main Concepts

GA work under some main common concepts as summarized in Figure 4.2.

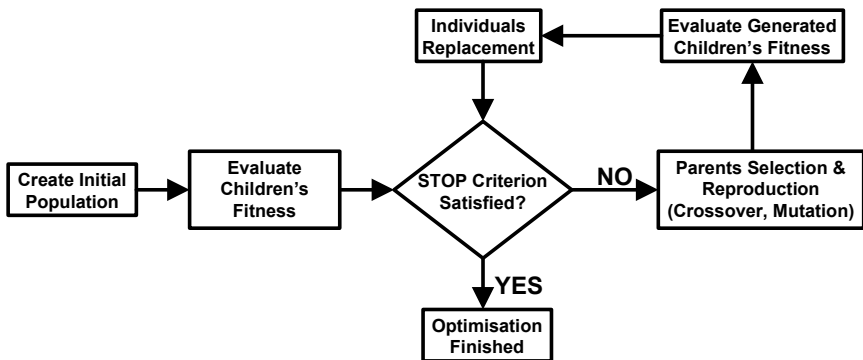


Figure 4.2: Schematic Representation of a Basic GA

It is worth remembering that FE simulations with ANSYS software are time consuming operations. The evaluation of an individual implies the building of the geometric model, meshing and finding a solution for each node of the meshed geometry. So, the *fitness* function evaluation of a population or the fitness evaluation of the generated children are operations very costly in computer calculation time.

An interesting propriety of the GA is their modularity particularity. In other words, many parts are independent of the others and can be, at least partially, considered and improved separately. For example, it is possible to modify the selection process of an algorithm while keeping the reproduction strategy.

4.4.1.1 Individual Representation

Within the framework of GAs, an individual $\mathbf{X} = (X_1, \dots, X_p)$ corresponds to one solution of a given problem. The individual includes in his phenotype the data of the different parameters that specify that solution.

As an example, with a multivariable function $f(X_1, \dots, X_p)$ to be optimized, an individual contains the information of p variables X_i . Another example is the traveling salesman problem [10], where the information corresponds to the round-trip route that visits each city exactly once and then returns to the starting point.

The information contained in each parameter can be represented in different ways, e.g. in a binary mode sequence of values or with real values. The representation type is called *genotype* or *genome*.

$$\mathbf{X} = (X_1, X_2, X_3, \dots, X_p) \quad (4.2)$$

$$\equiv (0, 1, 1, \dots, 1) \quad \text{Binary Genotype} \quad (4.3)$$

$$\equiv (2.3, 105, -52.6, \dots, 0.7) \quad \text{Real Values Genotype} \quad (4.4)$$

The choice of representation type (chromosomes or genotype of the genome) of candidate solutions (individuals, creatures or phenotypes) is important due to its direct and sometimes deciding effect on the used algorithms. Some papers [14] deal with this kind of accurate cases problems.

4.4.1.2 Initial Population

The initial population, to be evolved toward more optimal solutions, is composed by N individuals $\mathbf{X}_1, \dots, \mathbf{X}_N$ from the search space.

The individual distributions in the search space is frequently an uniform probability law, without any justification. However, as shown in [8], this choice is reasonable and comparable to other solutions.

4.4.1.3 Fitness Function vs Objective Function

The *fitness function* aims to quantify, with a real value, the quality of an individual in the given population, in particular envisioning its selection.

The *objective function* $f(\mathbf{X})$, quantifies, as well with a real value, the criterion to optimize (the criterion is frequently defined in such a way that the problem becomes a maximization or minimization problem).

In order to select optimal individuals, the *fitness* function value (simply called *fitness*) of an individual can be the same as the objective function value.

Nevertheless, the two functions have not to be mistaken; indeed, their values are not always identical, in particular in optimization problems with constraints (Section 4.4.2.1). The *fitness* of a single individual, in certain cases, can even depend on the objective function value of other individuals [7].

4.4.1.4 Parents Selection Rules

The individuals X_i of a given population undergo a selection, with intent to reproduce and then generate children (a new generation) that will replace all or only a part of the current generation population.

There are some selection methods or rules, all based on the *fitness* value of the individuals:

1. proportionate selection (or roulette-wheel selection)
2. rank selection
3. tournament selection
4. ...

4.4.1.5 Parents Reproduction Rules

In order to generate a second generation population of solutions, the selected parents combine its genetic material to generate a determined number of children (usually an even number).

Traditionally, an analogy is aptly done about biology (sexual reproduction), in which each child is the breeding from two parents. However, it is not always the case [1].

Traditionally also, a child is the result of a *crossover* between the genetic material of the two parents followed by a *mutation* (applied with a certain probability).

Crossover Rules Chromosomal *crossover*, is a phenomenon that occurs during meiosis and consists in pairing up and exchanging sections of DNA of two homologous chromosomes.

In GA, given that each individual has one single chromosome, the *crossover* operation from two parents generates each time two children for the next gen-

eration.

The *crossover* may be applied with different techniques that can be:

1. uniform crossover
2. arithmetic crossover
3. one-point crossover
4. two-point crossover
5. ...

As an example, the one-point crossover and the two-point crossover are represented in Figure 4.3.

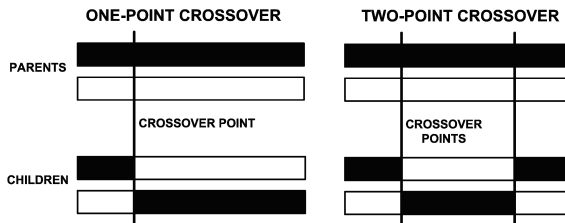


Figure 4.3: One-Point and Two-Point Crossovers

The type of *crossover* is related to the individual representation type; the *arithmetic crossover*, e.g. is related to a representation with real values.

For each position of two chromosomes of parents (X_1, X_2), the *uniform crossover* consists in reversing the values of the two corresponding p variables with a probability $1/2$, as can be shown in Figure 4.4.

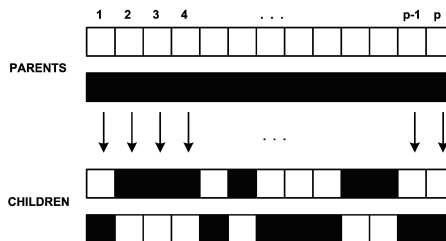


Figure 4.4: Uniform Crossover

For each variable or allele, the *arithmetic crossover* consists in the simple average of the values in the two current chromosomes.

Mutation Rules *Mutation* consists in modifying randomly a number of components of the individual genome $\mathbf{X}_1 = (X_{1,1}, X_{1,2}, \dots, X_{1,\rho})$. This operator is used to maintain a genetic diversity form one generation of population to the next generation.

Once again, the definition of a mutation operator is related to the representation type.

4.4.1.6 Replacement Strategy

The replacement strategy defines the manner in which the children, that are the individuals of the next generation, are inserted in the population.

A *total replacement* consists in a full replacement of the old population by the generated children.

A *reverse replacement* consists in replacing the k worst individuals of the old population by the k best children, with $k < N'$, N' is number of children.

4.4.1.7 Stop Criterion

A *stop criterion* defines a condition that, when satisfied, ends the running of the GA.

The stop criterion is often related to the number of iterations (maximum number of generations reached), the time or a convergence of the solution.

A useful stop criterion to compare the performance of many algorithms consists in fixing a maximal number of objective function evaluations [7].

4.4.2 Constraints and Convergence Problems

4.4.2.1 Optimization with Constraints

Some optimization problems are constrained. We just mention that the problems have been treated.

$$F(\mathbf{X}) = \begin{cases} f(\mathbf{X}) & \text{if } x \text{ satisfies the constraints} \\ f_{max} + \sum_{j=1}^m v_j(x) & \text{else} \end{cases} \quad (4.5)$$

with

$$v_j(x) = \max\{0, g_j(x)\} \quad (4.6)$$

4.4.2.2 Premature Convergence and Population Diversity

The premature convergence problem may occur when the function to optimize has many local minima. In that case, it is possible that the chosen algorithm converges quickly towards a local optimum which is different from the global maximum without taking into account the surrounding search domain.

In GA, the premature convergence is represented by a population of individuals in which the diversity quickly becomes very low. Even though the notion of diversity is relatively intuitive, it can be strictly defined as:

$$D = \frac{2}{N(N-1)} \sum_{i=1}^{N-1} \sum_{j=i+1}^N \frac{\|X_i - X_j\|}{\|a - b\|} \quad (4.7)$$

with X_i an individual, and a and b the lower and upper boundaries of the elements of X .

The diversity notion is very close to the convergence, as well as the exploration of the search domain of solutions.

Next Section 4.5, treats the case of that kind of problematic more in details.

4.5 Basic and New Genetic Algorithms

4.5.1 Preliminary Considerations

In order to find more successful algorithms, it is important to specify some determining criteria during the GA implementation; and there are the different assumptions done:

1. Mathematically, GA aims to find an individual $X = (X_1, \dots, X_p)$ with p parameters to be optimized such that an objective function $f(X)$ is minimized or maximized. It is easy to reduce a maximization problem to a minimization problem by doing a sign change.
2. Most of the time in a *run* (launch the algorithm until the convergence criterion is satisfied) is spent in evaluating the objective function. Calculation time due to the more or less algorithm complexity is considered negligible compared to the time spent in doing a complete FE simulation in FEA software.
3. An algorithm is considered more effective than others if the results obtained are on average (over many *runs*), higher in the same running time.

4. The determinant criterion retained for evaluating the effectiveness of an algorithm is the ratio between the solution value and the number of objective function evaluations.
5. If the number of objective function evaluations is in the order of ten thousand evaluations, and a FE simulation takes 5 seconds, a complete run will last 13 hours 53 minutes and 20 seconds.

The formulated assumptions provide a basis for the comparison of different GA's, while the number of objective function evaluations is limited by the calculation time spent for each simulation.

4.5.2 Basic Algorithm

The basic GA (*GAObasic*) implemented is based on [13].

The main concept of the algorithm is summarized in Figure 4.2, and is presented in the following manner, with the parameters values used in [13] shown between brackets:

- Step 1** Generate a population of N individuals ($N = 20$) and evaluate their *fitness*.
- Step 2** Select two parents with a selection rule (as tournament), the same parent is never selected twice.
- Step 3** Generate $N' \leq N$ children (N' even) from the two parents, with a probability P_c that an individual had a *crossover* ($P_c = 0.8$). Then, each allele of the N' children has a probability P_m to undergo a mutation ($P_m = 0.5$).
- Step 4** Evaluate the *fitness* of the children.
- Step 5** Reverse replacement: the best $R \cdot 100\%$ children replace the worst individuals of the current population ($R = 0.9$). Return to **Step 2**.

This algorithm represents the individuals with real values, which is kept with all algorithms the following.

Initially, the individuals are generated with a uniform probability law. The crossover operator is the *uniform crossover*, and the mutation operator for a component is the addition of a random value following a normal gaussian distribution.

4.5.3 Conditional Genetic Operators

The main problem with *GAbasic* is that the probability values of P_c and P_m have to be determined experimentally (trial-and-error) given that the values returning the best results may be different in each new case.

If the probability P_m is too low, a premature convergence may occur (i.e. exploration of the search domain not satisfactory). Conversely, if P_m is too high, the local search capacity may be reduced (i.e. exploitation of the search domain not satisfactory). The probability P_c also has an important effect on the domain search exploration quality.

The working principle of *conditional genetic operators* [15] is to avoid using hard to find probabilistic parameters, and instead using conditioned operators by an objective measure of the population diversity. The used measure is called the *difference-degree* d_i .

A minimal *difference-degree* $D_s \in]0; 1[$ is imposed at the beginning, that avoids a premature convergence and ensures some exploration of the domain search. The imposed diversity reduces progressively during the generations, that allows a more and more local search, however controlled.

The algorithm *GAO*i*1* based on [15] is presented:

- Step 1** Generate a population of N individuals and evaluate their *fitness*. Define a minimal $D_s \in]0; 1[$ to impose.
- Step 2** Select $\frac{N'}{2}$ pairs of parents ($N' \leq N$, N' even) with a selection method (as tournament). A same parent can be selected twice.
- Step 3** Evaluate the *difference-degree* d_i between the two parents, for each pair i of parents.
- Step 4** If $d_i < D_s$ for a given pair, both of the parents undergo a mutation, and return to **Step 3**. Otherwise, continue to next step.
- Step 5** Generate N' children from $\frac{N'}{2}$ pairs of parents by *crossover* (always applied). Here, no more mutation operator is applied.
- Step 6** Evaluate the *fitness* of the children.
- Step 7** Reverse replacement: the best $R \cdot 100\%$ children replace the worst individuals of the current population.
- Step 8** Relax the diversity constraint, with $D_s = \mu D_s$ and the cooling ratio $\mu \in]0; 1[$. Return to **Step 2**.

One difficulty resides in the fact that [15] uses a binary representation for the individuals, and then the *mutation*, the *crossover* operators and *difference-*

degree between two individuals have to be specifically defined for that representation.

Considering that we decide to keep the representation of individuals real-valued, the operators and the *difference-degree* measure defined in [15] are modified.

The *difference-degree* $d_i \in]0; 1[$ between two individuals \mathbf{X}_1 and \mathbf{X}_2 with p parameters (or variables to be optimized) for each individual; and where \mathbf{a} and \mathbf{b} the lower and upper boundaries of \mathbf{X} is:

$$d_i = \frac{1}{p} \sum_{i=1}^p \frac{X_{1,i} - X_{2,i}}{a_i - b_i} \quad (4.8)$$

The *crossover operator* used (as in [15]) is the *two-point crossover* consisting in the reversal of the parameters of the two individuals (corresponding here to real values and not a single bit) between randomly chosen positions.

The *mutation operator* is chosen nearby of its binary counterpart (the *simple random*); thus, the following random value X'_i is added to one of the real variables i (allele) of the considered individual:

$$X'_i = X_i + \tau \cdot (a_i - b_i) \cdot 2^{-\lfloor r \cdot z \rfloor} \quad (4.9)$$

with τ a variable that can equiprobable be ± 1 , r a random value in $[0, 1[$ and z the accuracy (in power of two) that each real value is supposed to be (binary representation analogy).

4.5.4 Crossover Rules and Integrated Local Search

In this section, *GAbasic* is considered as the departure algorithm. The improvements done here concern the definition of a particular *crossover operator* and the hybridization with a local search method. The improvements are based on [1] but the individual's representation is done also with real values.

According to [1], these improvements allows for avoiding a premature convergence and, on the other hand, avoids a lengthy or slow convergence.

The presented *GAOi2* algorithm is based on algorithm $GA(c_r, l)$ in [1] (i.e. *crossover* rule $n^{\circ}2$ with local search), is the following:

Step 1 Generate a population of N individuals and evaluate their *fitness*.

- Step 2** Select $\frac{N'}{2}$ triplets of parents ($N' \leq N$, N' even) with a tournament selection with two players. A same parent can be selected twice in the same triplet.
- Step 3** Generate N' children (N' even) from triplets of parents with help of a *crossover operator* defined below (always applied), each triplet of parents generates two children. Each allele of N' children has a probability P_m to be affected by the *mutation operator*.
- Step 4** Evaluate the *fitness* of the children.
- Step 5** Reverse replacement: the best $R \cdot 100\%$ children replace the worst individuals of the current population.
- Step 6** Local search (optional). Return to **Step 2**.

The *crossover operator* is defined, for each variable i , with \mathbf{X}_1 , \mathbf{X}_2 and \mathbf{X}_3 the three parents, \mathbf{X}_3 is the parent with the worst *fitness*, and \mathbf{Y}_1 and \mathbf{Y}_2 the two children:

$$Y_{1,i} = \frac{X_{1,i} + X_{2,i}}{2} + \sigma_i \left(\frac{X_{1,i} + X_{2,i}}{2} - X_{3,i} \right) \quad (4.10)$$

$$Y_{2,i} = X_{1,i} + \Phi_i (X_{2,i} - X_{3,i}) \quad (4.11)$$

with σ_i a uniform random number in $[0; 1]$, and Φ_i a uniform random number in $[0.4; 1]$ for each i .

The *mutation operator*, for a given variable i , is defined at generation k as:

$$X'_i = \begin{cases} X_i + \Delta(k, b_i - x_i) & \text{if } \tau = 0 \\ X_i - \Delta(k, x_i - a_i) & \text{if } \tau = 1 \end{cases} \quad (4.12)$$

where τ is a random bit that can take either 0 or 1, and

$$\Delta(k, y) = y \left(1 - r \left(1 - \frac{k}{T} \right)^b \right) \quad (4.13)$$

where r is a random number in $[0, 1]$, T is the maximal number of individual generations and b is a specified parameter by the user that determines the non-uniformity degree in the search domain (typically, $b = 5$).

4.5.4.1 Local Search

Local search works as follows:

1. Select an individual Y , different of the best individual X_l , in the current population.
2. Generate a new testing individual X_n .
3. If the new *fitness* $F_n < F_h$ of the worst individual X_h , then X_h and F_h are replaced respectively by X_n and F_n .
4. The process is repeated l_r times, with l_r a parameter specified by the user that gives the number of local searches to be done (e.g. $l_r = 5$).

Each component of X_n is calculated as follows:

$$X_{n,i} = (1 - \gamma_i)X_{l,i} - \gamma_i Y_i \quad (4.14)$$

the $\gamma_i \in [-0.5, 1.5]$ are uniform random numbers different for each i .

4.5.5 Combination of Both Improvements

In Sections 4.5.3 & 4.5.4, two improvements of the *GAObasic* algorithm (Section 4.5.2) have been made.

Here, a combination of the two preceding improvements is done; in the hopes that this combination will lead to a more efficient algorithm than both improvements taken separately.

Indeed, the two improvements concern separate parts of the GA, that are the application rules conditions of the operators, and the crossover operator with an added local search strategy.

Moreover, that algorithm generalizes the selection method in the sense that a method among others (tournament, wheel, etc.) can be specified by the user.

Thus, the *GAOi12* algorithm arises in the following manner:

- Step 1** Generate a population of N individuals and evaluate the *fitness* of each individual.
- Step 2** Select $\frac{N}{2}$ triplets of parents ($N' \leq N$, N' even) with a chosen selection method (e.g. tournament). A same parent can be selected twice in the same triplet.

- Step 3** Evaluate the triplets $d_{i,mean}$, defined as the mean of the *difference-degrees* $d_{i,12}$, $d_{i,23}$ and $d_{i,31}$ of the parents taken two by two of each triplet.
- Step 4** If $d_{i,mean} < D_{s,mean}$ for a given triplet, each of the three parents undergo a mutation following Equation (4.9) (does not depend on any probabilistic parameter to be specified) and back to **Step 3**. Else, **Step 5**.
- Step 5** Generate N' children (N' even) from the triplets of parents with the *crossover* operator (always applied) defined by Equations (4.10) & (4.11), each triplet of parents generates two children. No more mutation operator is any applied.
- Let us note that the *crossover* operator, that needs the parents *fitness* as inputs, uses here the fitness of the parents evaluated before any mutation at **Step 4**. Indeed, this approximation is useful to avoid a very large number of objective function evaluations and does not spoil the algorithm results in a significant manner.
- Step 6** Evaluate the children *fitness*.
- Step 7** Reverse replacement: the $R \cdot 100\%$ best children replace the worst individuals of the current population.
- Step 8** Local search (optional). Return to **Step 2**.

In this algorithm, the imposed *difference-degree* $D_{s,mean}$ depends on parameters other than a constant factor multiplication μ .

A correspondence between $D_{s,mean}$ and the mutation operator defined at Equation (4.12) is set up. More precisely, the imposed mean *difference-degree* $d_{i,mean}$ in a triplet of parents has to be of the same order as variable mutation of one of the three parents according to Equation (4.12). Thus, $D_{s,mean}$ at generation k is given by:

$$D_{s,mean} = \frac{1}{3p} \cdot \left(1 - 0.5^{\left(1 - \frac{k}{T}\right)^b}\right) \quad (4.15)$$

with p the number of variables of an individual, T the maximal number of individual generations and b a specified parameter by the user that determines the non-uniformity degree in the search domain (typically, $b = 5$).

To show the effect of the parameter b that can be chosen by the user, as an example, let us take a maximal number of generations $T = 5000$ and individuals with $p = 10$ variables. The resulting *difference-degree* $D_{s,mean}$ is shown in Figure 4.5.

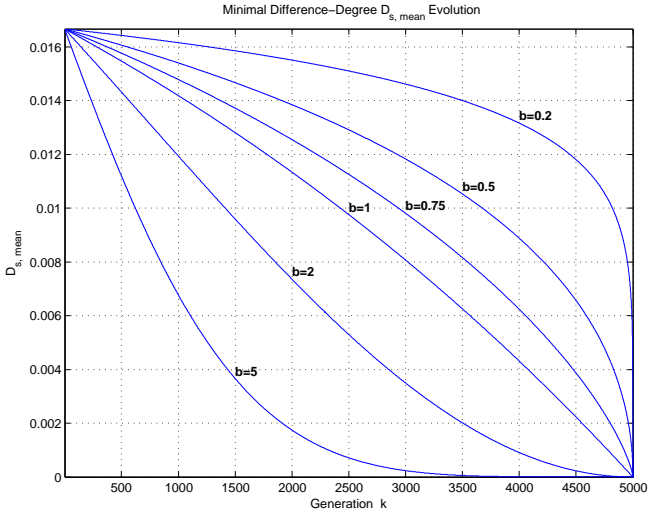


Figure 4.5: Minimal Difference-Degree Evolution

With high values of b , the *difference-degree* decreases strongly in the first generations. A slow decrease of $D_{s,mean}$ in the first generations and more accentuated in the last generations is obtained by values of b lower than 1. An intermediate behavior of $D_{s,mean}$ is obtained around the values of $b = 1$.

The presented solution, although it seems to have a superfluous degree of complexity, turns out to be more efficient than other possibilities considered with the *difference-degree* D_s evolving with a fixed cooling rate μ .

4.6 Test Functions

Many test problems [6] can be used to examine the performance of different optimization methods. The behavior of the test problems varies enough to cover a lot of difficulties faced in the domain of continuous global optimization.

4.6.1 Algorithms Comparison

The three developed algorithms *GAOi1*, *GAOi2*, *GAOi12* have to be evaluated and compared in order to measure their performance.

For that purpose, three unconstrained test functions are chosen to compare the performance of the algorithms: Rastrigin, Zakharov and Ackley test functions. An easy manner to see a representation of the functions is to plot them with $p = 2$ parameters as it is done in Figures 4.6 & 4.7.

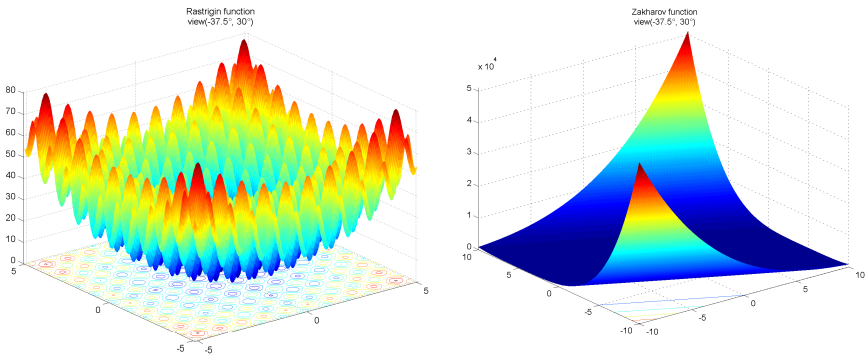


Figure 4.6: Rastrigin (left) & Zakharov (right) Test Functions

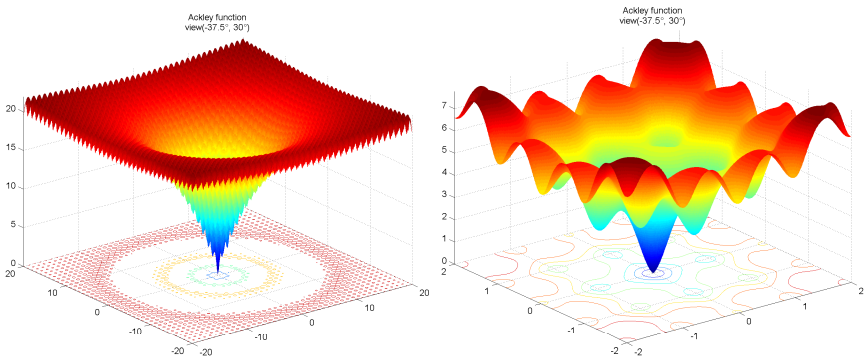


Figure 4.7: Ackley Test Function

The main reason for the choice of that three functions is that they can be calculated for any number of p variables or dimensions. Another point to mention is that the three functions have in common their global minimum

that is situated at zero for any number of p parameters. Some distinctive characteristics of the functions are:

- Rastrigin's function (as shown in Figure 4.6) has a lot of maxima and minima in the domain search.
- Ackley's function (Figure 4.7) also has a lot of maxima and minima. But unlike Rastrigin's function, the global minima is more accentuated than other local minima.
- Zakharov's function (Figure 4.6) is very flat near the global minima and can cause a lot of problems to some algorithms.

4.6.2 Algorithms Testing

To have a global idea of the behavior of the three implemented GA's, a common set of parameters is defined in Table 4.1.

Table 4.1: Parameters Used for Testing Algorithms

Parameter	Value	<i>GAOi1</i>	<i>GAOi2</i>	<i>GAOi12</i>
p	20	✓	✓	✓
N	10	✓	✓	✓
N'	2	✓	✓	✓
R	1	✓	✓	✓
T	10000	✓	✓	✓
E	10000	✓	✓	✓
selection	tournament	✓	-	✓
n_c	5	✓	-	✓
P_m	0.01	-	✓	-
$D_{s,i}$	0.5	✓	-	-
$D_{s,f}$	10^{-4}	✓	-	-
$n_{m,max}$	100	✓	-	✓
b	5	-	✓	✓
l_r	1	-	✓	✓

the parameter is available (✓) or not (-)

With FE optimizations, the main limiting factor is time or the number of times the simulations with FEA software will be launched, given that a simulation can take between 5 s and 5 min.

- The common parameters between the three algorithms are the number of dimensions $p = 20$, a population size of $N = 10$ individuals, $N' = 2$

children, a replacement rate $R = 1$ and the maximum number of generations $T = 10000$. The maximum number of objective function evaluations is $E = 10000$. Then, the *stop criterion* is either T or E .

- *GAOi1* has an initial minimal $D_{s,i} = 0.5$ and a final $D_{s,f} = 10^{-4}$ *difference-degree*. With $D_s = D_{s,i}$ and $D_s = D_{s,f}$ at the last generation, the cooling ratio μ can be determined.
- *GAOi2* has a mutation probability $P_m = 0.01$.
- *GAOi1* and *GAOi12* have a common *tournament* selection rule among $n_c = 5$ individuals. The maximum number of mutations by parent $n_{m,max} = 100$; indeed, the algorithms impose a diversity between parents that can in some cases not be reached and the algorithms can follow without stopping the process. The specified parameter $b = 5$ and a single local search $l_r = 1$.
- *GAOi12* replaces in the local search the individual with the *fitness* nearest to the mean and not the individual with the worst *fitness*; this allows maintaining control on the population diversity preventing the local search being too predominant in relation to other algorithm strategies.

The worst, best and the mean results obtained over 30 *runs* for the three test functions and the three implemented algorithms are available in Table 4.2.

Table 4.2: Test Function Results for Unconstrained Functions

f	p	Algorithm	Worst	Best	Mean
Ackley	20	<i>GAOi1</i>	0.02261	0.0020536	0.008481
		<i>GAOi2</i>	1.8364	1.8177e-007	0.35762
		<i>GAOi12</i>	0.0022434	0.00034515	0.0010439
Rastrigin	20	<i>GAOi1</i>	46.7634	15.9193	30.1145
		<i>GAOi2</i>	22.884	3.9798	13.1003
		<i>GAOi12</i>	3.9799	1.3777e-006	0.79629
Zakharov	20	<i>GAOi1</i>	46.6888	3.0732	19.4386
		<i>GAOi2</i>	226.207	27.3839	68.0506
		<i>GAOi12</i>	20.517	0.64947	5.3775

As a general comment, *GAOi12* obtained better results with the three functions tested. It is worth noting that *GAOi1* obtains better results than *GAOi2* for the Zakharov's function that is very flat near the global minimum, and confirms that a combination of *GAOi1* and *GAOi2* takes advantage of both algorithms.

4.6.3 Population and Children Size

In the above section, some parameters like the population size N or the children N' have not been justified. So to better understand the GAs implemented, one question has to be answered: is it better to have a big starting population size N and a lot of children N' at each generation or is the opposite better?

A test with *GAO_i12* on Rastrigin's function and the same parameters as in Table 4.1 is done. Unlike above, the population size N and the number of children N' are varied in the following manner: $N = 10i$ and $N' = 2i$ and $i = 1, 2, \dots, 10$. The results are depicted in Figure 4.8.

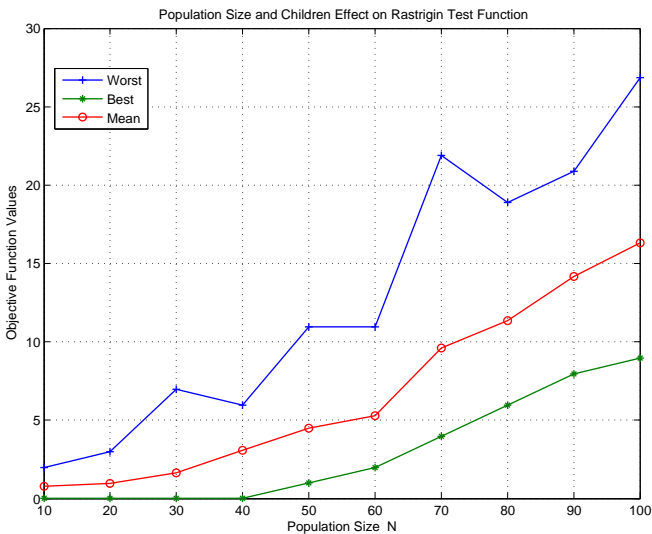


Figure 4.8: Population and Children Performance

With a limited number of objective function evaluations E , it is better to have a population size of $N = 10$ individuals and $N' = 2$ children. It also allows the conclusion that a lot of children at each generation is not useful, the number of generations is more important.

4.7 MATLAB and ANSYS Implementation

The optimization routines have been implemented in MATLAB software and the FE simulations are done using ANSYS software. One major difficulty is that the two softwares have not been designed to work together.

So, the communication between the two is done with the help of text files (*.txt). Each software can read or write data of external *.txt files that are in a predetermined format.

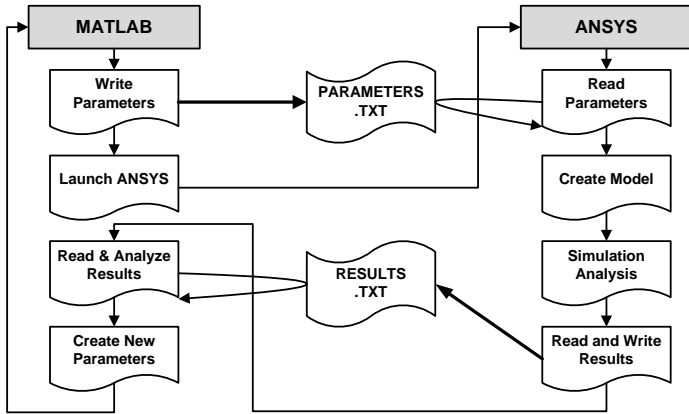


Figure 4.9: MATLAB and ANSYS Process Flow

MATLAB is used to:

1. Run and manage the GA routines. The GA creates the initial population and writes the parameters into an external PARAMETERS.TXT file.
2. Launch ANSYS software in batch processing.
3. Read the results of RESULTS.TXT file created by ANSYS and the GA analyzes them.
4. The GA creates a new set of parameters to be tested until the stop condition of the GA is satisfied.

When MATLAB launches **ANSYS**, the steps followed are:

1. Read the PARAMETERS.TXT file.
2. Create the geometry model and the meshing.
3. Simulate the model (static, harmonic or modal analysis) with the determined constrains.

4. Read and calculate the results. Export the results into a RESULTS.TXT file and close ANSYS.

The complete process is summarized and presented in Figure 4.9.

4.8 Conclusion

Different optimization methods have been discussed. Some methods have been implemented based on a pseudo-gradient have been used to optimize the analytical model of the transducer.

The aim in this chapter has been to study and develop new optimization methods more adapted to the requirements of FE simulations.

As a result, *GAOi1*, *GAOi2* and *GAOi12* genetic algorithms have been developed and implemented. The algorithms have also been tested with some functions and give satisfactory results.

In the following chapter, FE optimizations will be carried out with the *GAOi12* (Sec. 4.5.5) genetic algorithm developed.

Chap 5

Numerical Simulations and Optimizations

Summary

5.1	Introduction	86
5.2	Ultrasonic Transducer Parts	86
5.2.1	Piezoelectric Stack	86
5.2.2	Transmission Discs	87
5.2.3	Amplification Horns	87
5.2.4	Full Transducer Model	88
5.3	First Prototype	88
5.3.1	Displacement Amplitude	89
5.3.2	Impedance	90
5.3.3	Displacement and Impedance Comparisons	91
5.3.4	Mesh Size Effect	91
5.3.5	Optimization Objective Function	92
5.4	Second Prototype	93
5.4.1	Displacement Amplitude	93
5.4.2	Impedance	94
5.4.3	Amplitude and Impedance	94
5.4.4	Cannulation Size Effect	95
5.5	GAO Prototype	98
5.5.1	Transducer Model	98

5.5.2	Optimization Parameters	98
5.5.3	Results and Discussion	98
5.5.4	Conclusion	100

5.1 Introduction

In this chapter, the finite element (FE) models and simulations of different prototypes are discussed. Two prototypes have been realized and built in the machine shop, based on the results of pseudo-gradient analytical optimizations. For these two first prototypes, FE software (ANSYS) has been used as a means of verification of the analytical simulation results.

Another interesting approach is to optimize a FE model. This can only be achieved by a simplification of the transducer model; a 2D model is presented and the results after genetic algorithm optimizations (GAO) are discussed in details.

5.2 Ultrasonic Transducer Parts

Let us introduce the different constitutive parts of a typical piezoelectric ultrasonic transducer model.

5.2.1 Piezoelectric Stack

The first interesting part is the piezoelectric stack. The stack is composed of different piezoelectric discs. The FE model can be simplified and represented as a single ceramic disc with a total thickness being the number of discs times the height of one ceramic disc. The model is shown in Figure 5.1.

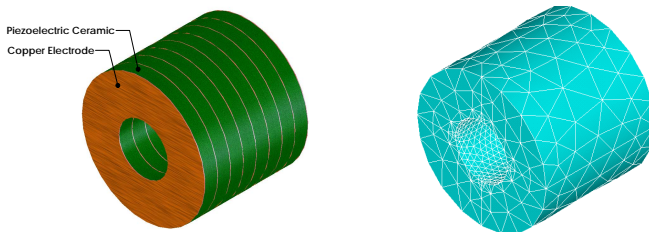


Figure 5.1: Piezoelectric Stack

When applying a voltage to a piezoelectric disc, the same voltage has to be applied to the nodes on the same area. A coupling of the nodes on the same area is needed. The DOFs used with piezoelectric materials are UX, UY, UZ and VOLT (to take into account piezoelectricity).

5.2.2 Transmission Discs

The transducer may have many transmission parts like simple rods or discs if there is a hole inside.

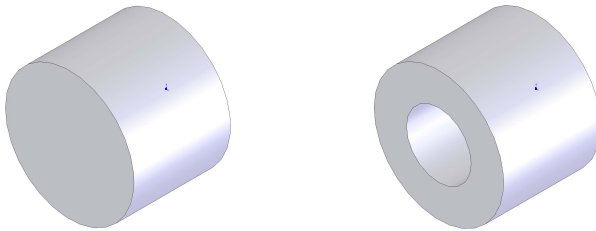


Figure 5.2: Transmission Rod Section

Transmission parts are metal parts and we only take into account the chosen aluminium alloy material EN-AW-7075 and the titanium alloy TI-6Al-4V-STA. Metal parts have displacements DOF that can be UX, UY, UZ to be calculated.

5.2.3 Amplification Horns

When two rods are connected together, this can result in a step horn as shown in Figure 5.3 if the rods have different diameters.

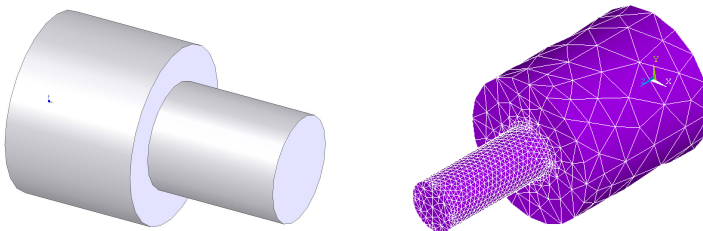


Figure 5.3: Step Horn Model

Another important amplification horn is the exponential horn as shown in Figure 5.4 which area $S(z)$ is defined by

$$S(z) = S_0 \cdot e^{-2\alpha z} \quad (5.1)$$

where $S_0 = S(z = 0)$, $S_L = S(z = L)$ and L is the length of the horn. Then α is given by

$$\alpha = \frac{1}{L^2} \ln \left(\frac{S_0}{S_L} \right) \quad (5.2)$$

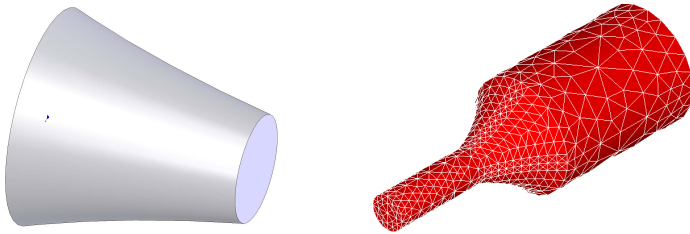


Figure 5.4: Exponential Horn Model

Amplification parts are also metal parts and only aluminium alloy EN-AW-7075 and titanium alloy TI-6Al-4V-STA are considered. Metal parts have displacements DOF that can be UX, UY, UZ to be calculated.

5.2.4 Full Transducer Model

A typical complete transducer model that will be considered to optimize is shown in Figure 5.5.

5.3 First Prototype

The first prototype modeled, as described in Figure 5.5, is composed of eight transmission parts or rods (2, 3, 4, 6, 8, 9, 10, 12), three exponential horns (5, 7, 11) and a piezoelectric stack (1) composed of eight PZ-54 piezoelectric discs.

The complete transducer model of the first prototype is shown in Figure 5.6 and the corresponding parameters are described in Table 5.1.

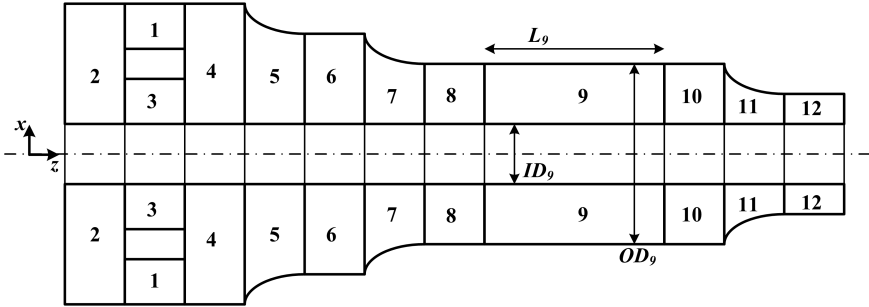


Figure 5.5: Complete Transducer Model

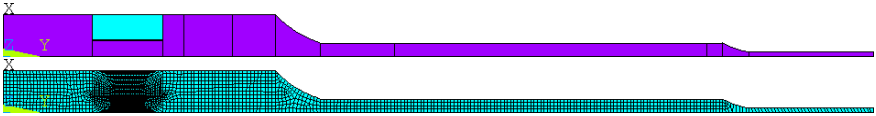


Figure 5.6: First Prototype 2D Model

Table 5.1: First Prototype Parameters

i	L_i [mm]	OD_i [mm]	ID_i [mm]	Material
1	16.9	20	8	PZ-54
2	21.66	20	0	EN-AW-7075
3	16.9	7.5	0	EN-AW-7075
4	5.21	20	0	EN-AW-7075
5	11.6	-	0	EN-AW-7075
6	10.36	20	0	EN-AW-7075
7	10.98	-	0	EN-AW-7075
8	17.8	6.35	0	EN-AW-7075
9	75.58	6.35	0	EN-AW-7075
10	3.78	6.35	0	TI-6Al-4V-STA
11	6.48	-	0	TI-6Al-4V-STA
12	30	2	0	TI-6Al-4V-STA

$f_r = 34.8$ kHz ; $V_a = 1$ V ; $n_{discs} = 8$

5.3.1 Displacement Amplitude

FE simulations of a 2D model are used to verify the the vibration amplitude in a frequency domain between 20 kHz and 40 kHz as shown in Figure 5.7.

The desired resonant frequency f_r at 34.8 kHz optimized in [12] only differs

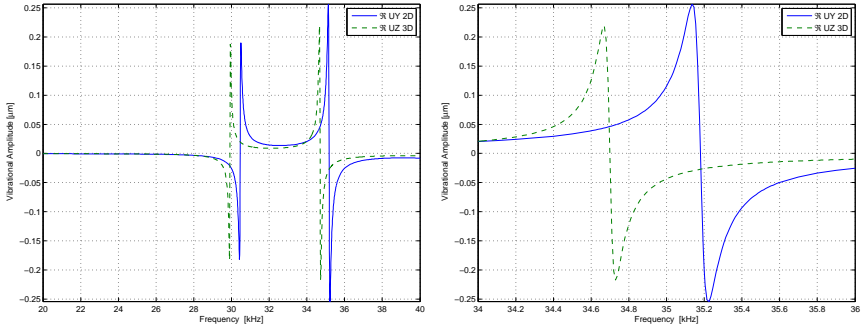


Figure 5.7: Vibration Amplitude for the 2D & 3D Models

a few hundred hertz from the resonant frequency in the 2D models that is about 35.1 kHz.

5.3.2 Impedance

With FE simulations, admittance can be determined with the sum of charges. This can be achieved in a 3D model. The disadvantage of 3D models is the large number of calculations depending on the number of nodes of the model. It is important to pay attention to the meshing size given that in a harmonic analysis one simulation can easily cost 5 min in time for each frequency.

The charges Q may also be obtained with 2D elements. The calculated impedance with ANSYS is shown in Figure 5.8.

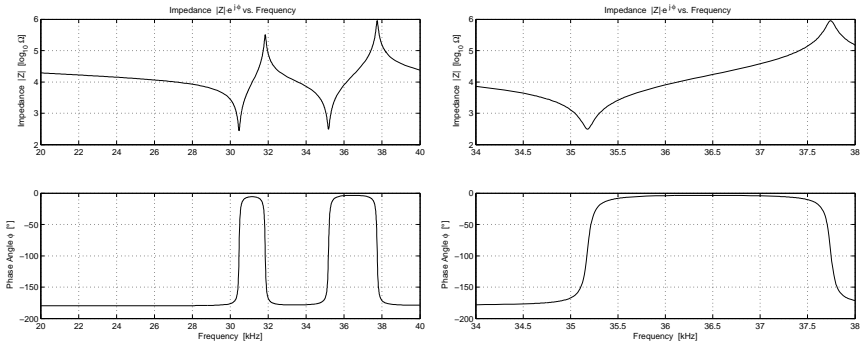


Figure 5.8: Impedance for the 2D Model

5.3.3 Displacement and Impedance Comparisons

The mechanical behavior of the transducer is represented by the amplitude displacement and the electrical behavior can be represented by the impedance Z of the transducer as shown in Figure 5.9.

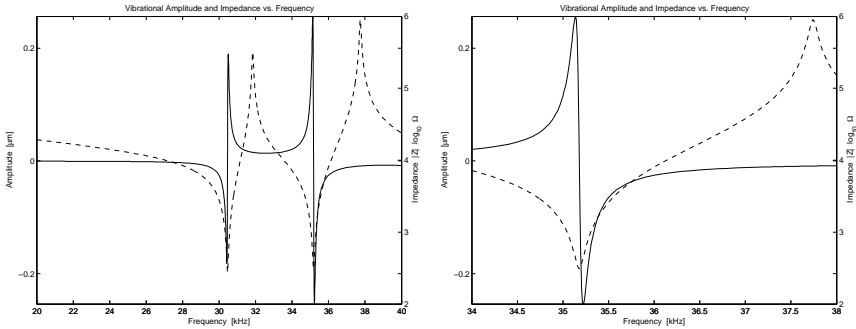


Figure 5.9: Vibrational Amplitude and Impedance for the 2D Model

The frequency f_m at which impedance $|Z|$ is minimum (maximum admittance; also called the resonance frequency f_r) approximates the series resonance frequency f_s .

As the frequency continues to increase, the impedance increases and the frequency f_n at which the impedance becomes maximum (minimum admittance; also called the anti-resonance frequency f_a) approximates the parallel resonance frequency f_p .

5.3.4 Mesh Size Effect

The size of the meshing in ANSYS is an important parameter that can be tuned to gain calculation time. The purpose here is to see if the general size of the mesh makes a difference near the resonant frequency on the displacement amplitude or the impedance.

As shown in Figure 5.10, mesh sizes varying from 0.5 mm to 1.2 mm have almost no effect on the general vibrational amplitude nor the impedance response.

Nevertheless, the boundary values chosen here for the mesh size variation are not chosen at random. They depend on the model and the user's experience. To build a good model, it is important to take into account the smallest

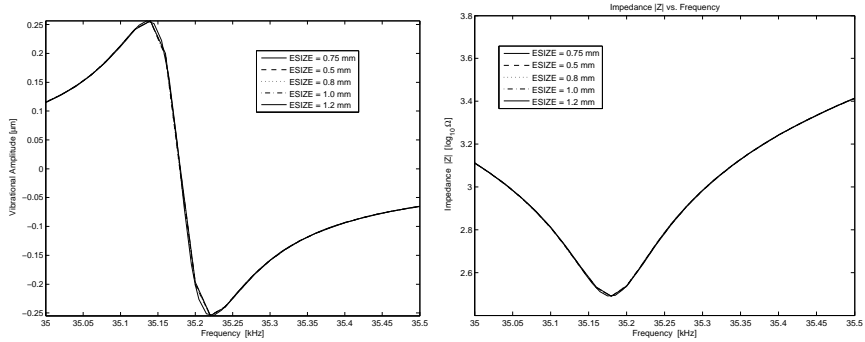


Figure 5.10: Displacement and Impedance in 2D Model at Varying Mesh Sizes

dimensions and mesh accordingly.

Here, the smallest dimension is $OD_{12} = 2$ mm. A coarse value of 2 mm for the mesh size can produce a poor meshing given that in a 2D model the geometrical dimensions are divided by two for the radial dimensions.

On the other hand, a finer mesh can help to have more precise results due to the more calculation points, but the price to pay is proportional in calculation time.

In Figure 5.10, an ANSYS simulation with a mesh size of 0.5 mm can take 12 s and with 1.2 m takes less than 5 s.

5.3.5 Optimization Objective Function

Until now, no justification has been given for the objective function that is to be minimized. The vibration amplitude is the objective function to minimize and the main reasons are:

- At the resonant frequency f_r , the vibration displacement is zero. Then it makes no sense to minimize a value to a fixed value of zero because it becomes impossible to differentiate one resonant frequency from another.
- Nevertheless, a few hundred hertz from the resonant frequency f_r gives the maximum or minimum vibration displacement for the transducer. This maximum or minimum gives a good measurement of the optimized solution quality.
- Impedance at the resonance frequency $f_m = f_r$ is also minimum and this could be a valid parameter to optimize. In ANSYS, the sum of charges Q

can be obtained with some elements.

- As already said, maximizing the impedance makes no sense due to when the impedance is maximum there is no mechanical vibration.

5.4 Second Prototype

The second prototype modeled (Nucleus Removal System) is an ultrasonic system consisting of a handpiece with disposable end effectors, cables, and a control console that will be used to remove spinal nucleus material from the lumbar discs. The console will contain electronics, an irrigation pump and a suction pump. The electronics will provide control functionality [see 12, Chap. 8], transducer drive, and the user interface. The handpiece is a mechanically resonant cannulated actuator tuned to a particular frequency [12, Chapters 2 & 3]. Ultrasonic waves generated by the transducer are passed into the end effector. The irrigation pump in the console pumps fluid from the console to the end effector where it is transformed into a cavitation jet by the ultrasonic motion of the tip. The tip has a special shape to augment the production of cavitation in the fluid. The jet is directed at the nucleus material, thereby fragmenting it for subsequent aspiration.

The first version of the second prototype built at the machine shop and as optimized and presented by Murphy [12], Appendix B is shown in Figure 6.3.



Figure 5.11: Second Prototype ANSYS 2D Model

The final prototype has underwent some modifications and the corresponding optimized and adapted parameters are shown in Table 5.2.

5.4.1 Displacement Amplitude

FE simulations of a 2D model are used to verify the amplitude of the vibration amplitude in the frequency domain between 20 kHz and 40 kHz as shown in Figure 5.12.

The desired resonant frequency f_r at 22.5 kHz optimized in [12] only differs a few hundred hertz from the resonant frequency in the 2D models that is about 22.2 kHz.

Table 5.2: Nucleus Removal System Parameters

i	L_i [mm]	OD_i [mm]	ID_i [mm]	Material
1	24.9	15	7	PZ-28
2	40	15	2	TI-6Al-4V-STA
3	24.9	6	2	TI-6Al-4V-STA
4	25	15	2	TI-6Al-4V-STA
5	24.3	-	2	TI-6Al-4V-STA
6	27	8.25	2	TI-6Al-4V-STA
7	20.2	-	2	TI-6Al-4V-STA
8	9.3	6.35	2	TI-6Al-4V-STA
9	105.5	6.35	2	TI-6Al-4V-STA
10	7.8	6.35	1.25	TI-6Al-4V-STA
11	14.1	-	1.25	TI-6Al-4V-STA
12	39.2	3.4	1.25	TI-6Al-4V-STA

$f_r = 22.5$ kHz ; $V_a = 1$ V ; $n_{discs} = 8$

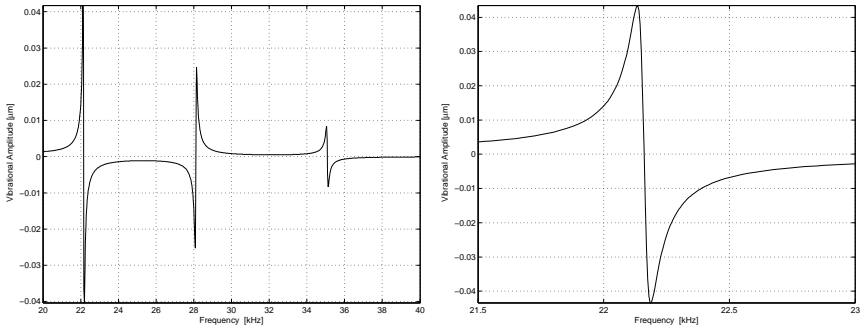


Figure 5.12: Vibration Amplitude for the 2D & 3D Models

5.4.2 Impedance

The charges Q may also be obtained with 2D elements. The calculated impedance with ANSYS is shown in Figure 5.13.

5.4.3 Amplitude and Impedance

The mechanical behavior of the transducer is represented by the amplitude displacement and the electrical behavior can be represented by the impedance Z of the transducer as shown in Figure 5.14.

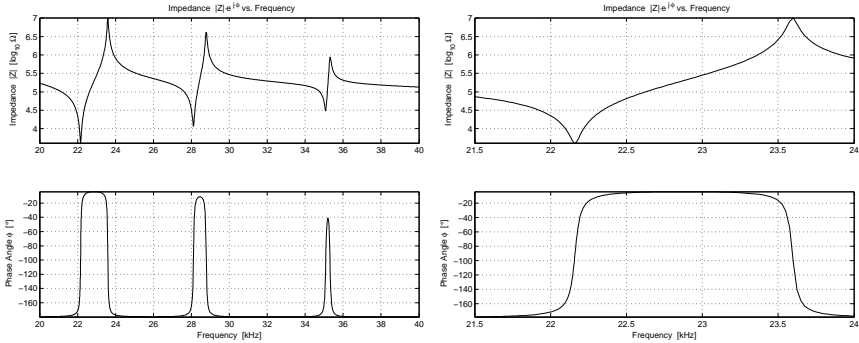


Figure 5.13: Impedance for the 2D Model

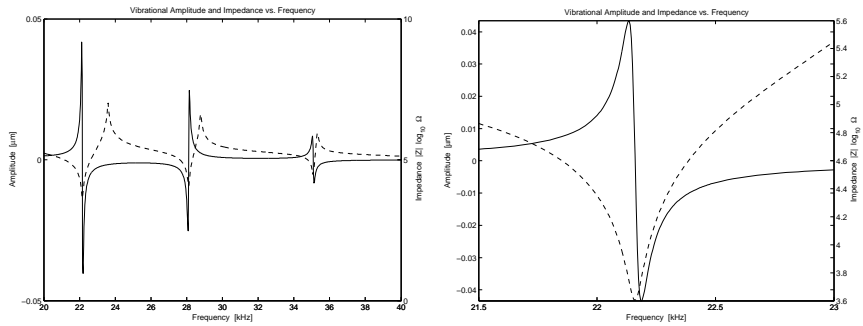


Figure 5.14: Vibrational Amplitude and Impedance for the 2D Model

5.4.4 Cannulation Size Effect

Let us remember that the second prototype is a cannulated handpiece. The cannulation is represented by an input diameter ID_i in the different parts of the transducer model. It is interesting to see the behavior of the optimized transducer around the resonant frequency f_r of 22.5 kHz when the inner diameter ID_i of the different parts of the transducer vary from 0 to 2 mm.

The results for the displacement amplitude are shown in Figure 5.15.

It is relevant to note that the resonance frequency f_r increases as the cannulation ID_i increases. Though the transducer parts have less material, the vibration amplitude at the end of transducer (part 12) increases.

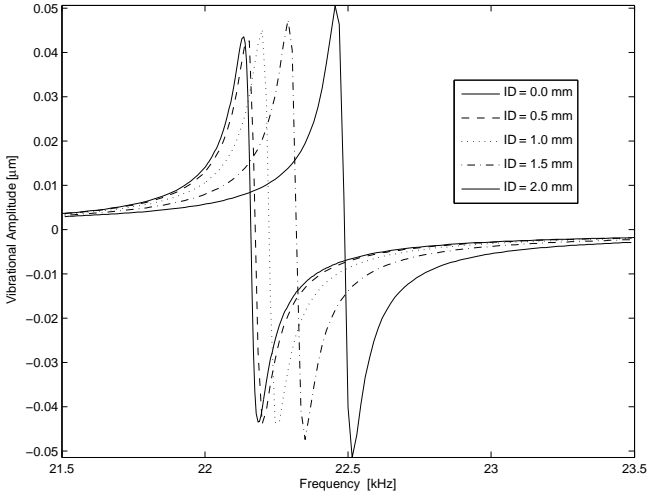


Figure 5.15: Vibrational Amplitude with Cannulation Effect in the 2D Model

Figure 5.16 shows the impedance variation with different cannulation diameters. The minimum impedance approaches the resonant frequency f_r of 22.5 kHz with the increasing inner diameter.

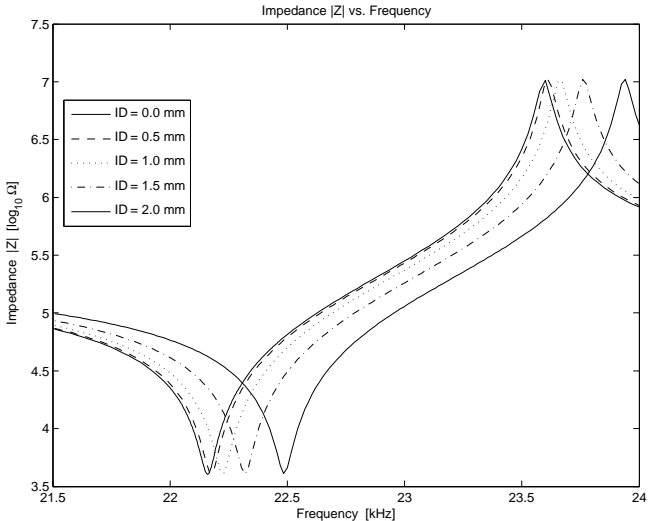


Figure 5.16: Impedance with Cannulation Effect for the 2D Model

5.5 GAO Prototype

The GA optimization routines developed (Sec. 4.5.5) with MATLAB software and combined with 2D axi-symmetric finite element (FE) simulations in ANSYS are used to maximize the vibrational displacement amplitude of the cutting tip at the resonance frequency f_r and the vibrational displacement along the actuator.

5.5.1 Transducer Model

A 2D axi-symmetric ultrasonic transducer model (Figure 5.17) composed of a piezoelectric stack (1), eight mechanical transmission parts (2, 3, 4, 6, 8, 9, 10, 12) and three exponential horns (5, 7, 11) for the movement amplification is defined.

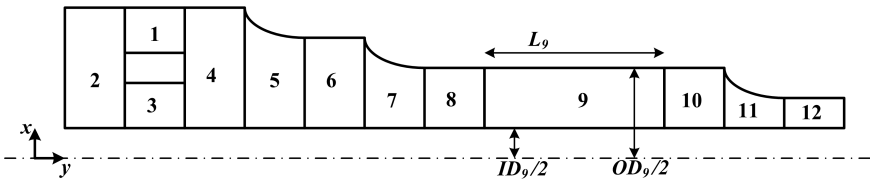


Figure 5.17: 2D Axi-symmetric Ultrasonic Transducer Model

5.5.2 Optimization Parameters

The transducer has eleven geometric parameters to be optimized, that are diameters OD_i or lengths L_i , cf. values in square brackets in Table 5.3.

The materials for that case are chosen but could also be optimized. The piezoelectric stack is composed of eight discs of PZ-28 material. All other metal parts are made of titanium alloy TI-6Al-4V-STA. The resonance frequency f_r is fixed at 22.5 kHz and the applied voltage V_a to the piezoelectric stack is 100 V.

5.5.3 Results and Discussion

In less than 5000 function evaluations (ANSYS simulations), at the resonant frequency f_r of 22.5 kHz, the GA optimizations give an amplitude of the

Table 5.3: Parameters Dimensions to be Optimized

i	L_i [mm]	OD_i [mm]	ID_i [mm]	Material
1	[5; 50]	15	0	TI-6Al-4V-STA
2	L_3	6	ID_1	TI-6Al-4V-STA
3	24.9	OD_1	7	PZ-28
4	[2; 50]	OD_3	ID_2	TI-6Al-4V-STA
5	[5; 50]	-	ID_4	TI-6Al-4V-STA
6	[5; 50]	$[OD_8; OD_4]$	ID_5	TI-6Al-4V-STA
7	[5; 50]	-	ID_6	TI-6Al-4V-STA
8	[5; 50]	6.35	ID_7	TI-6Al-4V-STA
9	[5; 200]	OD_8	ID_8	TI-6Al-4V-STA
10	[5; 50]	OD_9	ID_9	TI-6Al-4V-STA
11	[5; 50]	-	ID_{10}	TI-6Al-4V-STA
12	[5; 40]	3.4	ID_{11}	TI-6Al-4V-STA

$f_r = 22.5 \text{ kHz} ; V_a = 100 \text{ V}$

cutting tip of about $4.8 \mu\text{m}$ and the total length of the transducer is about 340 mm. The used algorithm is *GAOi12*.

A 3D view of the optimized transducer is shown in Figure 5.18 with the piezoelectric stack represented in green color.

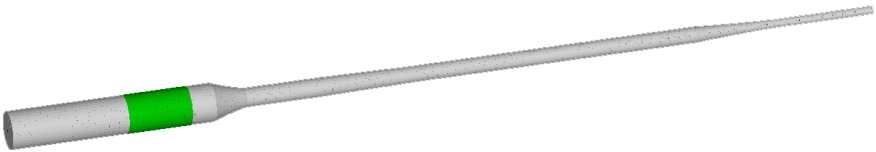


Figure 5.18: 3D View of the Optimized Transducer

The optimized transducer parameters are summarized in Table 5.4.

Table 5.4: Optimized Parameters Results

$L_1 = 45.89$ [mm]	$L_4 = 9.49$ [mm]	$L_5 = 13.20$ [mm]
$L_6 = 28.79$ [mm]	$OD_6 = 7.55$ [mm]	$L_7 = 38.86$ [mm]
$L_8 = 31.23$ [mm]	$L_9 = 43.05$ [mm]	$L_{10} = 35.20$ [mm]
$L_{11} = 30.94$ [mm]	$L_{12} = 39.28$ [mm]	

The objective function, corresponding to the vibrational amplitude displacement calculated in ANSYS, evolution and the diversity through the generations are shown in Figure 5.19.

The number of generations (1663) depends on the specified or desired parameters for each algorithm (number of parents, children, local search), and is different from the number of function evaluations (5000).

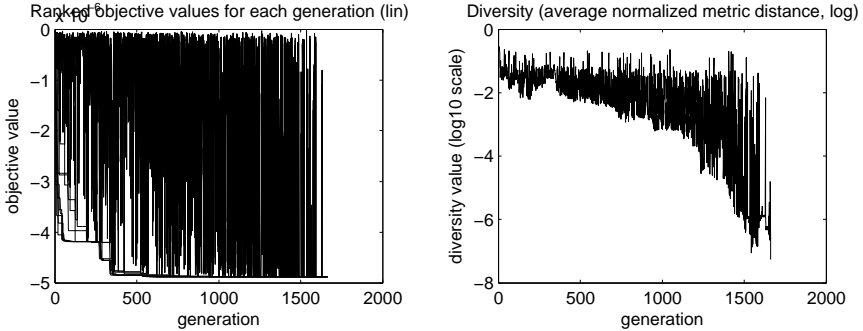


Figure 5.19: Diversity and Objective Values

At the resonant frequency f_r of 22.5 kHz, the harmonic displacement in the transducer nodes in the y -axis direction is shown in Figure 5.20. The amplitude of the cutting tip is about $4.8 \mu\text{m}$.

The transducer has three nodes where there is no vibrational amplitude and that are very useful to hold the transducer in ones hands. The position of nodes in the transducer can only be seen in Figure 5.20.

It is also relevant to verify the resonant modes of the transducer near the resonant frequency to avoid disturbing modes. The frequency analysis between 15 kHz and 30 kHz is shown in Figure 5.21.

5.5.4 Conclusion

In a previous work [11], an optimization of a piezoelectric transducer has been done with a pseudo-gradient method based on an analytical developed model. When comparing the vibration amplitude with the two methods (pseudo-gradient and genetic algorithms), the results are almost the same. The advantage of the GA resides in the low number of simulations needed to obtain good results. Which makes optimizations of full FE models realistic.

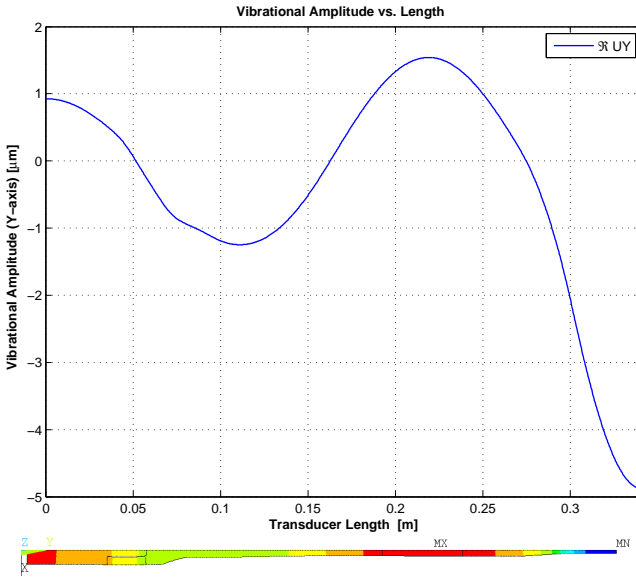


Figure 5.20: Real Amplitude Displacement in Transducer Nodes

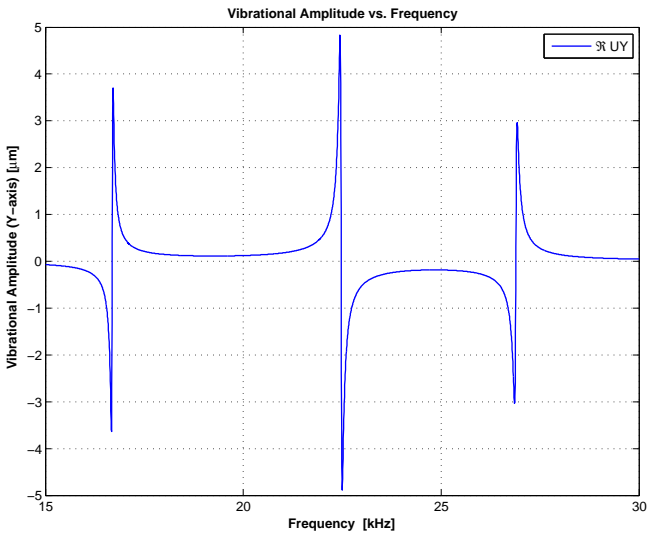


Figure 5.21: Harmonic Frequency Response

Chap 6

Measurements and Testings

Summary

6.1	Electronics	104
6.2	First Prototype Measurements	105
6.3	Second Prototype Measurements	106
6.3.1	Cracked Parts and Cannulation	106
6.3.2	Piezoelectric Stack Mounting	108
6.3.3	Displacement and Impedance Measurements	109
6.4	Cutting Testings	112
6.4.1	Test Setup	112
6.4.2	Test Results	113
6.5	Conclusions	114

In this chapter the different prototypes built are measured and tested. First, a recall of the electronics used to drive and control the different prototypes is done. Without the electronics, the different transducers would be useless because they must operate close to the resonance frequency and that frequency must be continuously tracked.

After that, the first prototype built is discussed and some general comments are made. Then, the second prototype built is presented with the corresponding encountered problems: breaking parts and cannulation. The mounting of the piezoelectric stack of this second prototype is also treated. Impedance measurements of the improved second prototype built are presented.

To realize some cutting tests, a small fixture that mimics an intervertebral disc has been built. The different prototypes, especially the second one, are tested on their ability to cut different animal tissue materials, and then overall conclusion is done.

6.1 Electronics

All that concerns the electronics has already been treated in Murphy [12]. As a visual recall, the electronics appear in Figure 6.1.

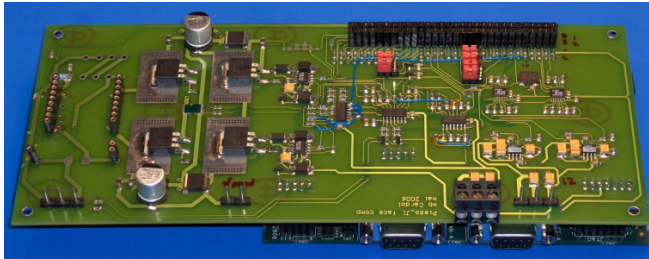


Figure 6.1: Electronics

In [12, Chap. 5], the integration of the system electronics into a larger system, the electrical characteristics of the load and issues associated with the effects of heat changes in the transducer have all been considered to generate a basis for the design of the system electronics. The type of drive signal has been established as a high voltage ultrasonic sinusoid that corresponds to the resonant frequency of the transducer.

The drive electronics necessary for proper operation of the transducer are explained in [12, Chap. 6]. The proposition and design of a transformer to address impedance matching and the need for elevated drive voltages are exposed. A discussion of an H-Bridge that is used to provide the high frequency drive from the 48 V DC power supply.

The control electronics are defined and each block is explained along with the circuitry necessary to perform the function and the prototype electronics are presented in [12, Chap. 7].

Digital control or the system integration of the different parts are explained in [12, Chap. 8].

6.2 First Prototype Measurements

The first prototype built at the machine shop is shown in Figure 6.2.



Figure 6.2: First Prototype Built

This prototype had already successfully been measured by Murphy [12], Chapter 4.4.3. The two measurements were the amplitude spectrum of transducer vibrations and the electrical impedance. The transducer movement measurements have been made with a *CLV 1000 Laser Vibrometer* and the optimized resonance frequency $f_r = 34.8$ kHz varies only a few hundred hertz from the measurements. The electrical impedance has been measured with an impedance analyzer *Agilent 4294 A* and the comparison with simulations showed to be very close.

Let us note some important changes that differ from analytical or numerical models and the prototype drawings necessary to build the transducer and thus may modify the transducer's performance:

- In FE simulations, the different transducer parts (L_i, OD_i, ID_i) are considered as if they were glued together. When building a prototype, some parts (e.g. parts with different materials) have to be attached physically together. Usually parts with threaded end sections meet that function.
- As the transducer has to be taken in the surgeon's hands, some locations are envisioned for that purpose. This corresponds to the rectangular part after

the first exponential horn. Each position along the transducer corresponding to minimal amplitude of standing waves is called a *node*.

- The backing part (part 2 in Figure 5.5) has been separated into two parts to facilitate the mounting of the piezoelectric stack.
- Some flat parts have been added to facilitate tightening of the piezoelectric stack with a determined preload.

This prototype has validated the analytical models developed and the optimization procedure. Further, the validity of the numerical models is also verified.

6.3 Second Prototype Measurements

The first version of the second prototype built at the machine shop and was optimized and presented by Murphy [12], Appendix B is shown in Figure 6.3.



Figure 6.3: First Trial of the Second Prototype Built

This prototype has underwent modifications due to some problems encountered while they were driven with electronics.

6.3.1 Cracked Parts and Cannulation

Initially, only the backing and cutting parts were made on titanium alloy Ti-6Al-4V-STA. The two other parts were made using the aluminium alloy EN-

AW-7075. Though the electronics have controlled and driven the prototype successfully at the correct resonant frequency, the prototypes quickly fatigued and cracked at the exit of the second horn section as shown in Figure 6.4.



Figure 6.4: Second Prototype Cracked Parts

The cracked region is around a *node* (because of the rectangular part used to hold the transducer). As said, a *node* corresponds to minimum displacement but at the same time this is a region where the mechanical strain or the stress is maximum. A paper drawing shows a cutaway view of the cracked region in Figure 6.5(a) and it can be seen that a screw is used to attach the two parts together. Moreover, this screw is threaded and cannulated. So, the strength of the aluminium alloy material may have been reduced below the fatigue stress applied during the operation and thus the transducer became fragile, even though the previous calculations did not reveal any stress problems.

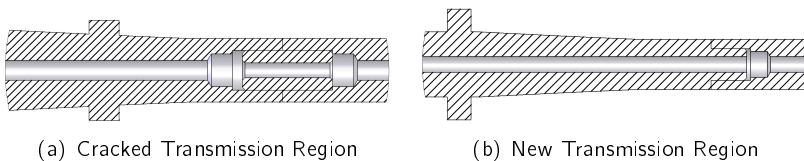


Figure 6.5: Drawings of the Transmission Region

In the same manner, a second horn section was fabricated but quickly broke after only a few minutes of operation in roughly the same spot as the first. A third aluminum prototype cracked and broke at the exit of the transmission section near the cutting tip, as it can be seen in Figure 6.6.

Given that the cannulation weakens the transducer and reduces its fatigue strength, a new transducer with the titanium alloy TI-6Al-4V-STA material



Figure 6.6: Second Prototype Cracked Transmission

in all parts has been designed. Then, optimization routines have been rerun, drawings regenerated and the transducers re-fabricated. The new transducer joint section has been modified to have the most material possible in the high stress regions as shown in Figure 6.5(b).

This transducer was difficult to fabricate due to the long cannulated sections, the bores of which are not perfectly straight. Although the new prototype resonates at the proper frequency, the imperfect cannulation results in the excitation of a secondary mode and some power is lost. This can be partially overcome by applying slightly more drive voltage, but the additional voltage required changes in the H-Bridge electronics. Unfortunately the transistors in the bridge were not sized for a higher drive voltage nor were the capacitors and it was necessary to replace them to get the electronics to function properly.

6.3.2 Piezoelectric Stack Mounting

Another interesting point to note is piezoelectric stack mounting. When the drawings of the backing part (L_2, OD_2, ID_2) have been made, it seemed unnecessary to split the backing part as it has been done in the Section 6.2 above with the first prototype built. The mounted piezoelectric stack is shown in the following Figure 6.7.

Finally, with eight ceramic discs, it is not evident at all to tighten the stack with a good alignment of the ceramics and keep the electrodes from making a short-circuit with the titanium alloy part inside. The copper electrodes are always moving when tightening because of the friction between the backing part and stack, whose movement is not easily controlled. This problem might not appear with two or four ceramics discs but, when building future prototypes,

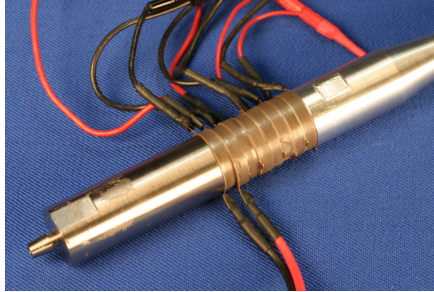


Figure 6.7: Piezoelectric Stack Mounting

the necessity of splitting the backing part should be considered.

6.3.3 Displacement and Impedance Measurements

With the first prototype (Section 6.2), it was possible to measure the amplitude of the vibration with a *CLV 1000 Laser Vibrometer*. The end of the cutting part is flat and there is no problem with focusing the laser beam.

In this second prototype, the end of the cutting tip is not flat but has a curved shape as shown in Figure 6.8.

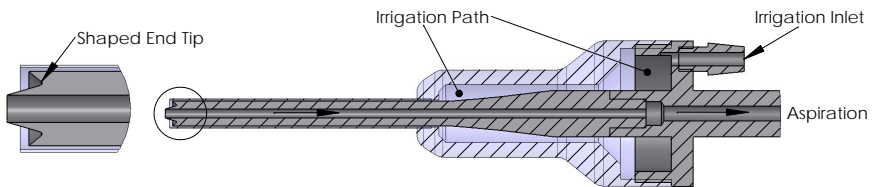


Figure 6.8: Shaped End in Cutting Tip

Several problems make the measurement difficult. First, the end of the cutting tip has a curved shape that diffuses the laser beam instead of focusing it. Second, the cutting tip is cannulated and trying to focus the laser is nearly impossible because the laser beam goes through the transducer cannulation. Unfortunately, for this kind of cannulated transducer with a shaped end, it has not been possible to measure the movement vibration amplitude at first.

The cutting tip has been modified to allow some measurements. A screw M 1.4×5 mm has been used to stick an aluminium flat disc onto it with



Figure 6.9: Modified Cutting Tip to Allow Measurements

Cyanolit. Figure 6.9 shows the modified cutting tip.

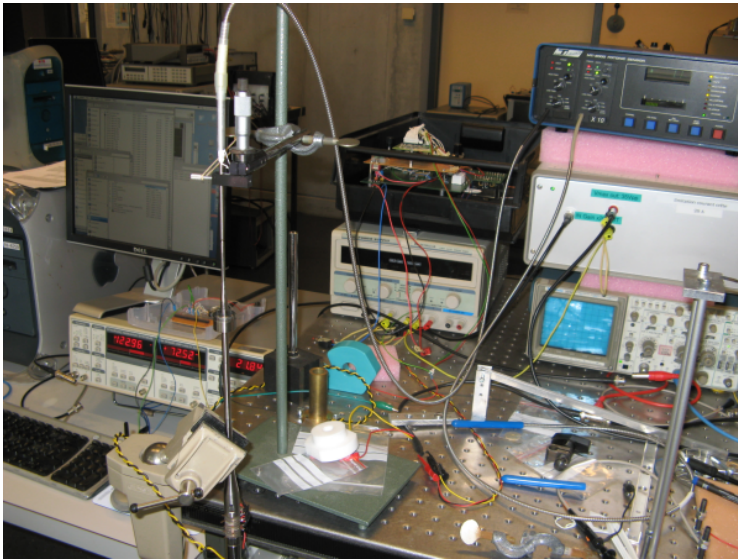


Figure 6.10: Measurements Test Setup

A *MTI 2000 Fotonic Sensor* has been used to measure the displacement and vibration on the flat disc. The measurements test setup is shown in Figure 6.10.

The vibrational displacement has been measured with an applied voltage of about 35 V peak to peak to the ceramic discs and the results are shown in Figure 6.11.

The first resonance frequency is at 21.85 kHz and the displacement amplitude is of 7.53 μm peak to peak. For the second resonance frequency at

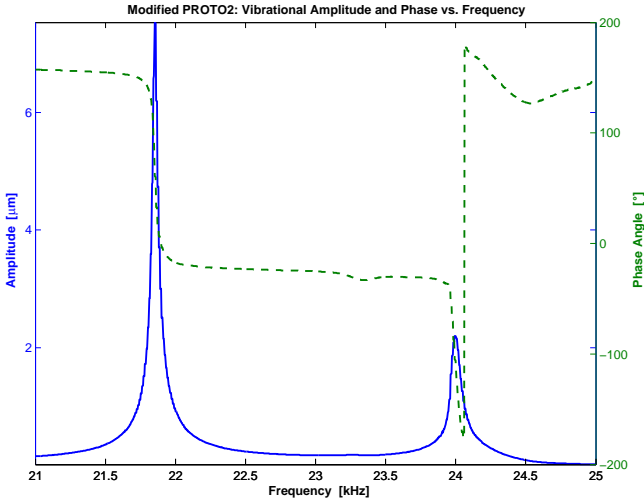


Figure 6.11: Second Prototype: Vibrational Amplitude Displacement

24 kHz, the displacement amplitude is of $2.2 \mu\text{m}$.

The electrical impedance has been measured with the impedance analyzer *Agilent 4294 A* and the results are shown in the following Figure 6.12.

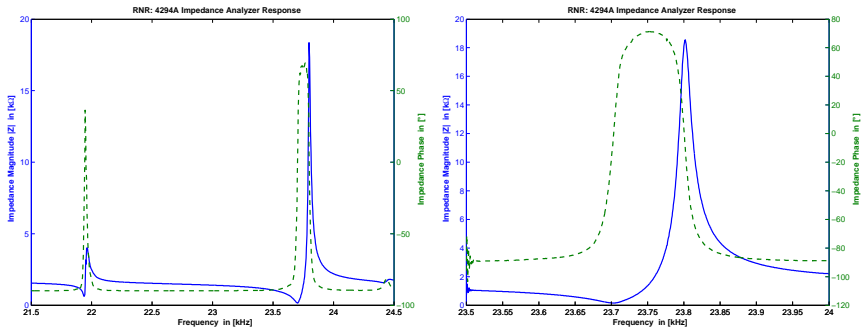


Figure 6.12: Electrical Impedance and Phase

The electrical impedance measurements give a resonant frequency $f_r = 23.7 \text{ kHz}$ at the minimum impedance and an anti-resonant frequency $f_a = 23.8 \text{ kHz}$ at the maximum impedance. It can also be seen that a new resonant

mode appears at 22 kHz that can disturb or result in power loss when driving the transducer.

It has also been remarked that the preload of this piezoelectric stack can easily make the resonance frequency f_r vary some hundred hertz. Nevertheless, the overall behavior of the transducer is correct in the sense that it can be controlled and the resonant frequency corresponds well enough with the predictions.

6.4 Cutting Testings

This section discusses the different tests done to validate and measure the ability of the cutting effect of the developed prototypes.

The objective of the project is the cutting of intervertebral spinal discs, and also the cutting or removal of cartilage, bone and soft tissue. Intervertebral discs consist of an outer *annulus fibrosus*, which surrounds the inner *nucleus pulposus*. The *annulus fibrosus*, peripheral, is the *hard* material of the disc and consists of several concentric layers of fibrocartilage. The *nucleus pulposus*, situated at the heart of the disc, is soft, deformable and is an incompressible gel with a jelly consistency.

6.4.1 Test Setup

The first purpose was to recreate the interior of a spinal disc. A small fixture with a similar shape and size of a disc has been built, as seen in Figure 6.13.

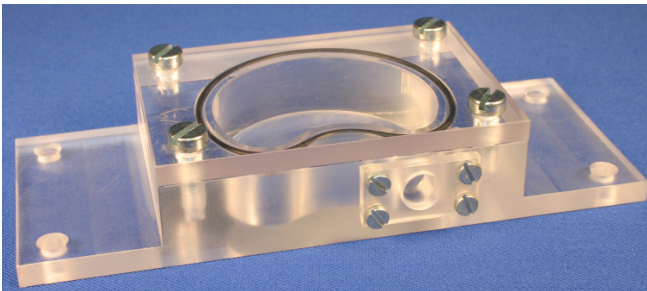


Figure 6.13: Spinal Disc Test Bench

The fixture is made from a clear acrylic so that the results could be evaluated easily and clearly seen. Fabricated in two pieces, the bottom was milled

out so that it contained a cavity characteristic of a lumbar *nucleus* space. The top is fitted with an O-ring and a lid that could be secured with four screws to give it a good seal. A small hole in the front side permits the cutter to be passed to the inside of the disc as it would be in a normal minimally invasive procedure, as in Figure 6.14.

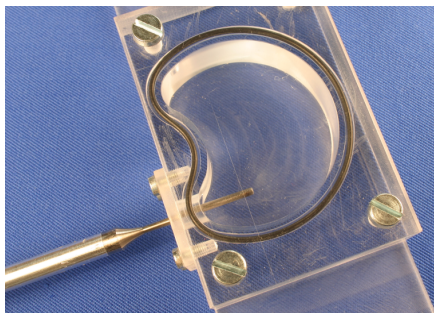


Figure 6.14: First Proto Cutting Procedure

The entry hole was fashioned in such a way that a stretchable membrane could be secured to the side of the fixture over the hole. The membrane serves to keep the tissue contained in the disc space and provides a means to apply a small amount of positive pressure that results from the jet produced by the cutter. A slit large enough for the cutter to pass through was then made in the membrane.

6.4.2 Test Results

The fixture was filled with chicken breast. This tissue has some interesting properties and is often used for this kind of tests. Then, the fixture has been closed with the screws and the cutter has passed through the entry hole. Aspiration by the central cannulation of the transducer and irrigation (Figure 6.8) has also been engaged before the cutter has been actuated.

A fixed voltage has been applied to the device during about ten minutes and the removed tissue is estimated.

As the cutting process is tedious, here are the main essential remarks:

- It was necessary to move the cutter closer to the target tissue to remove material. This was not possible to maintain the cutter so close during the procedure.

- Under application of the cutting tip, the tissue was liquified in the best cases and has been aspirated. Sometimes the pieces of tissue were too large to pass through the cannulation. These pieces of tissue being separated from the big piece of chicken become difficult to liquify as they would move away from the cutter.
- Though a cavitation effect exists, this effect is not important enough to allow a fast procedure. Neither the chicken's liquefaction nor the region with the irrigation accentuated the cavitation phenomenon.
- It was difficult to play with the irrigation and aspiration flows because a high irrigation rate floods the operating area and the aspiration cannot remove the water fast enough through the transducer's small cannulation.
- It took a lot of time to remove a small quantity (only a few grams) of tissue.
- The shape of the current developed cutters are not well adapted to access the annulus with a single hole as this can be clearly seen in Figure 6.13.

A surgical annulus disc removal procedure should take between three and five minutes at maximum and should only require one access hole to the disc. Unfortunately, the tissue removal rate is very slow and is not well-suited for a nucleotomy product offering even though it could be possible to reduce the duration of the procedure or improve the designs.

The cavitation jet produced is not strong enough to provide the desired cutting effect. Indeed, the cavitation depends on a minimum level of the acoustic intensity defined in W/m^2 . So, the vibrating surface should be increased to favor the cavitation phenomenon. Unfortunately, the combination of the desired cannulation inside the device and a necessary small tip diameter to have a minimally invasive access to the site, conflict with each other when attempting to obtain enough cavitation effect. Usually, the cutting and the material aspiration or removal are two different functions realized with two different devices.

6.5 Conclusions

The different prototypes have been tested with the electronics and it has been verified that they can be actuated and controlled. Moreover, it has been shown that any future device designed by the same method should operate at the correct frequency with good vibrational amplitude.

After having solved the problems encountered with the first version of the cracked second prototype by doing new designs, optimizations and a new fabrication, the cutting effect of the new device has been proven. Unfortunately,

the efficiency of this device is not high enough due to the slow tissue removal rate and a reduced cavitation effect. At the moment, this prototype is not well-suited for a minimally invasive surgical annulus disc removal or cutting intervention.

Chap 7

Conclusions

Summary

7.1	Overview	117
7.2	Originality	118
7.3	Outlook	119

7.1 Overview

In the domain of intervertebral spinal surgery interventions with minimally invasive methods, *ultrasonics* has clearly appeared as the technology to investigate. New devices that are small enough to pass through a small opening in the skin or through a small portal are presented as a solution for the rapid removal of spinal nucleus and annulus disc material.

This thesis has presented the design methodology that has been employed to design new ultrasonic transducers for the cutting of spinal disc material. The identification and decomposition of the device in three partial functions has allowed for making a complete catalogue of solutions for each partial function. For each of the *transmission*, *amplification* and *cutting* partial functions, a list of selection criteria has been chosen and the corresponding proposed solutions have been compared and evaluated to assess their viability. The transmission function consists of a resonant beam and the amplification function is done with a resonant horn. For the cutting function many solutions are proposed.

Finite element methods (FEM) have been employed to simulate the 3D numerical models developed. With the numerical optimization of new ultrasonic transducer designs in prospect and the computation time as a key problem, the different existing or developed optimization methods –absolutely valid with the correspondent analytical models– have shown their limitations. An optimization method based on genetic algorithms (GA) has been envisioned thanks to its ease of programming and its intrinsic modularity. The developed and implemented new algorithms have been tested with many test functions and have shown satisfactory results. Consequently, new 2D models of ultrasonic transducers have been conceived and optimized with the developed GAs with accurate results and enough fast computation time.

The prototypes have been built and measured. The electrical impedance and the vibration amplitude displacement measurements are in accord with the numerical and analytical models. The electronics has permitted actuation and control of the prototypes at the desired working point near the tracked resonance frequency. The cutting effect of the prototype has also been tested and proved. Though it has been possible to cut and remove some tissue, the efficiency of this device is not high enough due to the slow tissue removal rate and a reduced cavitation effect. Unfortunately, at the moment, this prototype is not well-suited for a minimally invasive surgical annulus disc removal or cutting intervention.

Nevertheless, this project has lead to a global cover of minimally invasive spinal surgery with piezoelectric transducers field. The experience acquired in the piezoelectric domain and in the design, the numerical optimization and prototyping of ultrasonic transducers is very solid.

7.2 Originality

The design methodology employed for the design of ultrasonic transducers for the cutting of spinal disc material offers an overall view of the different possible solutions available to fulfil the desired global cutting function. The evaluated and classified catalogues of solutions are a reference that allows fast further developments of new transducers since all the solutions to the different desired functions have already been analyzed. Furthermore, this design methodology can easily be adapted to new projects.

Nowadays, numerical FEMs are used successfully and provide solutions in more and more research domains. Nevertheless, the use of FEM to optimize a model can become very difficult to do. In this thesis, 2D models of ultrasonic

transducers that can be simulated enough fast to be part of an automated optimization process have been developed. The advantage of these models is that they are adaptable and can be modified on request in an easy manner.

A new optimization method based on GAs has been developed. Unlike other methods based on gradient calculations where the number of parameters to optimize increases the number of simulations needed, the GAs do not increase their complexity and stay efficient. The strong point of GAs is that they can easily be used and adapted to a large variety of problems without previous knowledge. Moreover, their modularity allows improvements of each part (reproduction, selection, mutation, crossover,...) separately as it has been done.

The combination of the 2D models and the developed GAs has allowed the numerical optimization of ultrasonic transducers. The originality is undoubtedly to have succeeded in the full optimization of an ultrasonic transducer with FE, especially when the calculation time is a limiting factor. With this project, we passed from an old traditional technique of quarter wavelengths designs to the optimization of numerical models without restrictions. From now, we can say that ultrasonic transducers can be modeled and optimized with analytical methods or numerical FE methods.

7.3 Outlook

During the prototype testings, the cavitation phenomenon has been used at ultrasonic frequencies during the tests. It would be interesting to make further studies to understand how the cavitation effect appears and how it could be used to facilitate or increase the cutting or removal of the human tissue. A direction to follow could be the use of FEMs to study the cavitation.

The end effector and the cutter developed have shown a bad efficiency and a slow tissue removal rate. Different shapes of cutters could be studied in order to obtain a better efficiency. Though the properties of the cutters could be studied with FE simulations, the cutting efficiency cannot be estimated in FEMs. In this case, an iterative process to build, test and modify the cutter prototypes, has to be undertaken until the desired results are obtained.

Finally, even though the developed ultrasonic transducer is not well-suited for a minimally invasive surgical annulus disc removal or cutting intervention, new opportunities for that kind of transducers can be found. Ultrasonic transducers are used in many medical or industrial domains and most probably these developed products are not optimized. This leaves many open doors

and optimization improvements in perspective.

Bibliography

- [1] M. Ali and P. Kaelo. Integrated crossover rules in real coded genetic algorithms. *Eur. J. Oper. Res.*, 176:60–76, 2007.
- [2] H. Allik and T. J. R. Hughes. Finite element method for piezoelectric vibration. *International Journal for Numerical Methods in Engineering*, 2:151 – 157, 1970. doi: 10.1002/nme.1620020202.
- [3] A. Bourquard. Optimisation d’un instrument chirurgical ultrasonique par algorithmes génétiques. Projet de Semestre, EPFL-LAI, 2008.
- [4] R. Clavel. *Méthodologie de Construction*. EPFL, 1987.
- [5] J. Fernandez Lopez. *Modeling and optimization of ultrasonic linear motors*. PhD thesis, EPFL, 2006. URL <http://library.epfl.ch/theses/?nr=3665>.
- [6] A.-R. Hedar. Global optimization test problems. URL http://www-optima.amp.i.kyoto-u.ac.jp/member/student/hedar/Hedar_files/TestG0.htm.
- [7] A. Lemonge and H. Barbosa. An adaptive penalty scheme for genetic algorithms in structural optimization. *Int. J. Numer. Methods Eng.*, 59:703–736, 2004.
- [8] H. Maaranen, K. Miettinen, and A. Penttinen. On initial populations of a genetic algorithm for continuous optimization problems. *J. of Global Optim.*, 37:405–436, 2007.
- [9] S. Moaveni. *Finite Element Analysis, Theory and Application with ANSYS, 3rd Edition*. Prentice Hall, 3 edition, 2008.
- [10] C. Moon, J. Kim, G. Choi, and Y. Seo. An efficient genetic algorithm for the traveling salesman problem with precedence constraints. *Eur. J. Oper. Res.*, 140:606–617, 2002.
- [11] J. Murphy, D. Porto, and Y. Perriard. Ultrasonic transducer model for optimization of a spinal tissue ablation system. In *Industry Applications Conference, 2006. 41st IAS Annual Meeting. Conference Record of the 2006 IEEE*, volume 1, pages 379–384, Oct. 2006. doi: 10.1109/IAS.2006.256550.

- [12] J. M. Murphy. *Analytical design and optimization of ultrasonic vibrational transducers for spinal surgery*. PhD thesis, EPFL, Lausanne, 2007. URL <http://library.epfl.ch/theses/?nr=3756>.
- [13] T. Schaffter. Optimisation d'un moteur synchrone à l'aide d'algorithmes génétiques. Projet de Semestre, EPFL, 2007.
- [14] L. Snyder and M. Daskin. A random-key genetic algorithm for the generalized traveling salesman problem. *Eur. J. Oper. Res.*, 174:38–53, 2006.
- [15] R.-L. Wang and K. Okazaki. An improved genetic algorithm with conditional genetic operators and its application to set-covering problem. *Soft Comput.*, 11:687–694, 2007.
- [16] www.mathworks.com. Genetic algorithm and direct search toolbox 2. User's guide, Matlab, 2007.

List of Figures

1.1	Normal Spinal Disc Segment and Manual Disc Removal Technique	2
2.1	Sliding Wire Axial and Rotational	13
2.2	Linked Tube with Internal Sliding Wire	14
2.3	Resonant Beam	15
2.4	Resonant Horn	15
2.5	Floating Head	16
2.6	Rubber Inside Flexible Tube	16
2.7	Bellows Coupling	17
2.8	Bendable Tube with Internal Sliding Wire on Guides	18
2.9	Flexible Electrical Cable	18
2.10	Flexible Tube with Incompressible Liquid	19
2.11	Combination Resonant Beam and Flexible Tube with Incompressible Liquid	19
2.12	Resonant Horn	24
2.13	Expanding Ball	25
2.14	Impact Printer Concept	25
2.15	Scissored Beams	26
2.16	Pinching Fingers	27
2.17	Cantilever Foot	27
2.18	Rotational Lever	28
2.19	Bow Strain	28
2.20	4 Bar Linkage	29
2.21	Molecular Scale Mechanical Amplifier	29
2.22	Bimorph Trimorph	30
2.23	Dual Fixed End Bimorph	30

2.24	Hydraulic Amplifier	31
2.25	Integrated Lever	32
2.26	Multiple Element Piezoelectric Stack	32
2.27	Free Mass	33
2.28	Constrained Mass	33
2.29	Simple Blade with a Tip and Knife Blade	38
2.30	Blade with a Fixed Base	39
2.31	Needle Blade	39
2.32	Scissors Ball	39
2.33	Scissors Piezo	39
2.34	Cavitation Jet	40
2.35	Multiple Pyramidal Cutter	40
2.36	Curved Shank Cutter	41
2.37	Rasp	41
2.38	Apposing Cutters	42
2.39	Apposing Cutters II	42
2.40	Resonant Tube	43
2.41	Resonant Tube with Sharpened Screen	43
2.42	Large Area Tips	44
2.43	Combination of the Different Partial Function Solutions	48
3.1	Young's Modulus Definition	50
3.2	Quarter Wavelength $\lambda/4$ for Metal Materials Used	54
3.3	Quarter Wavelength $\lambda/4$ for Piezoelectric Materials	55
3.4	Piezoelectric 2D Elements	58
3.5	Piezoelectric 3D Elements	58
3.6	Equivalent Circuit	59
4.1	Local and Global Maxima or Minima	63
4.2	Schematic Representation of a Basic GA	65
4.3	One-Point and Two-Point Crossovers	68
4.4	Uniform Crossover	68
4.5	Minimal Difference-Degree Evolution	77
4.6	Rastrigin (left) & Zakharov (right) Test Functions	78
4.7	Ackley Test Function	78
4.8	Population and Children Performance	81
4.9	MATLAB and ANSYS Process Flow	82
5.1	Piezoelectric Stack	86

5.2	Transmission Rod Section	87
5.3	Step Horn Model	87
5.4	Exponential Horn Model	88
5.5	Complete Transducer Model	89
5.6	First Prototype 2D Model	89
5.7	Vibration Amplitude for the 2D & 3D Models	90
5.8	Impedance for the 2D Model	90
5.9	Vibrational Amplitude and Impedance for the 2D Model	91
5.10	Displacement and Impedance in 2D Model at Varying Mesh Sizes	92
5.11	Second Prototype ANSYS 2D Model	93
5.12	Vibration Amplitude for the 2D & 3D Models	94
5.13	Impedance for the 2D Model	95
5.14	Vibrational Amplitude and Impedance for the 2D Model	95
5.15	Vibrational Amplitude with Cannulation Effect in the 2D Model	96
5.16	Impedance with Cannulation Effect for the 2D Model	97
5.17	2D Axi-symmetric Ultrasonic Transducer Model	98
5.18	3D View of the Optimized Transducer	99
5.19	Diversity and Objective Values	100
5.20	Real Amplitude Displacement in Transducer Nodes	101
5.21	Harmonic Frequency Response	101
6.1	Electronics	104
6.2	First Prototype Built	105
6.3	First Trial of the Second Prototype Built	106
6.4	Second Prototype Cracked Parts	107
6.5	Drawings of the Transmission Region	107
6.6	Second Prototype Cracked Transmission	108
6.7	Piezoelectric Stack Mounting	109
6.8	Shaped End in Cutting Tip	109
6.9	Modified Cutting Tip to Allow Measurements	110
6.10	Measurements Test Setup	110
6.11	Second Prototype: Vibrational Amplitude Displacement	111
6.12	Electrical Impedance and Phase	111
6.13	Spinal Disc Test Bench	112
6.14	First Proto Cutting Procedure	113

List of Tables

1.1	Power Source Selection Criteria	3
1.2	Power Source Results	4
2.1	Transmission Selection Criteria	12
2.2	Transmission Merit Comparisons	21
2.3	Definition of Pass-Fail Criteria	22
2.4	Amplification Selection Criteria	23
2.5	Pass Fail Solution Analysis	34
2.6	Merit Comparisons of Narrowed Solutions	35
2.7	Augmentation Solution Merit Analysis	35
2.8	Cutting General Selection Criteria	36
2.9	Cutting Function Specific Criteria	37
2.10	Cutting Solution Comparisons - Soft Material	45
2.11	Cutting Solution Comparisons - Coarse Material	45
2.12	Material Removal Solutions	45
2.13	Material Shaping Solutions	45
2.14	Coagulation Solutions	45
3.1	Piezoelectric Matrices	52
3.2	Piezoelectric Capability in ANSYS Elements	57
4.1	Parameters Used for Testing Algorithms	79
4.2	Test Function Results for Unconstrained Functions	80
5.1	First Prototype Parameters	89
5.2	Nucleus Removal System Parameters	94
5.3	Parameters Dimensions to be Optimized	99
5.4	Optimized Parameters Results	99

A.1 Selection Matrix of Cutting Methods	132
---	-----

Appendices

Appendix A

Technology Narrowing

Table A.1: Selection Matrix of Cutting Methods

Cutting Method: Scalpel		
C1	false	Has no power source
C2	1	Cuts any tissue provided there is enough force applied
C3	1	Rigid Body
C4	1	Makes singles cuts that must be connected to remove a portion of material.
C5	1	No means to cause a cauterizing effect unless the scalpel were heated.
Cutting Method: Ultrasonics		
C1	true	Provides power to the source
C2	8	Frequency and power output can be varied to obtain many different cutting characteristics based on the material properties of the work piece
C3	8	1. The standard piezo-driven ultrasonics can be guided to some degree and remain effective. 2. Other magnetostrictive materials allow the transducer to be placed at the end of a steerable tool.
C4	9	Ultrasonics provide intense localized heating that can vaporize materials. In liquids it is also possible to generate cavitation bubbles that facilitates the removal of material in an ablative manner.
C5	10	Very good cauterizing effect when a tool that is optimized for cauterization is brought into contact with tissue to be sealed.
Cutting Method: Electro Mechanical Shaver		
C1	true	Provides power to the source
C2	3	Shaver blades can be designed that are more or less aggressive to allow for some selectivity
C3	3	Shaver blades can be shaped but retain that shape during the procedure. A rebending process or selection of a new blade would be necessary for constant variability.
C4	3	Particle size is determined by the holes in the stationary and rotating tubes or by a burr that can be used at the end of the rotating tube.
C5	1	No means to cause a cauterizing effect unless the blade were heated.
Cutting Method: Laser		
C1	true	Provides power to the source
C2	5	The frequency of light can be varied so that some materials are opaque while others are translucent. A drawback is the difficulty in changing the light frequency on the fly and the number of materials that can be selected in this manner.
C3	8	Laser light can be introduced into the site by means of a flexible fiber. This fiber can be bent and twisted to provide good access through a small access hole. The access would be limited by the bend radius of the fiber and the ability to keep the light at total internal reflection in the fiber.
C4	10	Localized high temperatures caused by the incident laser beam can be used to vaporize material.
C5	8	Could be used but would expect less control over the process than with other means, because the laser beam would tend to remove material while the coagulation process was occurring.

Appendix B

Material Properties

B.1 Aluminium Alloy EN-AW-7075

Density: $\rho = 2810 \text{ kg/m}^3$

Young's Modulus: $E_Y = 72 \cdot 10^9 \text{ N/m}^2$

Poisson's ratio: $\nu = 0.33$

B.2 Titanium Alloy T-6Al-4V-STA

Density: $\rho = 4430 \text{ kg/m}^3$

Young's Modulus: $E_Y = 114 \cdot 10^9 \text{ N/m}^2$

Poisson's ratio: $\nu = 0.33$

B.3 Piezoelectric PZ-28

Density: $\rho = 7700 \text{ kg/m}^3$

Compliance matrix:

$$s^E = \begin{bmatrix} 12.6 & -3.71 & -6.6 & 0 & 0 & 0 \\ & 12.6 & -6.6 & 0 & 0 & 0 \\ & & 18.3 & 0 & 0 & 0 \\ \text{Symmetric} & & & 39 & 0 & 0 \\ & & & & 39 & 0 \\ & & & & & 32.6 \end{bmatrix} \cdot 10^{12} \text{ m}^2/\text{N} \quad (\text{B.1})$$

Piezoelectric matrix:

$$\mathbf{d} = \begin{bmatrix} 0 & 0 & 0 & 0 & 403 & 0 \\ 0 & 0 & 0 & 403 & 0 & 0 \\ -114 & -114 & 275 & 0 & 0 & 0 \end{bmatrix} \cdot 10^{-12} \text{ C/N} \quad (\text{B.2})$$

Relative dielectric permittivity matrix:

$$\frac{\epsilon^T}{\epsilon_0} = \begin{bmatrix} 1220 & 0 & 0 \\ 0 & 1220 & 0 \\ 0 & 0 & 1300 \end{bmatrix}, \quad \epsilon_0 = 8.854 \cdot 10^{-12} \text{ F/m} \quad (\text{B.3})$$

B.4 Piezoelectric PZ-54

Density: $\rho = 7760 \text{ kg/m}^3$

Compliance matrix:

$$\mathbf{s}^E = \begin{bmatrix} 13.8 & -4.45 & -6.89 & 0 & 0 & 0 \\ & 13.8 & -6.89 & 0 & 0 & 0 \\ & & 18.6 & 0 & 0 & 0 \\ & \text{Symmetric} & & 35 & 0 & 0 \\ & & & & 35 & 0 \\ & & & & & 36.4 \end{bmatrix} \cdot 10^{12} \text{ m}^2/\text{N} \quad (\text{B.4})$$

Piezoelectric matrix:

$$\mathbf{d} = \begin{bmatrix} 0 & 0 & 0 & 0 & 500 & 0 \\ 0 & 0 & 0 & 500 & 0 & 0 \\ -201 & -201 & 479 & 0 & 0 & 0 \end{bmatrix} \cdot 10^{-12} \text{ C/N} \quad (\text{B.5})$$

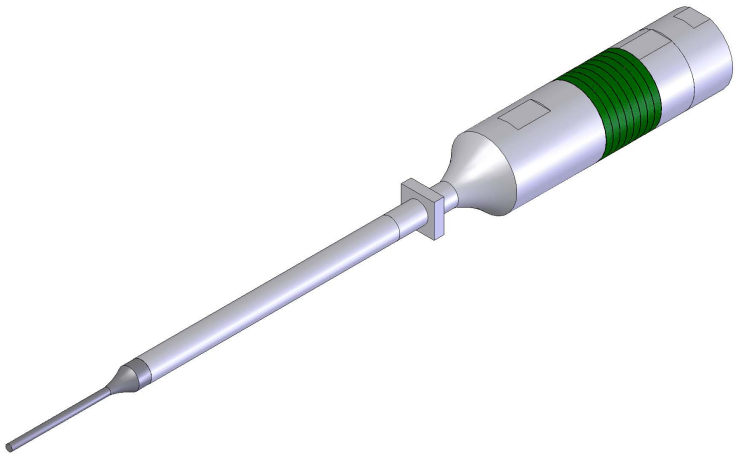
Relative dielectric permittivity matrix:

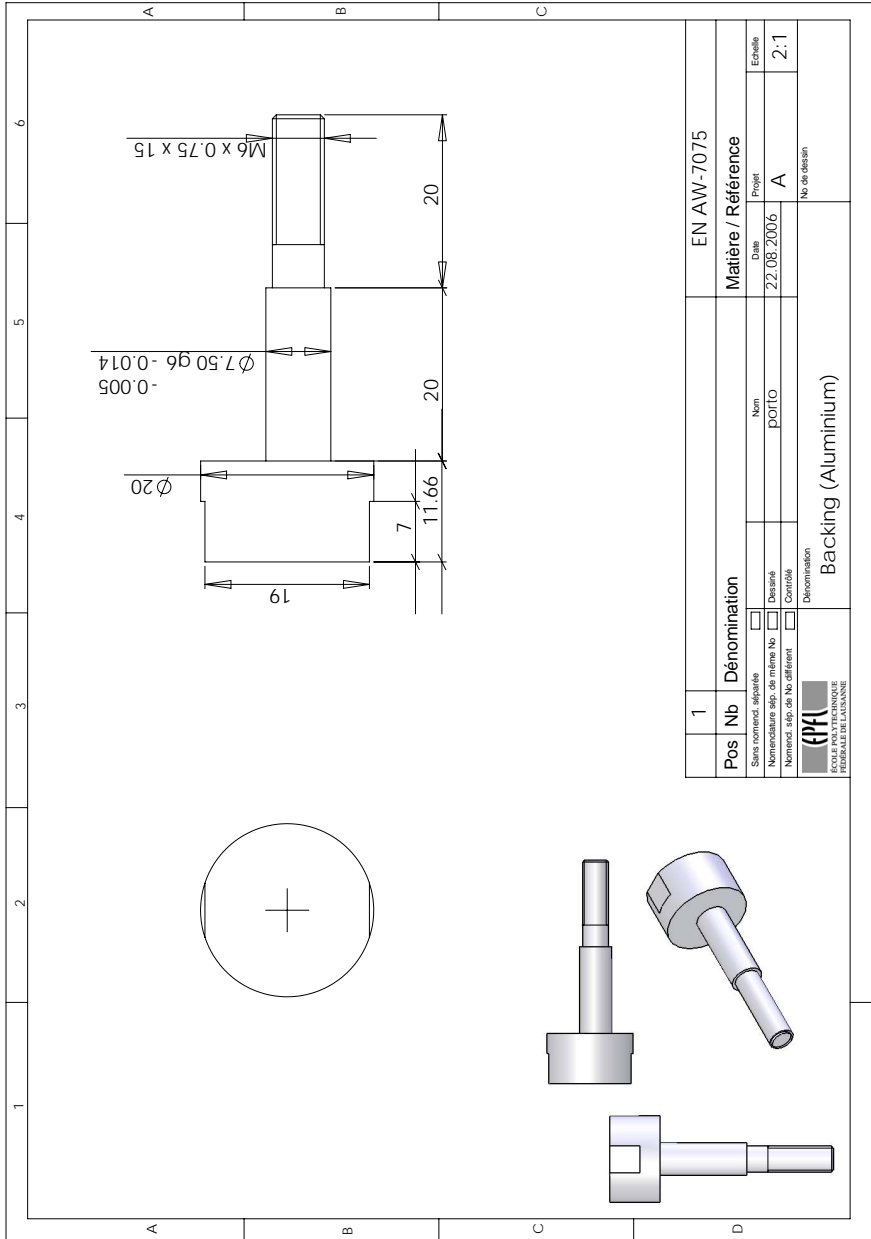
$$\frac{\epsilon^T}{\epsilon_0} = \begin{bmatrix} 2870 & 0 & 0 \\ 0 & 2870 & 0 \\ 0 & 0 & 2870 \end{bmatrix}, \quad \epsilon_0 = 8.854 \cdot 10^{-12} \text{ F/m} \quad (\text{B.6})$$


Appendix C

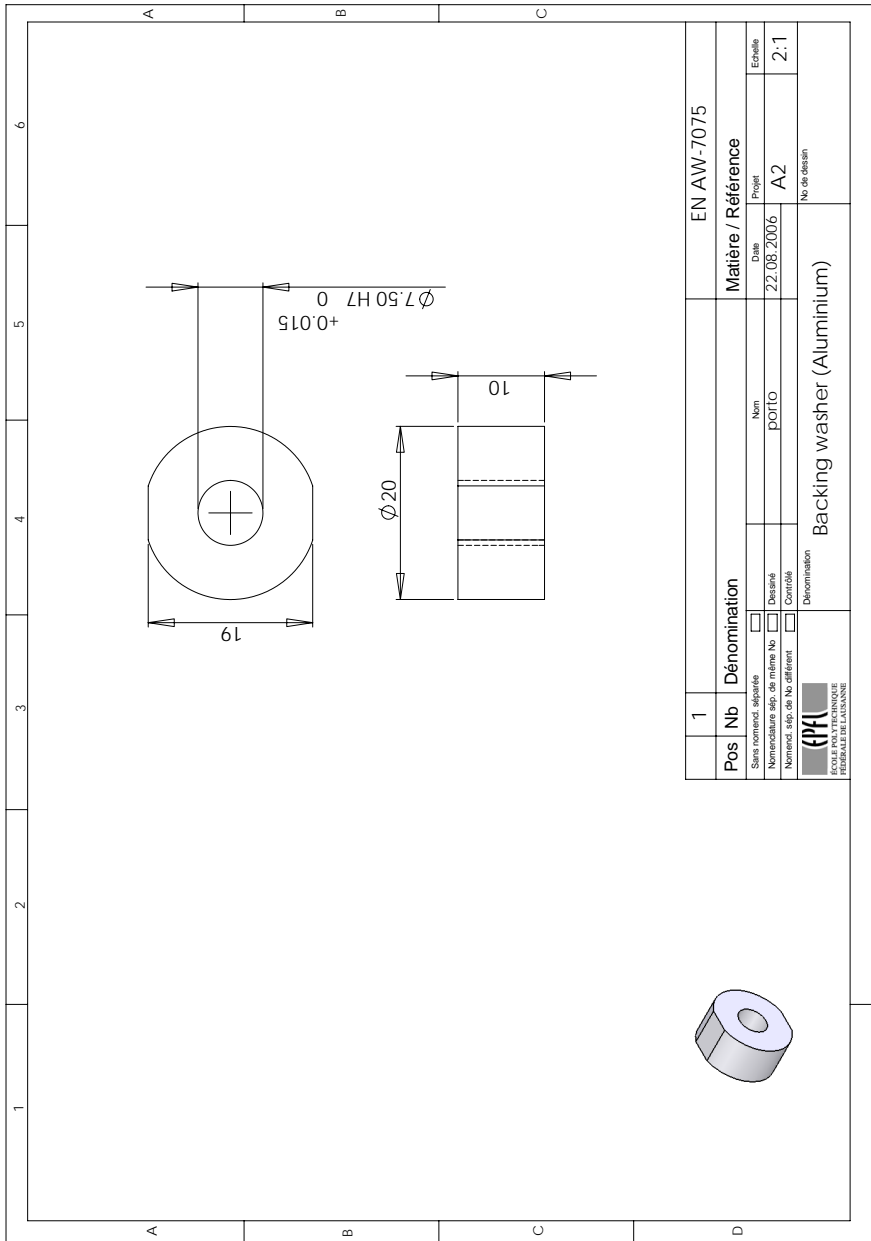
Mechanical Drawings


C.1 First Prototype

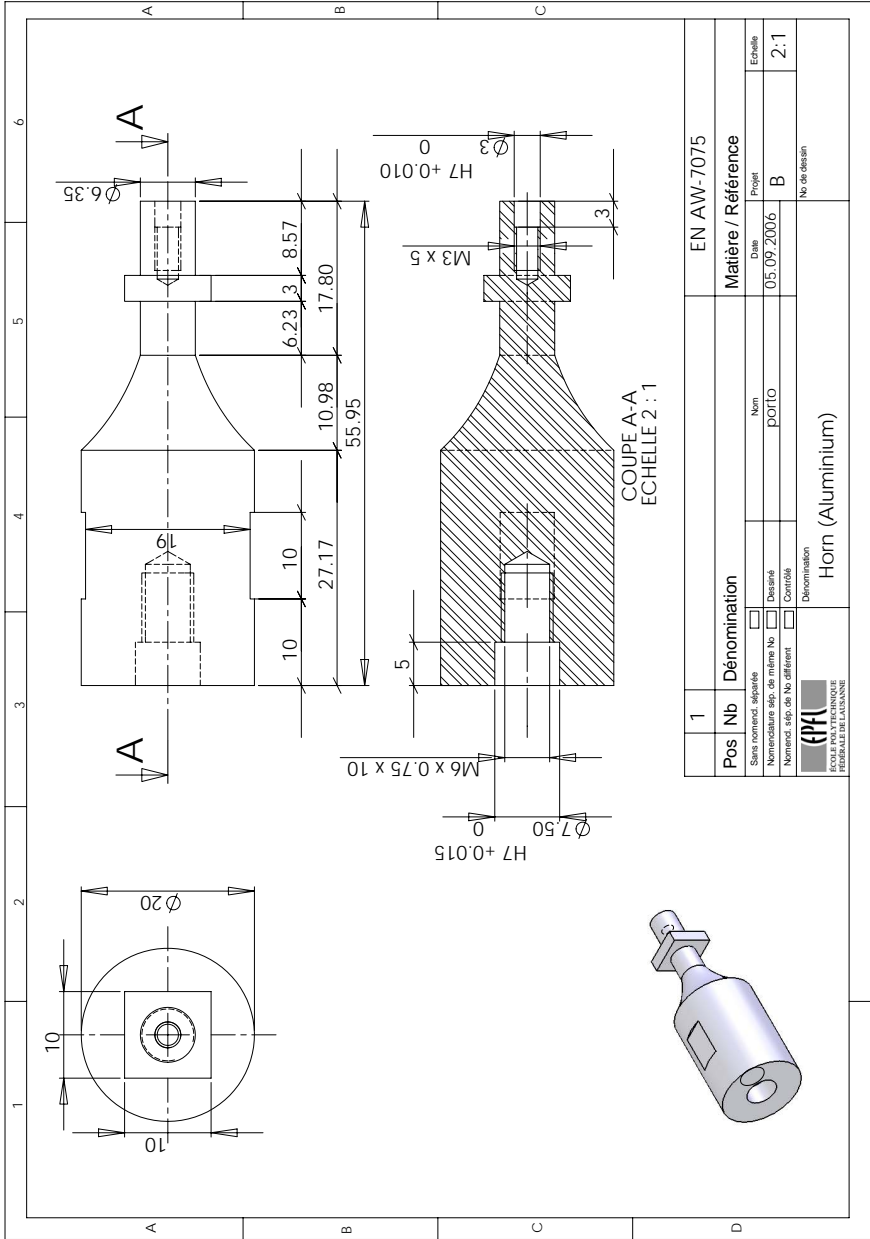





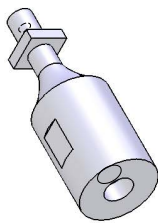
1	EN AW-7075	
Pos Nb	Dénomination	
	Matière / Référence	
	Date	
	Projet	
Sans nomenc. spéciale		Nom
Nomenclature séc. de même No		
Nomencl. séc. de No différent		Contrôle
Date		
22.08.2006		A
Dénomination		
Backing (Aluminium)		2:1
 ÉCOLE POLYTECHNIQUE FÉDÉRALE DE LAUSANNE		

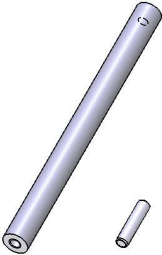
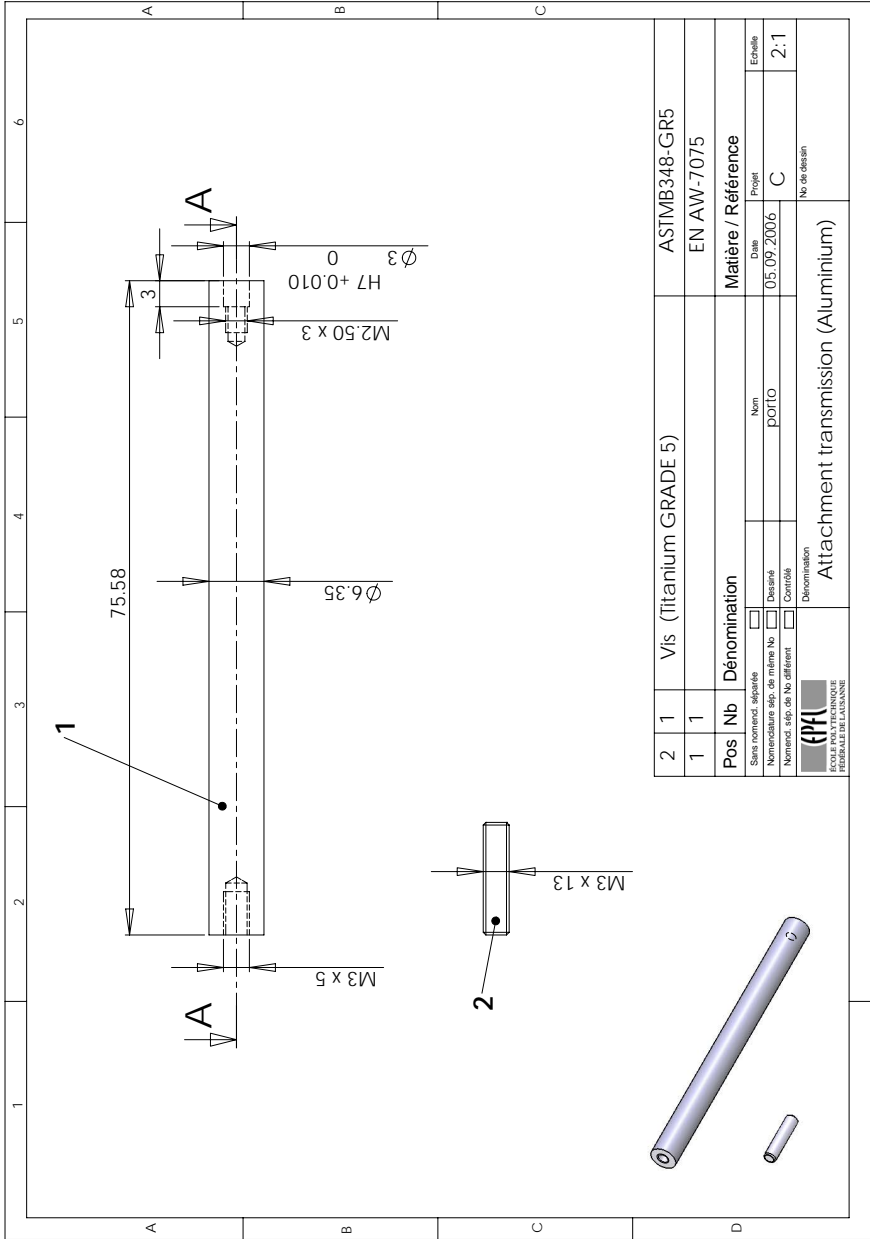


1						EN AW-7075	
Pos	Nb	Dénomination	Matière / Référence				
		<input type="checkbox"/> Sans nomenc. spéciale <input type="checkbox"/> Nomenclature spé. de même Nb <input type="checkbox"/> Nomencl. spé. de No. différent	<input type="checkbox"/> Dessiné <input type="checkbox"/> Contrôlé	Nom porf10	Date 22.08.2006	Projet A2	
 ÉCOLE POLYTECHNIQUE FÉDÉRALE DE LAUSANNE			Dénomination Backing washer (Aluminium)				Nr de dessin 2:1



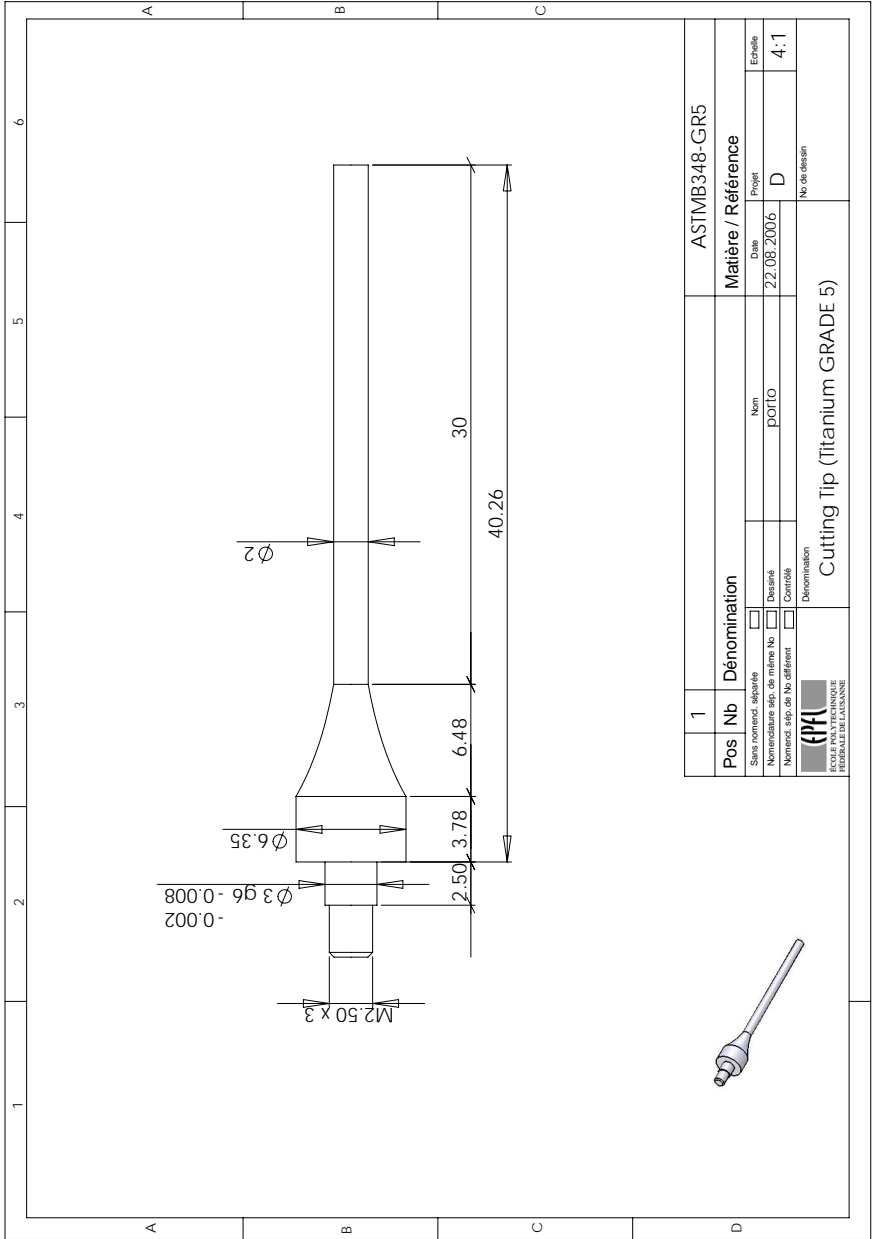
1	Pos Nb	Dénomination	Matière / Référence	EN AW-7075
<input type="checkbox"/> Sans numéro spéciale <input type="checkbox"/> Nomenclature séq. de même No <input type="checkbox"/> Désigné <input type="checkbox"/> Nomencl. séq. de No. différent <input type="checkbox"/> Contrôlé		Nom	Date	Projet
 <small>ÉCOLE POLYTECHNIQUE FÉDÉRALE DE LAUSANNE</small>		Dénomination	05.09.2006 B	
		Horn (Aluminium)		
				Nr de dessin
				2:1




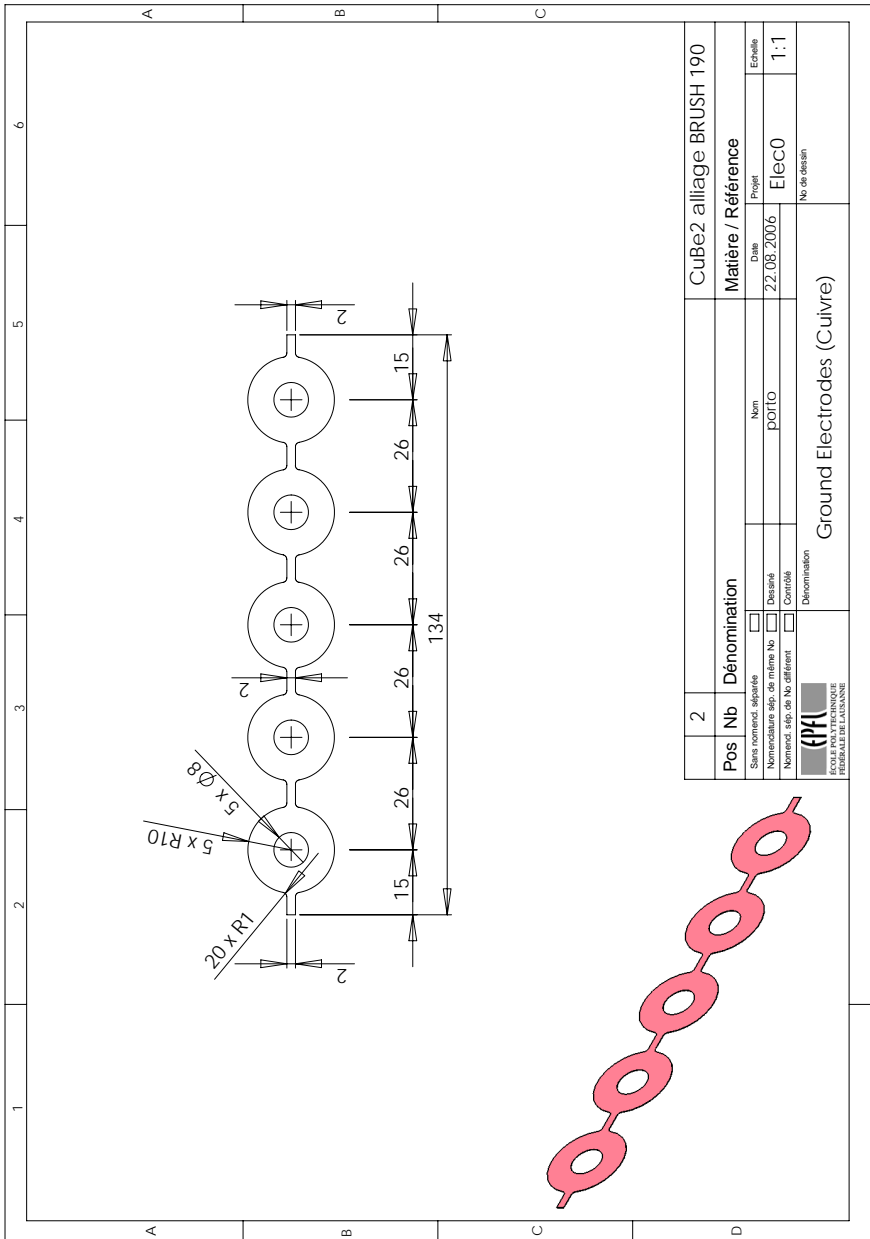


2	1	Vis (Titanium GRADE 5)	ASTMB348-GR5
1	1		EN AW-7075
Pos	Nb	Dénomination	Matière / Référence
		<input type="checkbox"/> Sans nomenc. spéciale <input type="checkbox"/> Nomenclature spécifique <input type="checkbox"/> Nomenclature de même No. <input type="checkbox"/> Nomenclature de No. différent	Date: 05.09.2006 Projet: C No. de dessin:
		<input type="checkbox"/> Désigné <input type="checkbox"/> Contrôlé Dénomination: Attachment transmission (Aluminium)	Echelle: 2:1





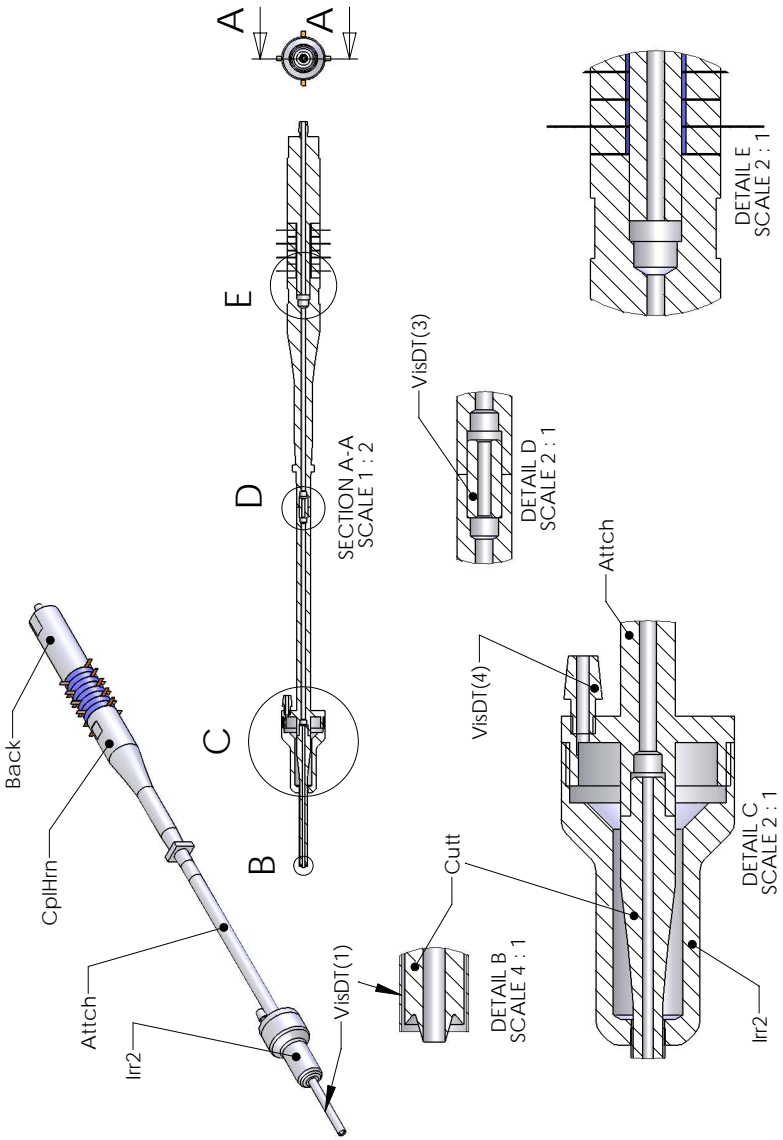
1						ASTM B348-GR5	
Pos	Nb	Dénomination	Matière / Référence				
		<input type="checkbox"/> Sans nommée spéciale <input type="checkbox"/> Nomenclature spécifique de même No <input type="checkbox"/> Nomenclature spécifique de No différent	Nom	Date	Projet	Echelle	
		<input type="checkbox"/> Dessiné <input type="checkbox"/> Contrôlé Dénomination	POUTO	22.08.2006	D	4:1	
 ÉCOLE POLYTECHNIQUE FÉDÉRALE DE LAUSANNE			Cutting Tip (titanium GRADE 5)				Nr de dessin

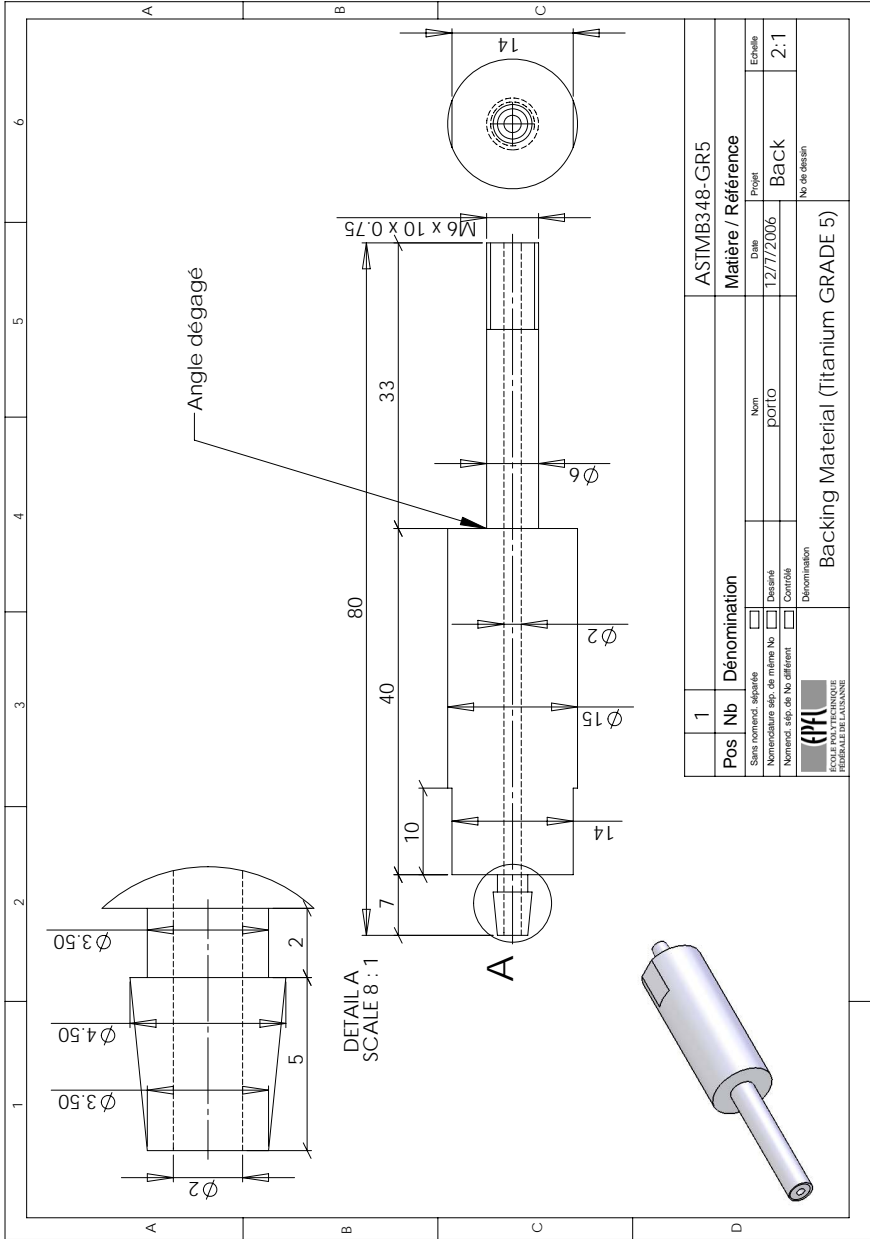


2		CuBe ₂ alliage BRUSH 190		
Pos	Nb	Dénomination	Matériau / Référence	
			Date	Projet
Sans connect. séparée				Echelle
Nomenclature séq. de même No				1:1
Nomenclature séq. de No différent			22.08.2006	Eleco
Contrôle				Nr de dessin
		Ground Electrodes (Cuivre)		
		EPFL ÉCOLE POLYTECHNIQUE FÉDÉRALE DE LAUSANNE		

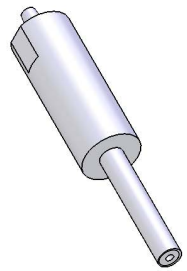
C.2 Second Prototype

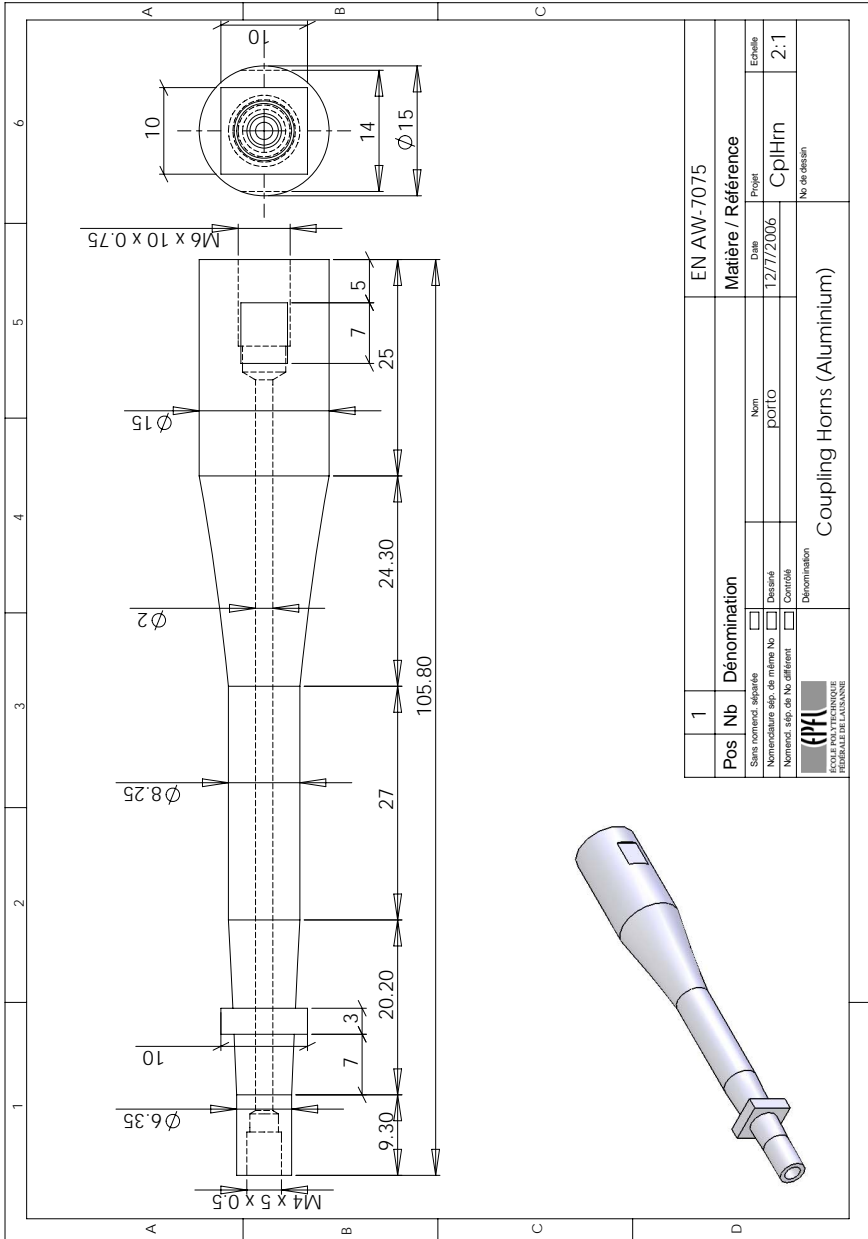





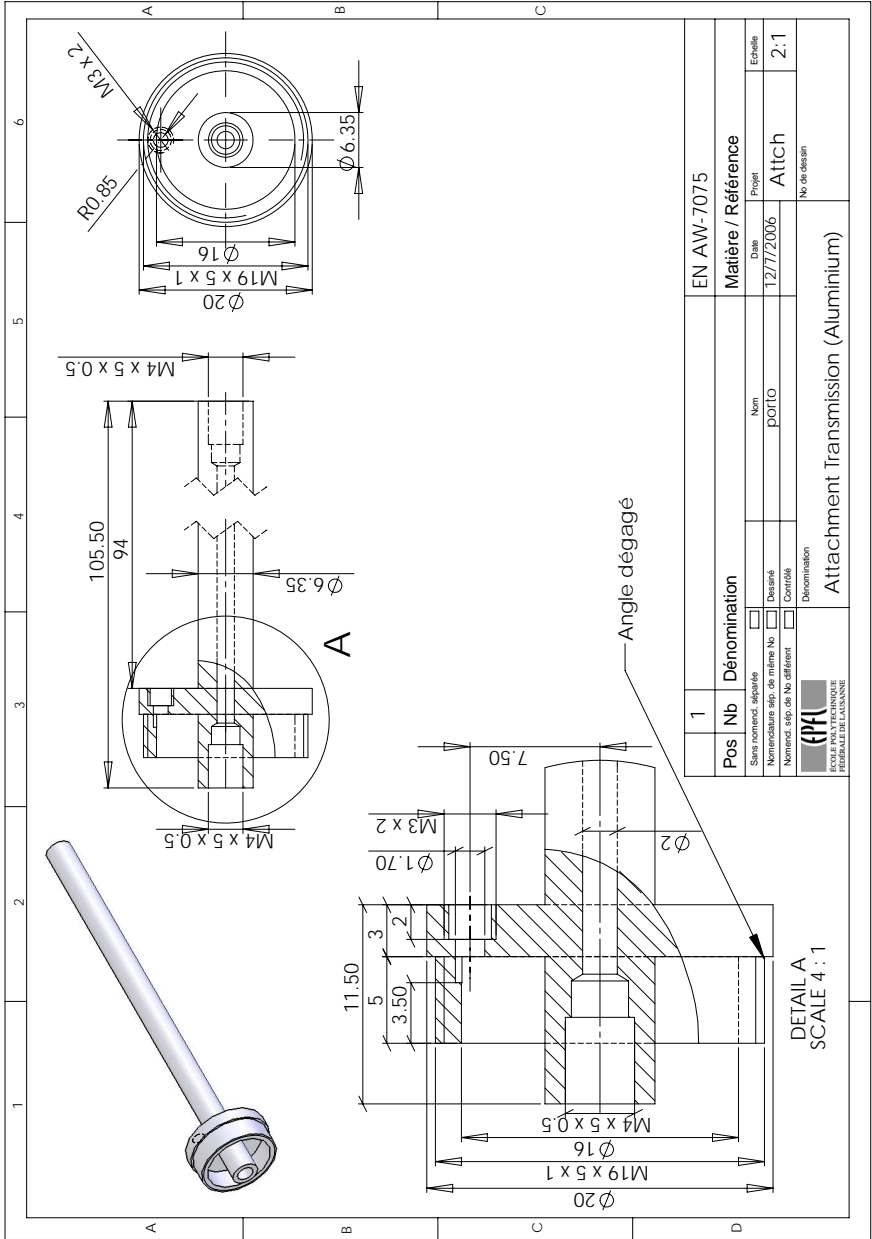


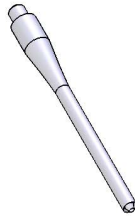
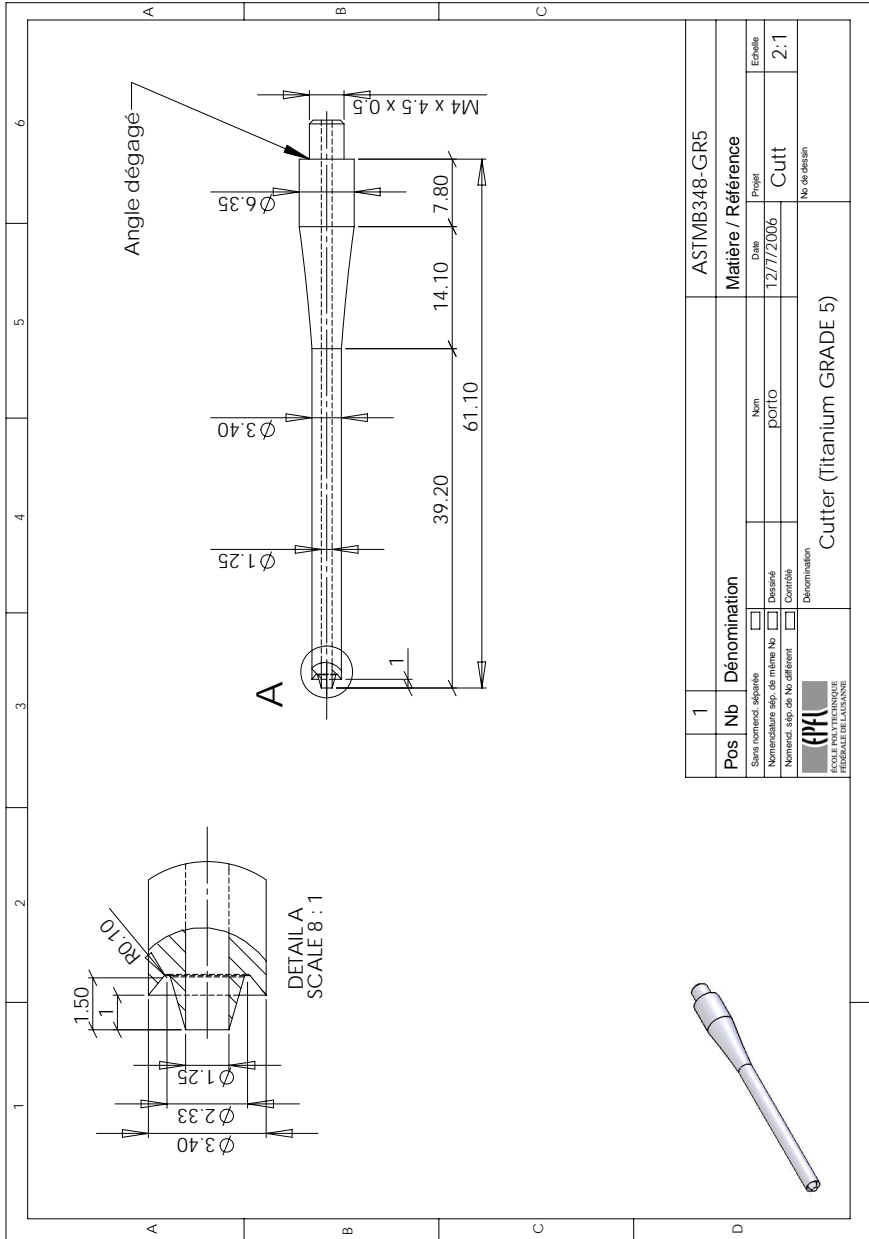
1										ASTMB348-GR5	
Pos	Nb	Dénomination	Nom		Date	Matière / Référence		Projet	Echelle		
		<input type="checkbox"/> Sans command. séparée <input type="checkbox"/> Nomenclature séc. de même No. <input type="checkbox"/> Dessiné <input type="checkbox"/> Nomencl. séc. de No. différent <input type="checkbox"/> Contrôlé	porfo		12/7/2006	Back		2:1			
		Dénomination		No. de dessin							
		EPFL ÉCOLE POLYTECHNIQUE FÉDÉRALE DE LAUSANNE		Backing Material (Titanium GRADE 5)							

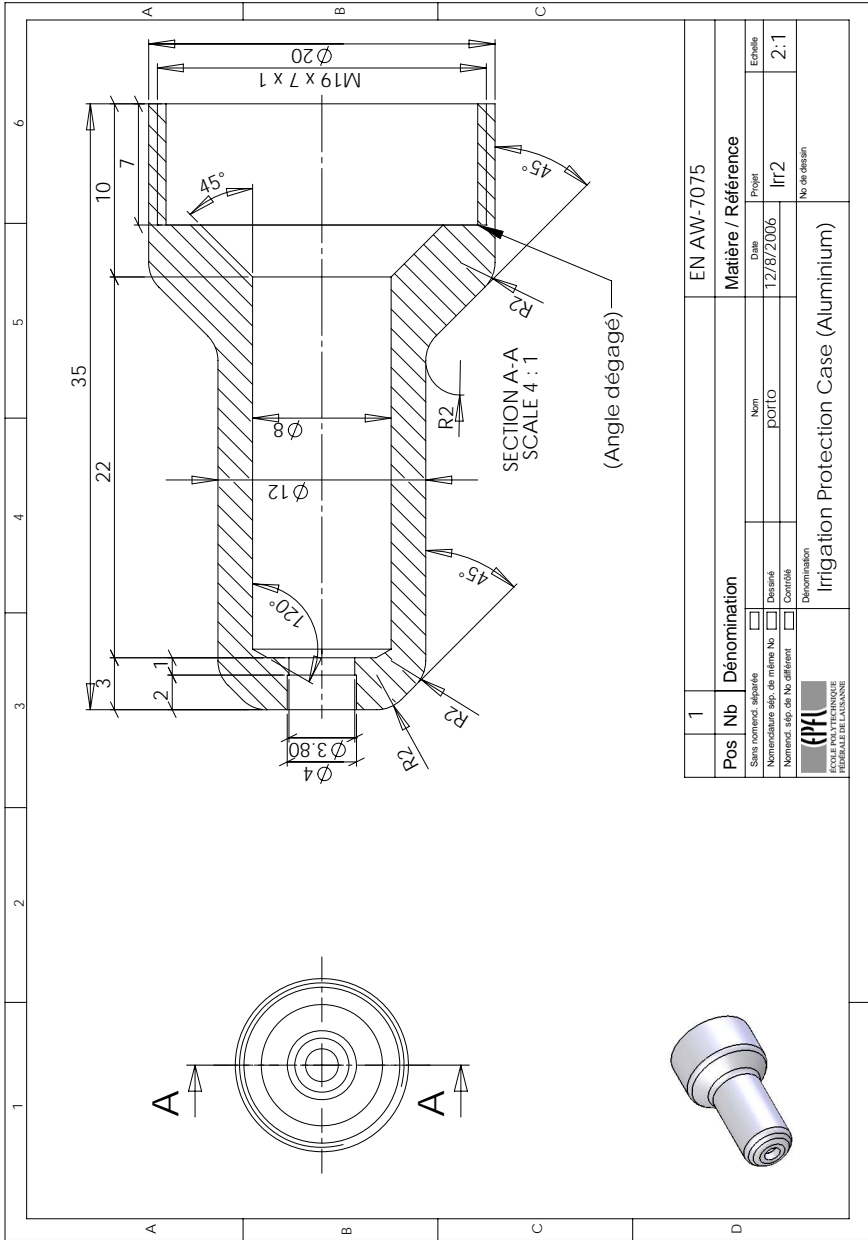





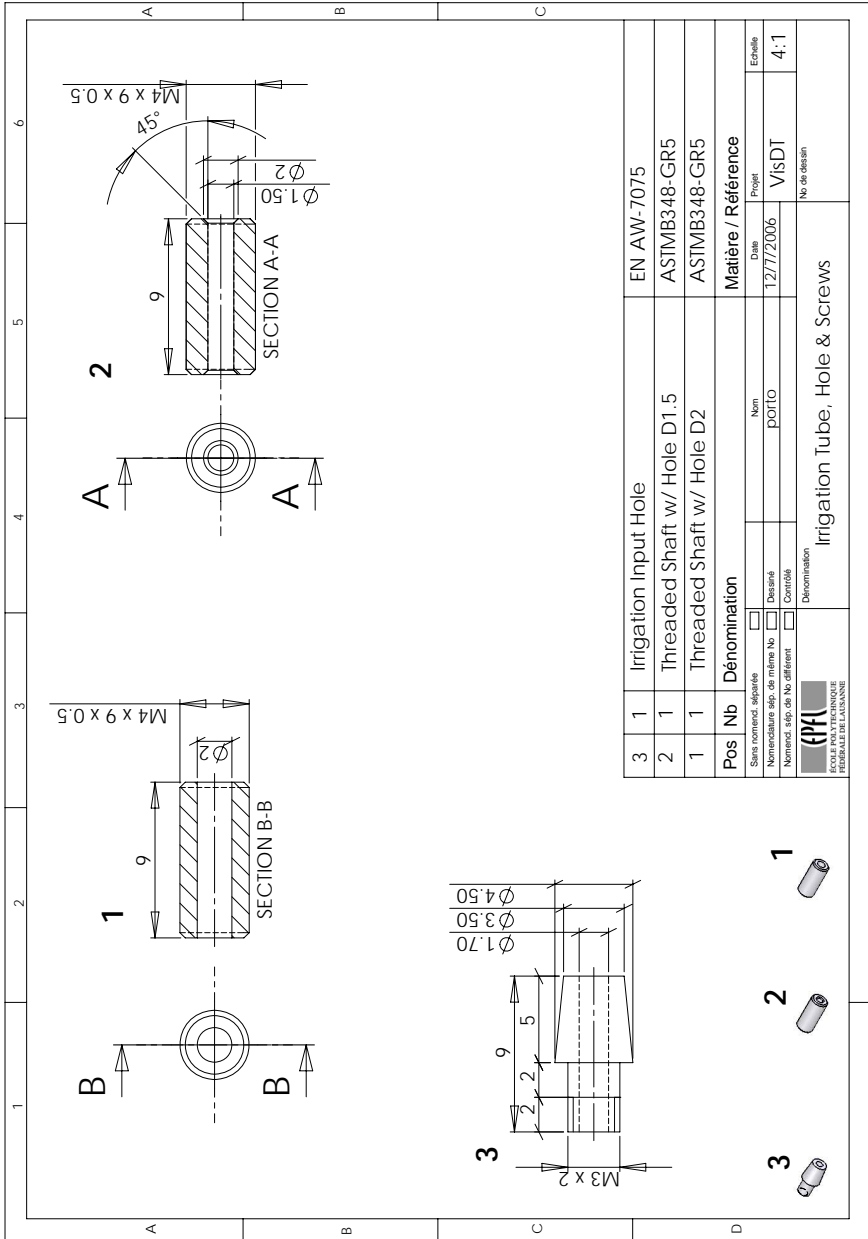
1						EN AW-7075	
Pos	Nb	Dénomination	Matière / Référence		Date		
		<input type="checkbox"/> Sans cotation spéciale <input type="checkbox"/> Nomenclature spécifique de même No <input type="checkbox"/> Désigné <input type="checkbox"/> Nomenclature spécifique de No différent <input type="checkbox"/> Contrôlé	Nom	Date		Projet	
			portFD	12/7/2006		CplHrn	
 Dénomination COUPLAGE ÉCOLE POLYTECHNIQUE FÉDÉRALE DE LAUSANNE			Coupling Horns (Aluminium)				No de dessin 2:1

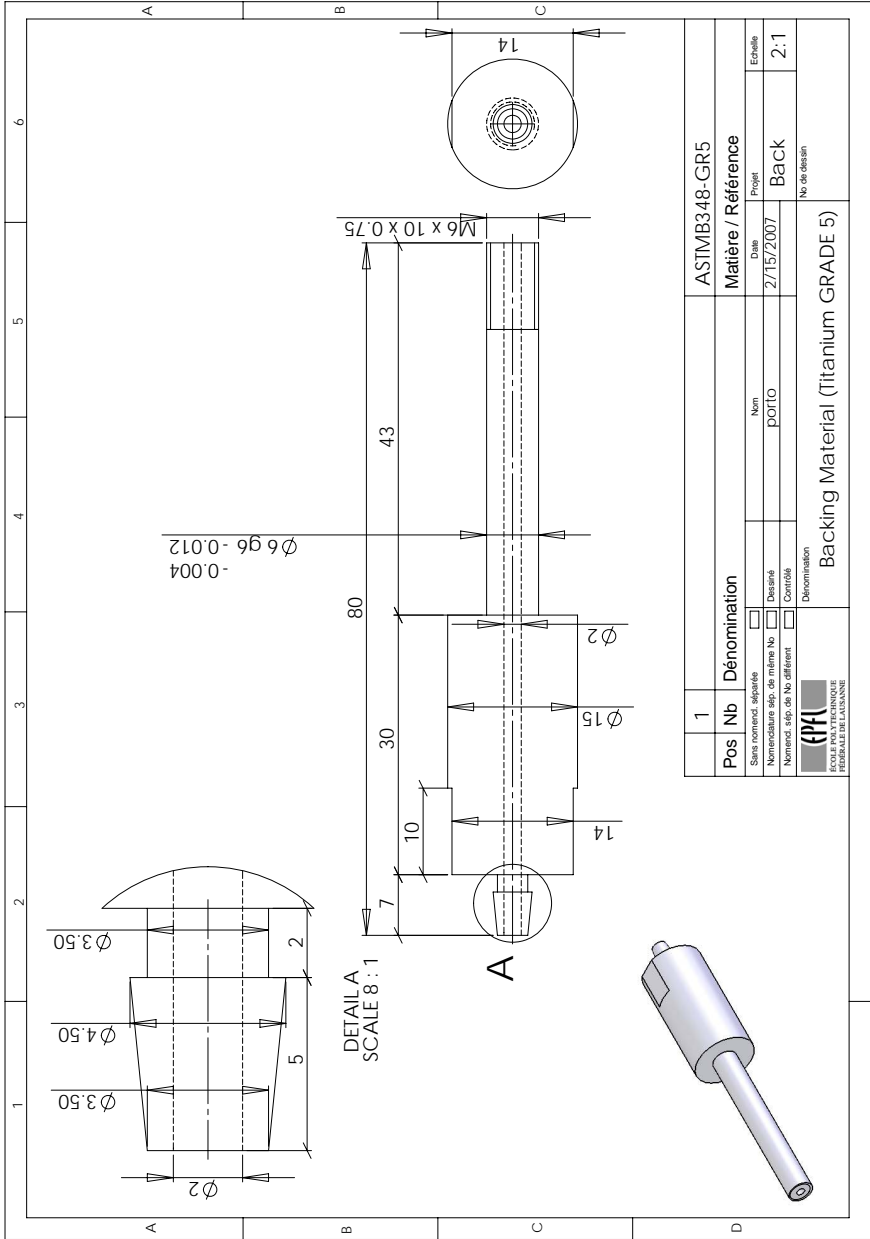


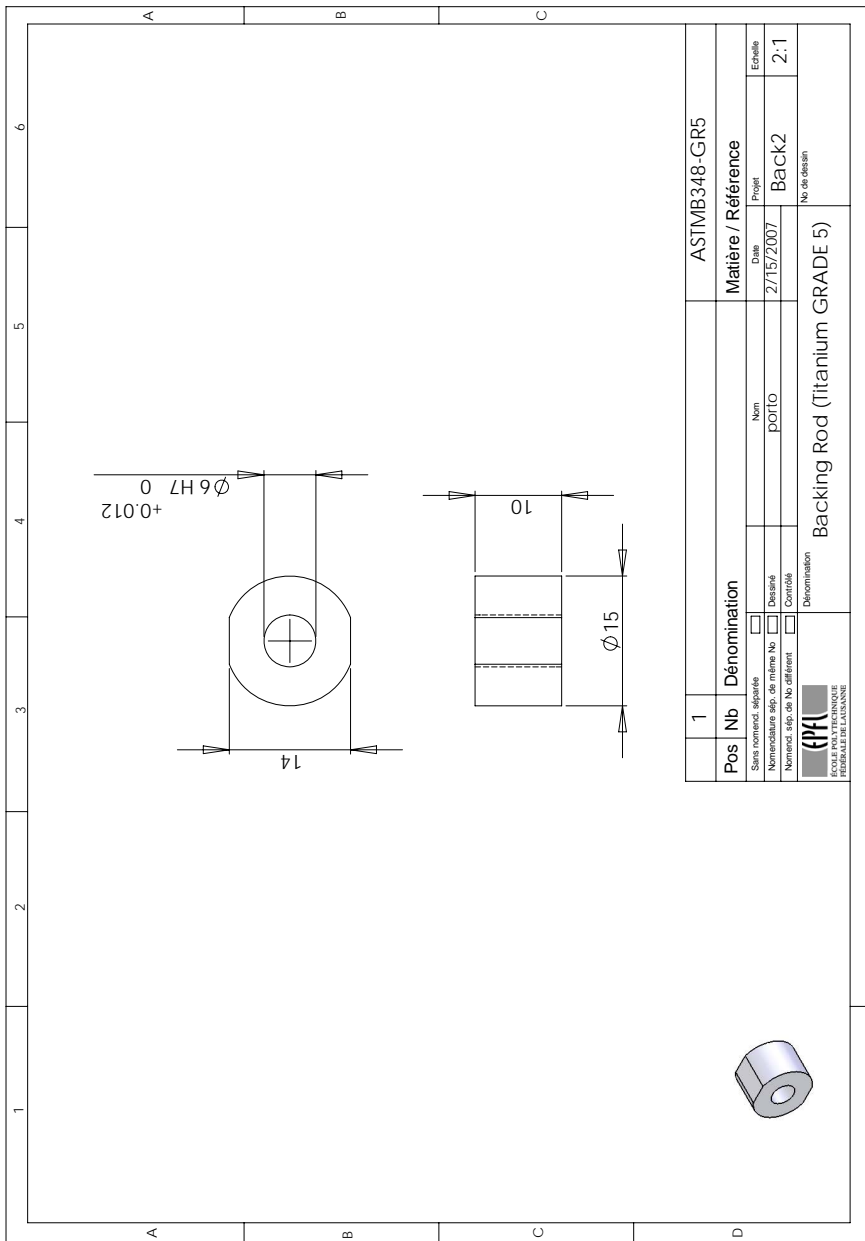





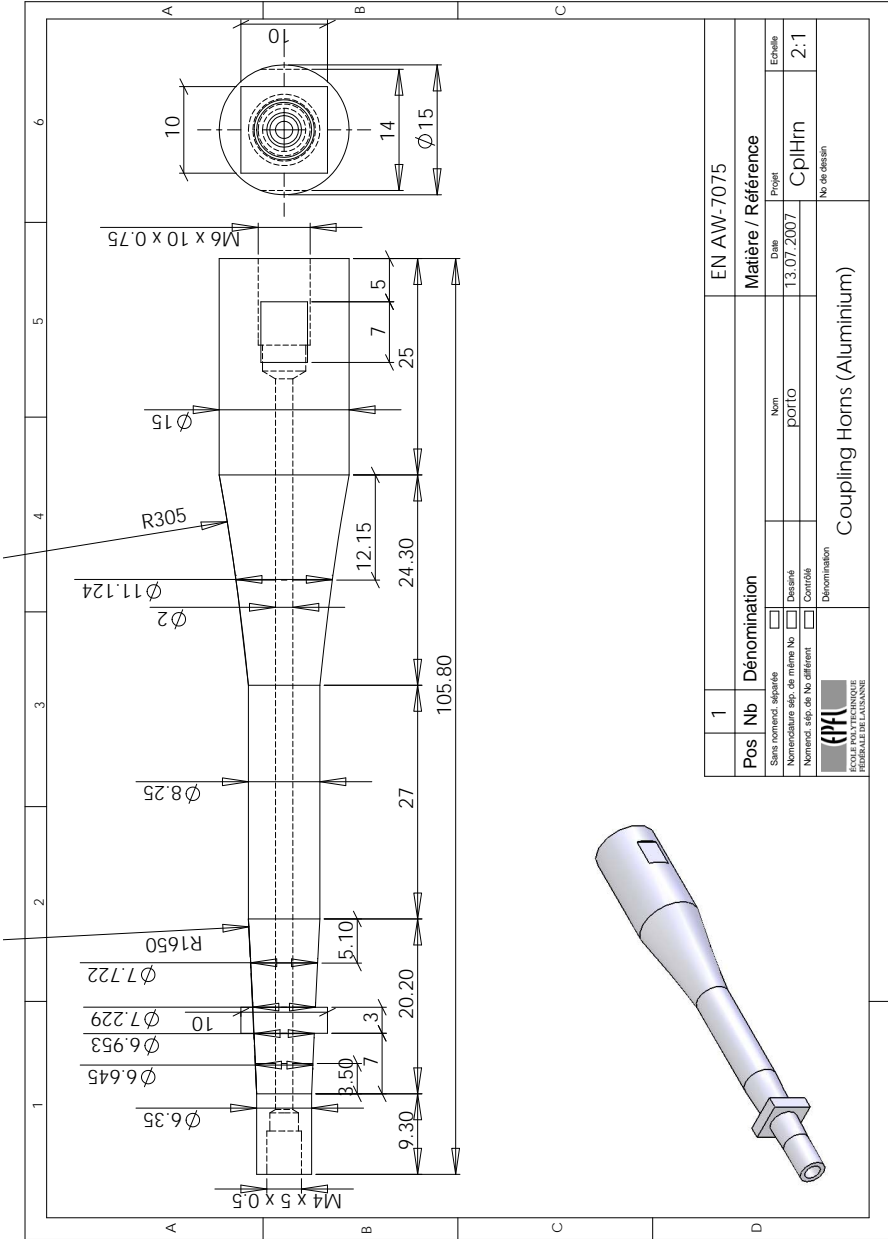
1	EN AW-7075	Matière / Référence	
Pos / Nb	Dénomination	Date	Projet
<input type="checkbox"/> Sans nommée spéciale <input type="checkbox"/> Nomenclature spécifique de même No <input type="checkbox"/> Désignée <input type="checkbox"/> Nomenclature spécifique de No différent <input type="checkbox"/> Contrôlée		12/8/2006	lrr2
 Dénomination Irrigation Protection Case (Aluminium)		No de dessin 2:1	

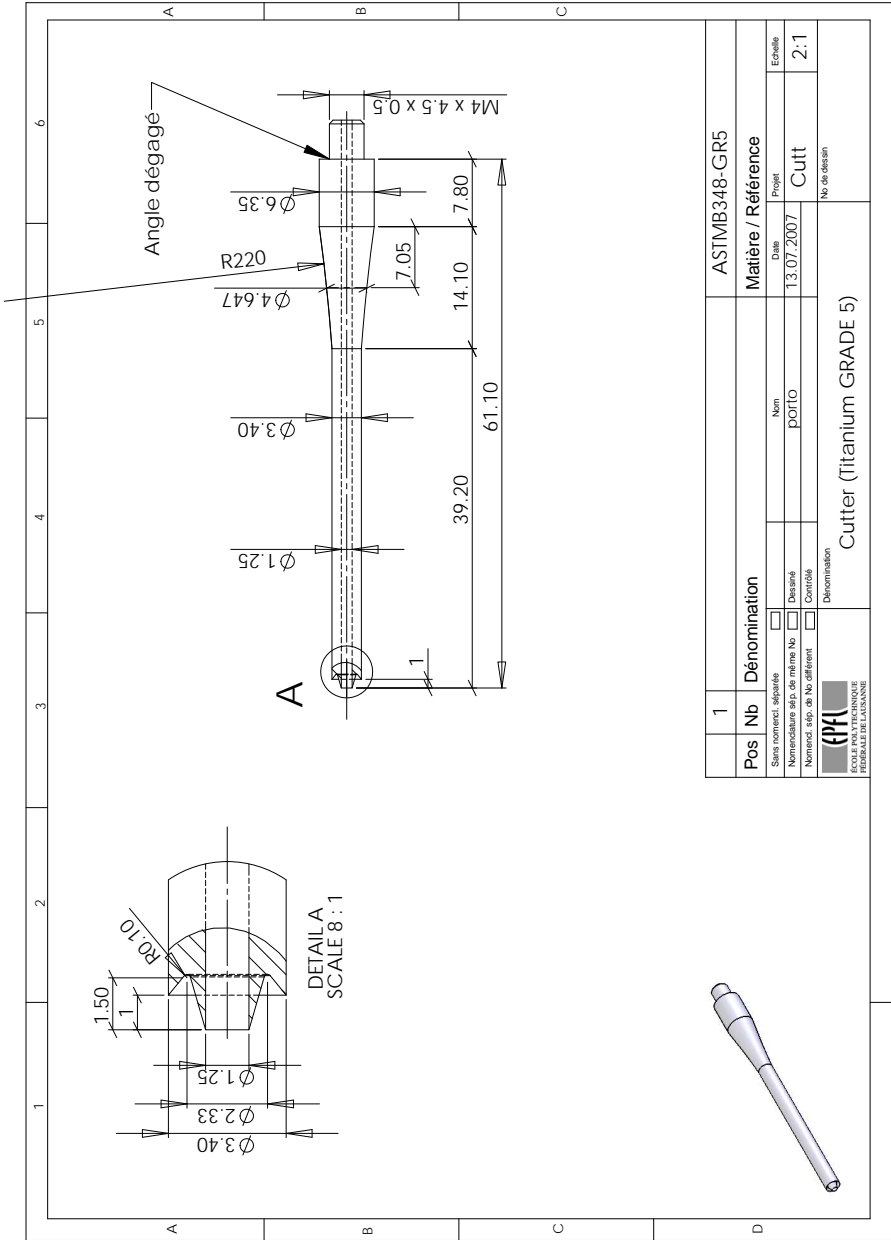




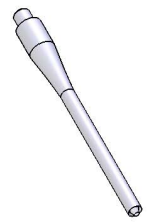


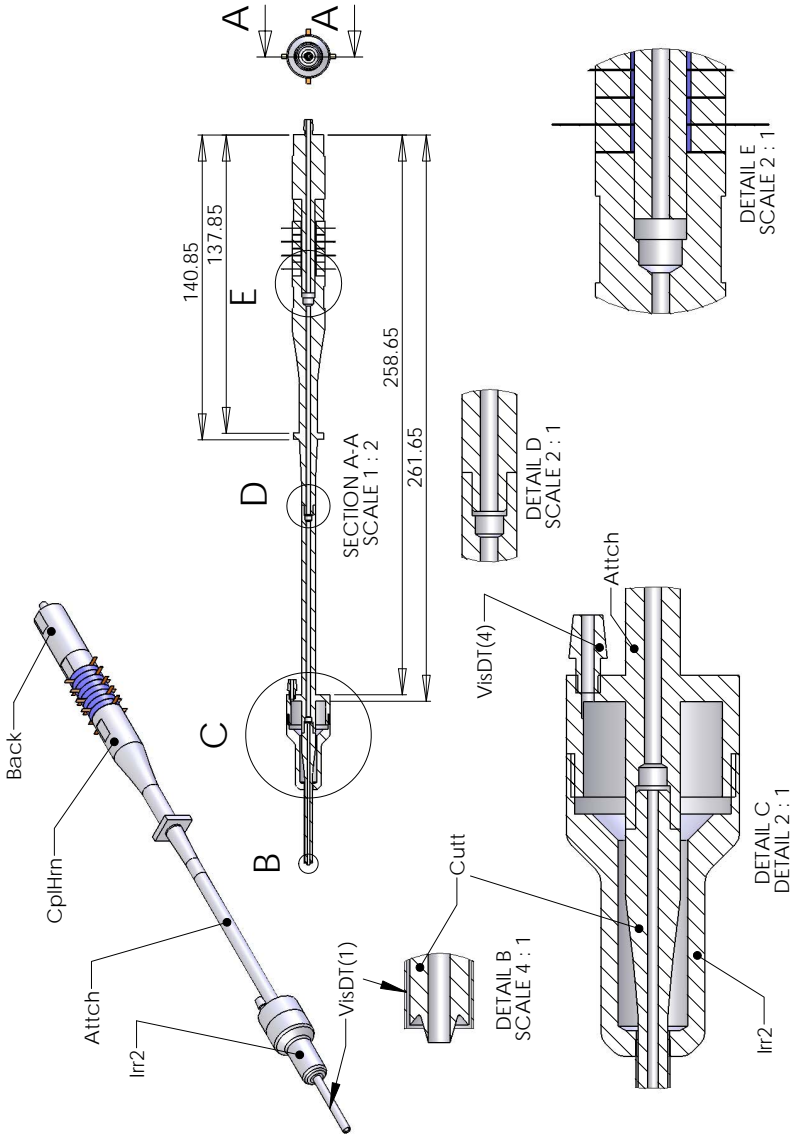
1							ASTM B348-GR5
Pos	Nb	Dénomination	Matière / Référence		Echelle		
		<input type="checkbox"/> Sans nomenc. spéciale <input type="checkbox"/> Nomenclature spé. de même No. <input type="checkbox"/> Dessiné <input type="checkbox"/> Nomenc. spé. de No. différent <input type="checkbox"/> Contrôlé	Nom	Date	Projet	Echelle	
			porf10	2/15/2007	Back2	2:1	
 Dénomination Backing Rod (Titanium GRADE 5)			No. de dessin				
ÉCOLE POLYTECHNIQUE FÉDÉRALE DE LAUSANNE							

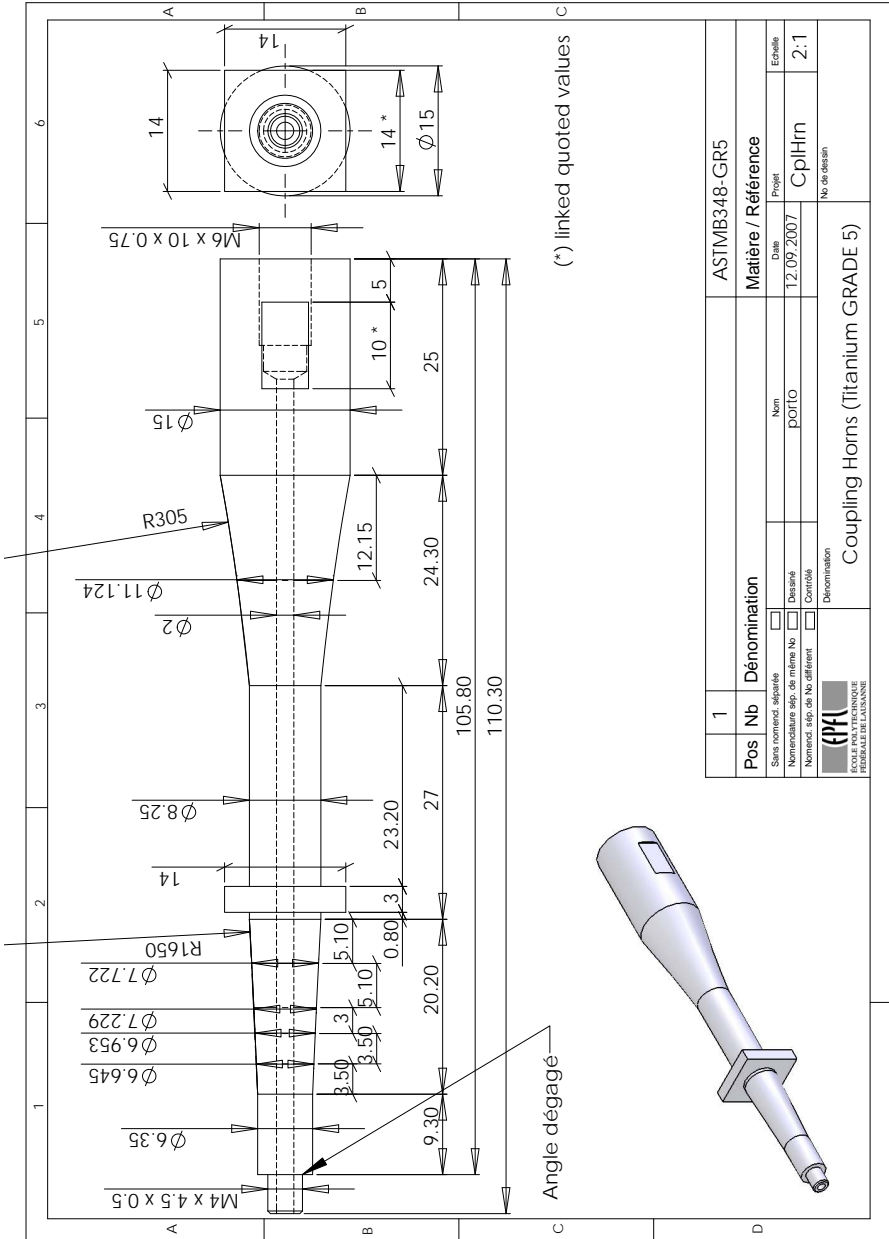




1		ASTMB348-GR5	
Pos	Nb	Matière / Référence	
		ASTMB348-GR5	
Sais commec. séparée		Date	
Nomenclature sûr, de même No		13.07.2007	
Nomencl. sûr, de No différent		Projet	
Contrôle		Cutt	
Dénomination		No de dessin	
Cutter (Titanium GRADE 5)		2:1	

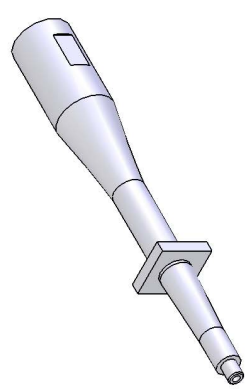


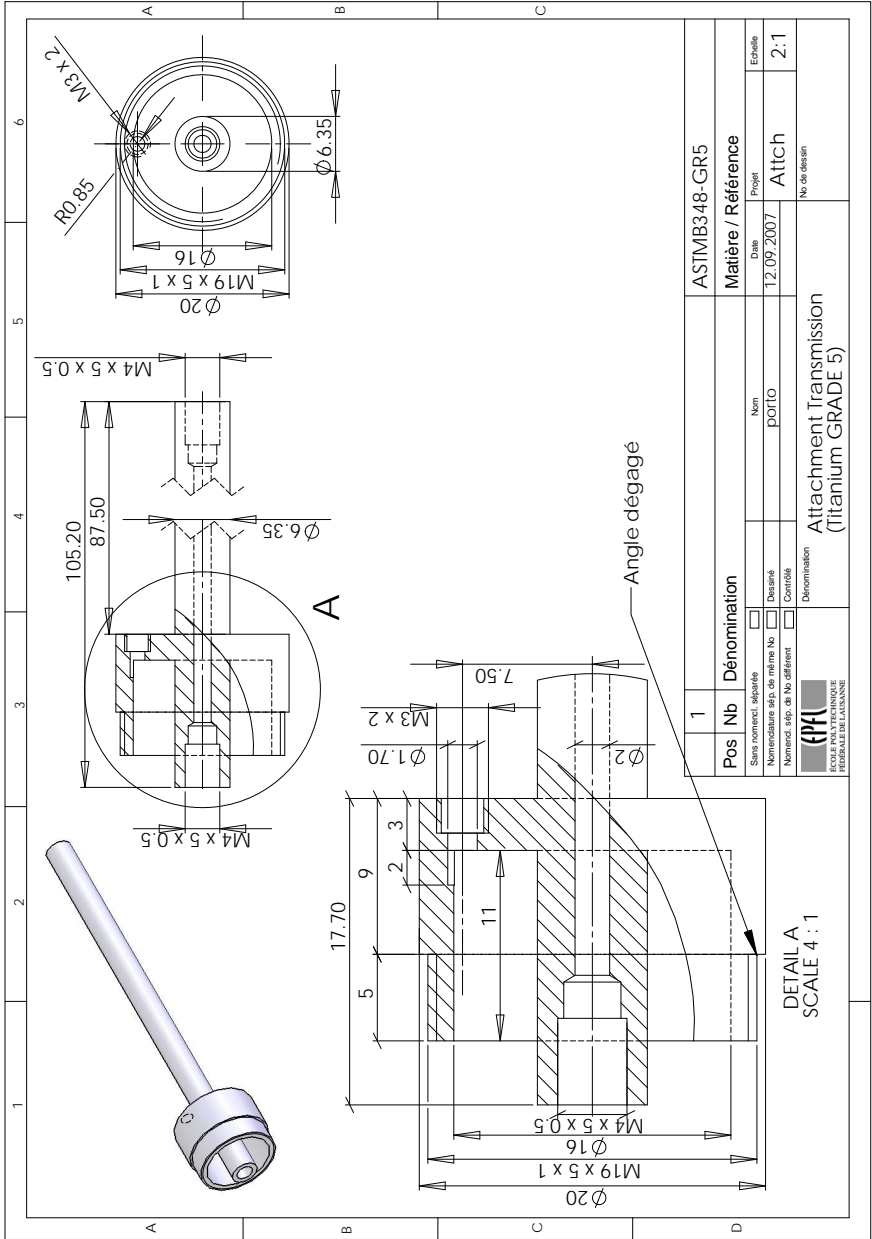




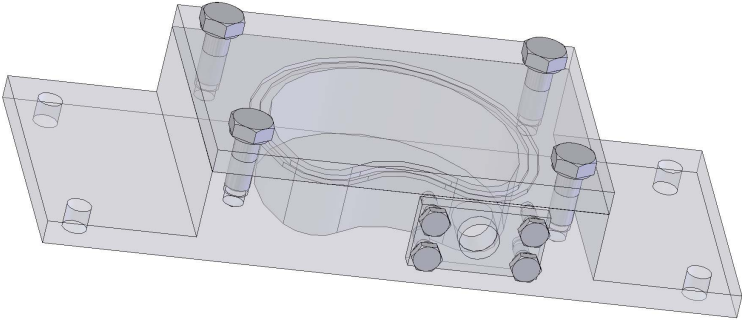
(*) linked quoted values

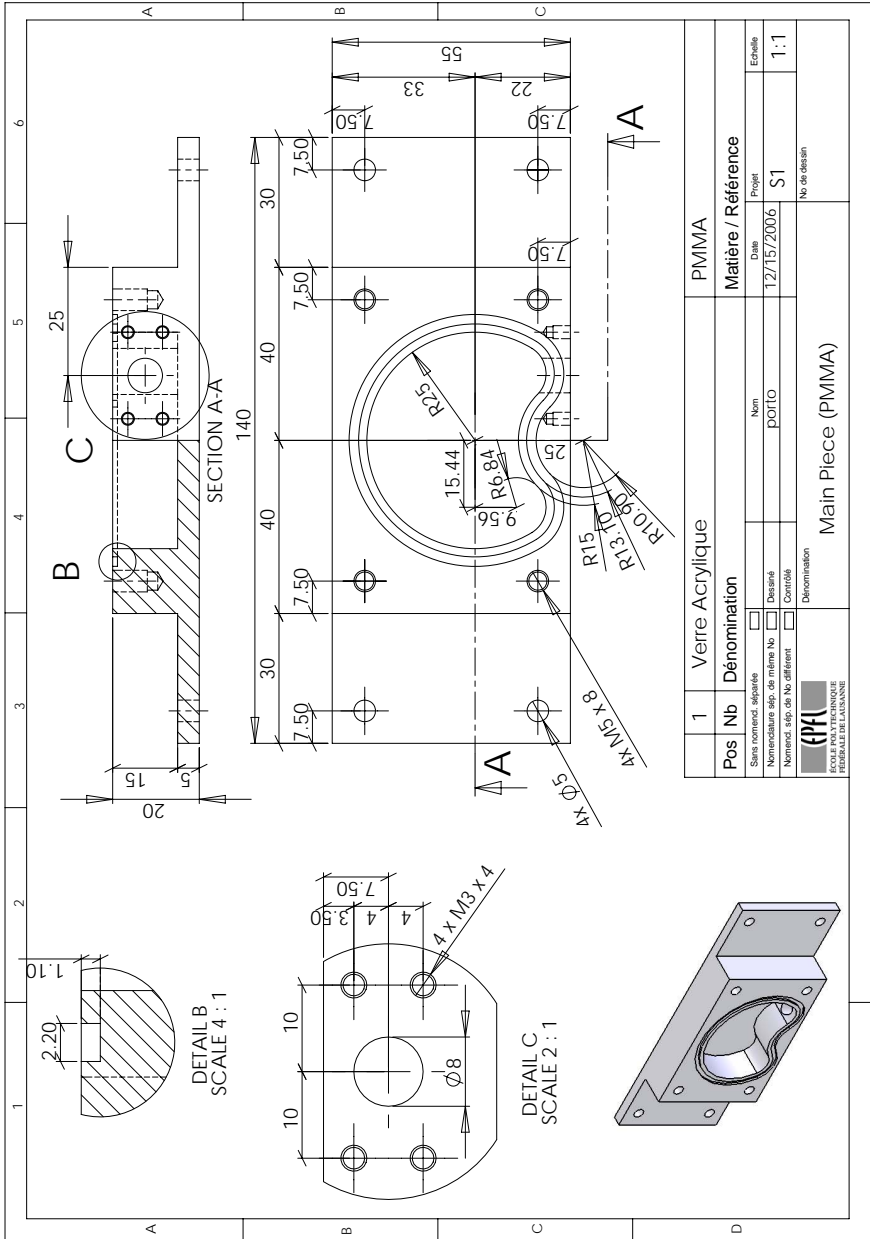
1	Pos / Nb	Dénomination	Matière / Référence	ASTMB348-GR5
		<input type="checkbox"/> Sans nommée spéciale <input type="checkbox"/> Nomenclature spécifique de même No <input type="checkbox"/> Désigné <input type="checkbox"/> Nom <input type="checkbox"/> Nommeé spécifique de No différent <input type="checkbox"/> Contrôlé <input type="checkbox"/> Contrôlé <input type="checkbox"/> Contrôle	Date	12.09.2007
			Projet	CplHrn
			No de dessin	
		Dénomination		
		Coupling Horns (Titanium GRADE 5)		
		ÉCOLE POLYTECHNIQUE FÉDÉRALE DE LAUSANNE		
		Echelle		
		2:1		



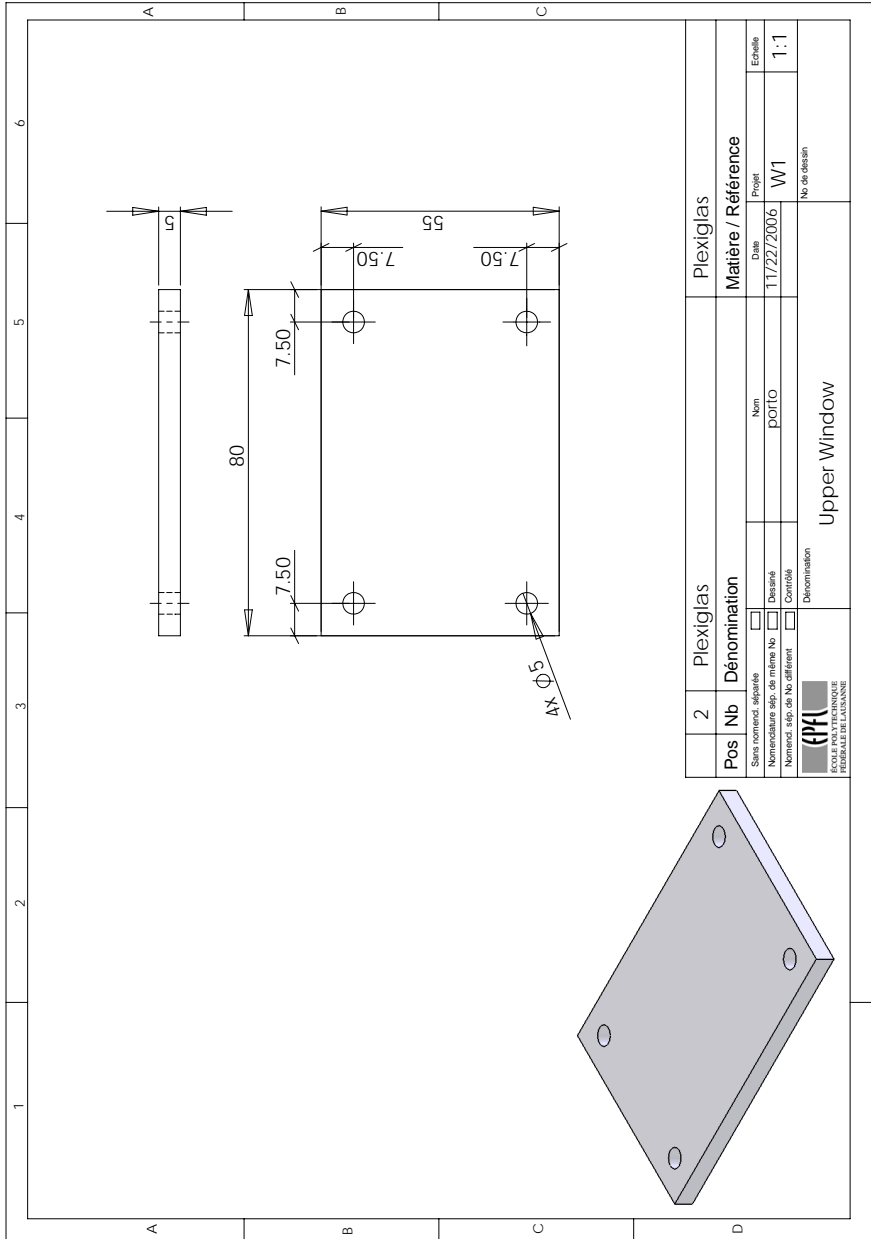


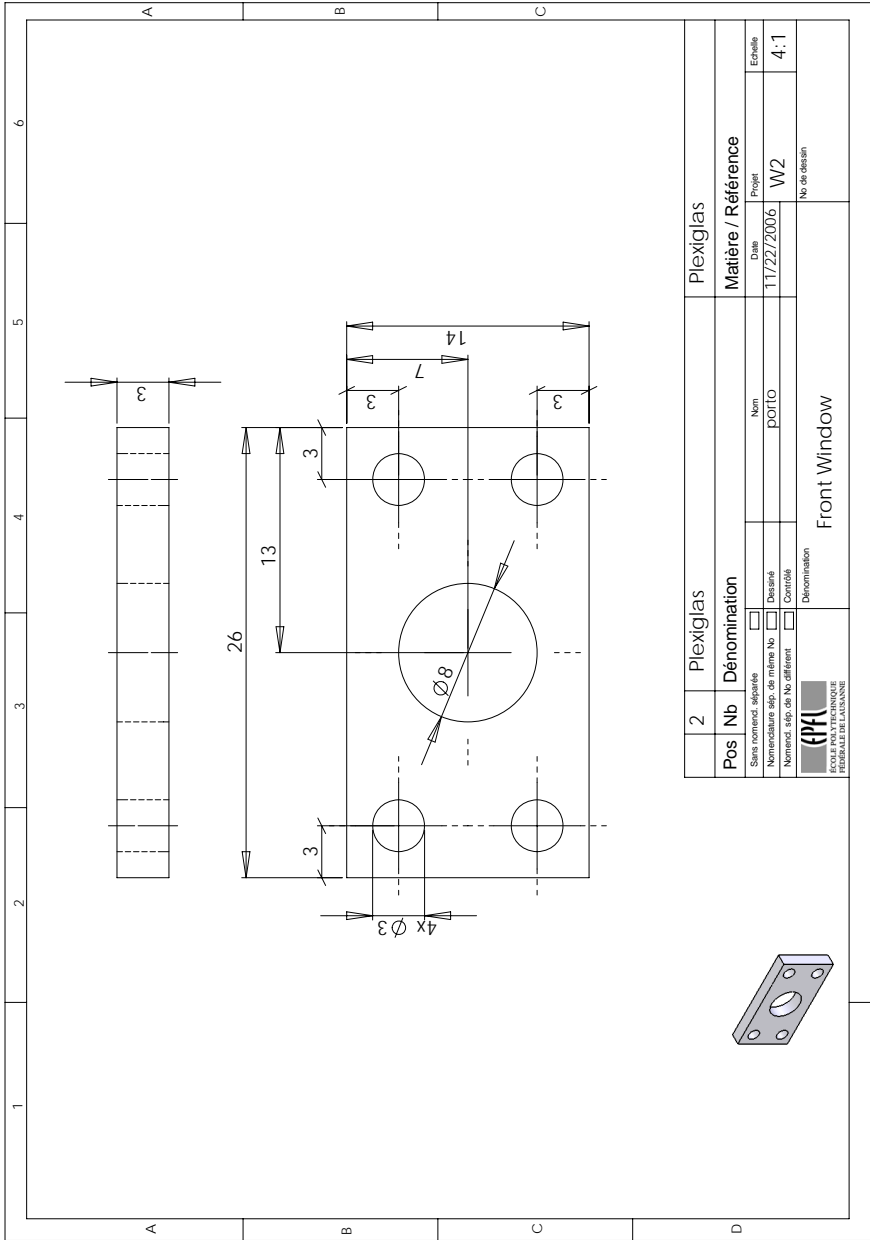
C.3 test Bench




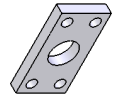


1	Verre Acrylique	PMMA
Pos	Inb	Dénomination
<input type="checkbox"/> Sans cotations séparées <input type="checkbox"/> Nomenclature séq. de même No <input type="checkbox"/> Désigné <input type="checkbox"/> Nomencl. séq. de No. différent <input type="checkbox"/> Contrôlé		
Dénomination		
Main Piece (PMMA)		
Matière / Référence		Nr de dessin
Date		Projet
12/15/2006		S1
Echelle		1:1





2		Plexiglas		Plexiglas	
Pos	Nb	Dénomination		Matière / Référence	
Sans comment séparé		<input type="checkbox"/>	Nom	Date	Projet
Nomenclature séc. de même Nb		<input type="checkbox"/>	POI10	11/22/2006	W2
Nomencl. séc. de Nb différent		<input type="checkbox"/>			
		<input type="checkbox"/>			
 ÉCOLE POLYTECHNIQUE FÉDÉRALE DE LAUSANNE		Dénomination		No de dessin	
		Front Window			
				Echelle	4:1



Appendix D

Test Functions

D.1 Ackley Function

$$f(\mathbf{x}) = 20 + e - 20e^{-\frac{1}{5}\sqrt{\frac{1}{p}\sum_{i=1}^p x_i^2}} - e^{-\frac{1}{p}\sum_{i=1}^p \cos(2\pi x_i)} \quad (\text{D.1})$$

$$-15 \leq x_i \leq 30, \quad i = 1 \dots p \quad (\text{D.2})$$

D.2 Rastrigin Function

$$f(\mathbf{x}) = 10p + \sum_{i=1}^p (x_i^2 - 10 \cos(2\pi x_i)) \quad (\text{D.3})$$

$$-5.12 \leq x_i \leq 5.12, \quad i = 1 \dots p \quad (\text{D.4})$$

D.3 Zakharov Function

$$f(\mathbf{x}) = \sum_{i=1}^p x_i^2 + \left(\sum_{i=1}^p 0.5 i x_i \right)^2 + \left(\sum_{i=1}^p 0.5 i x_i \right)^4 \quad (\text{D.5})$$

$$-5 \leq x_i \leq 10, \quad i = 1 \dots p \quad (\text{D.6})$$

Curriculum Vitae

Daniel PORTO

Nationality: Spanish

Date of birth: October 30th, 1976

Rte de la Maladière 4

CH-1022 Chavannes-Renens

Phone: +41 76 490 77 51

daniel.porto@a3.epfl.ch

Education

2004-to date Ph.D Student and Research Assistant at Integrated Actuators Laboratory (LAI), EPFL, Lausanne, Switzerland

1997-2004 Swiss Federal Institute of Lausanne (EPFL)

Degree: Dipl. Ing. EPFL

1993-1997 Senior High School, Lausanne

Degree: Matura Typus C

Languages

French, Spanish Mother tongues

English Fluent

German Good knowledge

Publications

D. Porto, A. Bourquard, Y. Perriard, "Genetic Algorithm Optimization for a Surgical Ultrasonic Transducer", 2008 IEEE International Ultrasonics Symposium (IUS), Beijing, China, November 2-5, 2008

J. Murphy, D. Porto, Y. Perriard, "Ultrasonic Transducer Model for Optimization of a Spinal Tissue Ablation System", Industry Applications Conference, 2006. 41st IAS Annual Meeting. Conference Record of the 2006 IEEE